

**Evaluation of Reducing Cement Content in NDOR Class R Combined Aggregate Gradations**

Miras Mamirov

Graduate Research Assistant

Department of Civil and Environmental Engineering

University of Nebraska-Lincoln

Jiong Hu, Ph.D.

Associate Professor

Department of Civil and Environmental Engineering

University of Nebraska-Lincoln

and

Yong-Rak Kim, Ph.D.

Professor

Department of Civil and Environmental Engineering

University of Nebraska-Lincoln

A Report on Research Sponsored by

Nebraska Department of Transportation

December 2019

1. Report No SPR-P1(18) M069	2. Government Accession No.	3. Recipient's Catalog No.	
4. Title and Subtitle Evaluation Reducing Cement Content in NDOR Class R Combined Aggregate Gradations		5. Report Date December 31, 2019	
		6. Performing Organization Code	
7. Author/s Miras Mamirov, Jiong Hu, and Yong-Rak Kim		8. Performing Organization Report No. 26-1121-4033-001	
9. Performing Organization Name and Address University of Nebraska-Lincoln, Department of Civil Engineering Peter Kiewit Institute, Omaha, NE 68182-0178		10. Work Unit No. (TRAIS)	
		11. Contract or Grant No.	
12. Sponsoring Organization Name and Address Nebraska Department of Transportation 1400 Highway 2, PO Box 94759, Lincoln, NE 68509		13. Type of Report and Period Covered	
		14. Sponsoring Agency Code	
15. Supplementary Notes			
16. Abstract The main objective of this research project was to achieve a cement reduction on Nebraska slip-form pavement concrete through aggregate particle packing optimization. A literature review was conducted to examine different aggregate optimization tools, quality control tests, and historical data of Nebraska Department of Transportation (NDOT) pavement mixtures. It was found that the Modified Toufar Model has good potential in optimizing particle packing and predicting packing degrees. The combined aggregate void content test was found to be useful to experimentally justify optimized aggregate gradations. The Box Test with a modified index and image analysis tool for surface void estimation was used to evaluate the effect of cement reduction and optimized aggregate gradation on pavement concrete workability. Considering one of the goals of the study was to maximize the use of local materials, locally available aggregates from both East and West Nebraska were selected. Analysis of different aggregate combinations has shown that experimental packing from the combined void content test has a high correlation with estimated packing from the Modified Toufar Model. Results also demonstrated that the current NDOT standard aggregate combination is not the optimum gradation and can be improved. The experimental program included in this study consisted of three Phases. Phase 1 focused on obtaining promising aggregate blends by maintaining the standard cement content (564 lb/yd <sup>3</sup> , 335 kg/m <sup>3</sup> ). Phase 2 included an evaluation of the performance of pavement concrete with cement content reduced by 0.5 sack (47 lb/yd <sup>3</sup> , 28 kg/m <sup>3</sup> ) steps for other reference and optimized aggregate blends. Results justified that when optimum gradation is used, cement could be reduced up to 94 lb/yd <sup>3</sup> (56 kg/m <sup>3</sup> ) with satisfactory key fresh and hardened concrete properties. Phase 3 is the performance evaluation phase, which included evaluating the reference mix and selected promising mixes for slump, air content, setting time, compressive strength, modulus of rupture, modulus of elasticity, surface and bulk resistivity, free shrinkage, restrained shrinkage, and freeze/thaw resistance. Finally, a mix design improvement procedure incorporating theoretical and experimental particle packing and using excess paste-to-aggregates ratio as the control parameter was proposed. Results from the study demonstrated that with the optimized aggregate gradation, cement content can be reduced without compromising key fresh, mechanical, and durability properties.			
17. Key Words Pavement concrete, Aggregate gradation optimization, Box test, Reduced cement content		18. Distribution Statement	
19. Security Classification (of this report) Unclassified	20. Security Classification (of this page) Unclassified	21. No. of Pages 79	22. Price

# TABLE OF CONTENTS

TABLE OF CONTENTS.....	i
LIST OF FIGURES .....	iv
LIST OF TABLES.....	vi
ACKNOWLEDGEMENTS.....	vii
DISCLAIMER .....	viii
ABSTRACT.....	ix
CHAPTER 1. INTRODUCTION.....	1
1.1 Introduction.....	1
1.2 Research Objectives.....	4
1.3 Organization of the report.....	4
CHAPTER 2. BACKGROUND.....	5
2.1 Introduction.....	5
2.2 Particle packing theories and models.....	5
2.2.1 Furnas model.....	5
2.2.2 Aim’s and Goff’s model .....	6
2.2.3 Modified Toufar’s model.....	7
2.2.4 The Linear Packing Density Model (LPDM).....	8
2.2.5 The Compressible Packing Model (CPM).....	8
2.2.6 Modified Andreasen and Andersen Model .....	10
2.3 Empirical gradation optimization methods .....	10
2.3.1 0.45 Power Chart .....	10
2.3.2 8-18 curve .....	11
2.3.3 Tarantula Curve .....	12
2.3.4 Coarseness Factor Chart.....	12
2.4 Factors impacting aggregate packing and workability of pavement concrete .....	13
2.4.1 Maximum size of aggregate.....	13
2.4.2 Gradation.....	14
2.4.3 Aggregate shape and texture .....	14
2.4.4 Micro fines content .....	14
2.5 Mixture design development.....	14
2.6 Quality control tests .....	15
2.7 NDOT historical data.....	16
2.8 Summary .....	18
CHAPTER 3. MATERIALS AND TEST METHODS.....	20

3.1 Introduction.....	20
3.2 Materials .....	20
3.2.1 Cement and cementitious materials .....	20
3.2.2 Aggregates .....	20
3.2.3 Chemical admixtures .....	23
3.3 Combined aggregate void content test.....	24
3.4 Concrete mixing.....	25
3.5 Fresh concrete tests .....	26
3.5.1 Slump test.....	26
3.5.2 Air content test.....	26
3.5.3 Setting time test.....	27
3.5.4 Box test .....	28
3.6 Specimen casting and curing.....	31
3.7 Hardened concrete tests .....	31
3.7.1 Compressive strength test .....	31
3.7.2 Flexural strength test.....	31
3.7.3 Static modulus of elasticity test .....	32
3.8 Durability tests.....	33
3.8.1 Freeze/thaw resistance .....	33
3.8.2 Surface and bulk resistivity.....	33
3.8.3 Free shrinkage.....	34
3.8.4 Restrained shrinkage.....	34
<b>CHAPTER 4.    EXPERIMENTAL DESIGN AND RESULTS.....</b>	<b>36</b>
4.1 Introduction.....	36
4.2 Aggregate system evaluation and selection .....	36
4.2.1 Experimental packing results .....	36
4.2.2 Theoretical packing results .....	38
4.3 Testing matrix development.....	40
4.4 Phase 1 - Aggregate Blends Study.....	41
4.4.1 Mix proportions .....	41
4.4.2 Fresh concrete properties .....	42
4.4.3 Hardened concrete properties.....	44
4.5 Phase 2 - Cement Content Study.....	46
4.5.1 Mix proportions .....	46
4.5.2 Fresh concrete properties .....	47



4.5.3 Hardened concrete properties.....	51
4.6 Phase 3 - Performance Evaluation .....	53
4.6.1 Mix proportions .....	53
4.6.2 Fresh concrete properties .....	54
4.6.3 Hardened concrete properties.....	55
4.6.4 Durability properties .....	57
4.7 Proposed changes in NDOT specifications.....	63
4.8 Summary .....	63
CHAPTER 5.    COST EFFECTIVENESS AND FEASIBILITY STUDY .....	66
5.1 Cost Effectiveness Analysis.....	66
5.1.1 Methodology.....	66
5.1.2 Results.....	66
5.2 Feasibility Analysis.....	67
CHAPTER 6.    CONCLUSIONS AND RECOMMENDATION FOR FUTURE STUDIES .	68
6.1 Conclusions.....	68
6.2 Recommendations for Future Studies .....	68
6.2.1 Potential modification of Tarantula Curve limits for Nebraska pavement .....	68
6.2.2 Air content requirement adjustment with the cement reduction .....	69
6.2.3 Mix design adjustment based on specific aggregate characteristics .....	70
REFERENCES .....	72
Appendix A - Excess Paste-to-Aggregates Calculation.....	76
Appendix B - Mix Design Improvement Methodology.....	77
B.1 Design Philosophy.....	77
B.2 Proposed Mix Design Procedure .....	78
B.3 Summary .....	79

# LIST OF FIGURES

Figure 1.1. Annual CO<sub>2</sub> emissions from cement production (Andrew, 2018). ..... 1

Figure 1.2. Comparison of shrinkage of aggregate, paste, and concrete. .... 2

Figure 1.3. Illustration of cement content reduction through aggregate gradation optimization ... 2

Figure 1.4. Aggregate sources in Nebraska and Iowa ..... 4

Figure 2.1. Wall effect and loosening effect (De Larrard 1999) ..... 6

Figure 2.2. Correlation between predicted and experimental packing degrees (Goltermann, 1997)  
..... 8

Figure 2.3. Compaction index versus packing degree (De Larrard, 1999)..... 9

Figure 2.4. 0.45 Power Chart of the current NDOT combined aggregate gradation..... 11

Figure 2.5. The current NDOT combined aggregate gradation on the IPR chart with ‘8-18’ limits  
..... 11

Figure 2.6. The current NDOT combined aggregate gradation Tarantula Curve..... 12

Figure 2.7. The current NDOT combined aggregate gradation on the Coarseness Factor Chart. 13

Figure 2.8 Nebraska gradation on 0.45 Power Chart..... 16

Figure 2.9. Nebraska gradations on Tarantula Curve ..... 17

Figure 2.10. Nebraska gradations on 8-18 Curve ..... 17

Figure 2.11. Nebraska gradations on Shilstone Chart..... 18

Figure 3.1. Nebraska aggregates gradations ..... 21

Figure 3.2. Selected aggregates ..... 22

Figure 3.3. Gradation curve of aggregates used in this curve..... 23

Figure 3.4. Combined void content test..... 25

Figure 3.5. Vibration plus pressure method sketch..... 25

Figure 3.6. Slump test setup..... 26

Figure 3.7. Air pressure meter ..... 27

Figure 3.8. Setting time test setup..... 27

Figure 3.9. Box Test setup ..... 28

Figure 3.10. Comparison of surface voids of box test rankings from different methods ..... 29

Figure 3.11. Examples of Box test results with different edge holding abilities ..... 30

Figure 3.12. Compressive strength test setup ..... 31

Figure 3.13. Flexural strength test setup..... 32

Figure 3.14. Static Modulus of Elasticity test setup ..... 32

Figure 3.15. Setup used for freeze/thaw resistance test..... 33

Figure 3.16. Resistivity test setup..... 34

Figure 3.17. Length comparator used for shrinkage measurement..... 34

Figure 3.18. Restrained shrinkage test setup ..... 35

Figure 4.1. Results of the combined aggregate void content test for binary blends..... 37

Figure 4.2. Results of the combined aggregate void content test for ternary blends..... 38

Figure 4.3. Comparison between experimental and theoretical packing degrees of East NE blends  
..... 39

Figure 4.4. Comparison between experimental and theoretical packing degrees of West NE  
blends ..... 39

Figure 4.5. Theoretical Optimum curve with the reference blend and promising ternary blends, $q=0.45$ , $d_{max}=1$ in, $d_{min}=75$ microns.....	40
Figure 4.6. Reference blend and blends chosen for further study plotted on Tarantula curve. ....	41
Figure 4.7. Mix identification .....	42
Figure 4.8. Box test images from Phase 1 East NE mixes.....	43
Figure 4.9. Box test images from Phase 1 West NE mixes .....	44
Figure 4.10. Mechanical properties of Phase 1 mixes .....	45
Figure 4.11. Surface resistivity results of Phase 1 mixes .....	46
Figure 4.12. Box test images for East NE mixes .....	50
Figure 4.13. Box test images for West NE mixes.....	51
Figure 4.14. Effect of cement content on mechanical properties .....	52
Figure 4.15. Effect of cement content on permeability .....	53
Figure 4.16. Mechanical properties of the promising mixes .....	56
Figure 4.17. Permeability properties of the promising mixes.....	57
Figure 4.18. Freeze/thaw resistance results of East NE mixes .....	58
Figure 4.19. Representative specimens of East NE mixes after 300 cycles of freezing-thawing.	59
Figure 4.20. Freeze/thaw resistance results of West NE mixes.....	60
Figure 4.21. Representative specimens of West NE mixes after 300 cycles of freezing-thawing	61
Figure 4.22. Free shrinkage results .....	62
Figure 4.23. Restrained shrinkage results of East NE mixes.....	63
Figure 6.1. Promising blends plotted on Tarantula Curve .....	69
Figure 6.2. Illustration of increase in paste air content when maintaining concrete air .....	70
Figure 6.3. AIMS 2 setup.....	71
Figure 6.4. Direct measurement of aggregate shape and texture.....	71
Figure B.1. Effect of $P_c\%/V_{B\_agg}\%$ ratio on surface voids.....	78
Figure B.2. The proposed mix design adjustment procedure .....	79

## LIST OF TABLES

Table 2.1. Compaction Index with different packing processes .....	9
Table 3.1. Chemical composition and physical properties of IP cement.....	20
Table 3.2. Aggregates properties .....	23
Table 4.1. Mix proportions for mixes of Phase 1 .....	42
Table 4.2. Fresh concrete properties of Phase 1 East NE mixes.....	42
Table 4.3. Fresh concrete properties of Phase 1 West NE mixes .....	44
Table 4.4. Mix proportions for mixes of Phase 2 .....	47
Table 4.5. Fresh concrete properties of Phase 2 East NE mixes.....	49
Table 4.6. Fresh concrete properties of Phase 2 West NE mixes .....	49
Table 4.7. Mix proportions for performance evaluation mixes .....	54
Table 4.8. Fresh concrete properties of East NE performance evaluation mixes .....	54
Table 4.9. Specification for 47B pavement concrete mix.....	63
Table 4.10. Summary table of Phase 3 mixes.....	65
Table 5.1. Unit costs of materials .....	66
Table 5.2. Base costs of promising mixes.....	67

## **ACKNOWLEDGEMENTS**

The authors would like to thank the Nebraska Department of Transportation (NDOT) for funding the research project and providing the opportunity to study pavement concrete. Special thanks to Technical Advisory Committee members Mr. Mick Syslo, Mr. Wally Heyen, Ms. Lieska Halsey, Mr. Andy Dearmont, Mr. Kurt Peyton, and Mr. Ray Wagner for their valuable inputs. Authors would like to thank Mr. Ben Ricceri from Lyman-Richey Corporation and Mr. Kevin Piper from Simon Contractors for donating materials for this research. Authors also would like to acknowledge Dulitha Fredrick, Joshua Jackson, Flavia Mendonca, Arman Abdigaliyev, and Joey Malloy for their assistance in the laboratory work.

## **DISCLAIMER**

The contents of this report reflect the views of the authors, who are responsible for the facts and the accuracy of the information presented herein. The contents do not necessarily reflect the official views or policies neither of the Nebraska Department of Transportations nor the University of Nebraska-Lincoln. This report does not constitute a standard, specification, or regulation. Trade or manufacturers' names, which may appear in this report, are cited only because they are considered essential to the objectives of the report. The United States (U.S.) government and the State of Nebraska do not endorse products or manufacturers.

This material is based upon work supported by the Federal Highway Administration under SPR-P1(18) M069. Any opinions, findings and conclusions or recommendations expressed in this publication are those of the author(s) and do not necessarily reflect the views of the Federal Highway Administration.

## ABSTRACT

The main objective of this research project was to achieve a cement reduction on Nebraska slip-form pavement concrete through aggregate particle packing optimization. A literature review was conducted to examine different aggregate optimization tools, quality control tests, and historical data of Nebraska Department of Transportation (NDOT) pavement mixtures. It was found that the Modified Toufar Model has good potential in optimizing particle packing and predicting packing degrees. The combined aggregate void content test was found to be useful to experimentally justify optimized aggregate gradations. The Box Test with a modified index and image analysis tool for surface void estimation was used to evaluate the effect of cement reduction and optimized aggregate gradation on pavement concrete workability. Considering one of the goals of the study was to maximize the use of local materials, locally available aggregates from both East and West Nebraska were selected. Analysis of different aggregate combinations has shown that experimental packing from the combined void content test has a high correlation with estimated packing from the Modified Toufar Model. Results also demonstrated that the current NDOT standard aggregate combination is not the optimum gradation and can be improved. The experimental program included in this study consisted of three Phases. Phase 1 focused on obtaining promising aggregate blends by maintaining the standard cement content ( $564 \text{ lb/yd}^3$ ,  $335 \text{ kg/m}^3$ ). Phase 2 included an evaluation of the performance of pavement concrete with cement content reduced by 0.5 sack ( $47 \text{ lb/yd}^3$ ,  $28 \text{ kg/m}^3$ ) steps for other reference and optimized aggregate blends. Results justified that when optimum gradation is used, cement could be reduced up to  $94 \text{ lb/yd}^3$  ( $56 \text{ kg/m}^3$ ) with satisfactory key fresh and hardened concrete properties. Phase 3 is the performance evaluation phase, which included evaluating the reference mix and selected promising mixes for slump, air content, setting time, compressive strength, modulus of rupture, modulus of elasticity, surface and bulk resistivity, free shrinkage, restrained shrinkage, and freeze/thaw resistance. Finally, a mix design improvement procedure incorporating theoretical and experimental particle packing and using excess paste-to-aggregates ratio as the control parameter was proposed. Results from the study demonstrated that with the optimized aggregate gradation, cement content can be reduced without compromising key fresh, mechanical, and durability properties.

# CHAPTER 1. INTRODUCTION

## 1.1 Introduction

Pavement concrete is one of the most widely used infrastructural materials with applications in highways, airports, streets, and roads. The optimization of pavement concrete mixtures is becoming essential as the industry is committing to promote economy and sustainability. The purpose of optimization is mainly to reduce cement, which is the most expensive ingredient in concrete and with the largest contribution to carbon dioxide emissions. Recent estimates have shown that cement production contributes about 5% of total global CO<sub>2</sub> emissions (Andrew, 2018), and the CO<sub>2</sub> emissions contributed by cement production is gradually increasing (Figure 1.1).

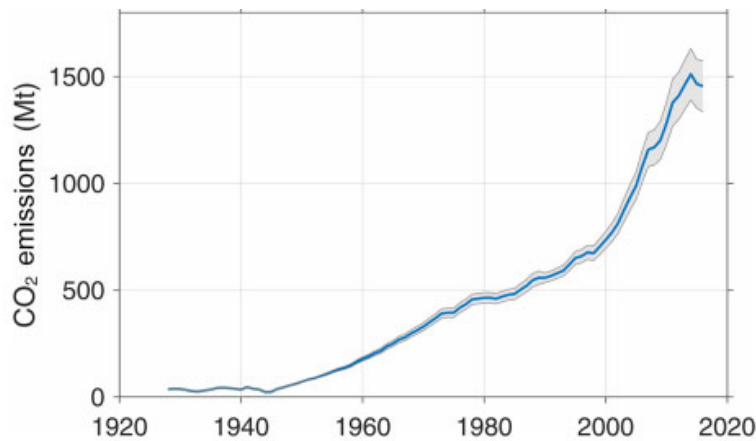


**Figure 1.1. Annual CO<sub>2</sub> emissions from cement production (Andrew, 2018).**

Shrinkage-induced cracking has been a major contributor to pavement concrete durability issues. As the shrinkage of aggregates is negligible, shrinkage of concrete, which is largely determined by the cement paste, can be reduced consequently through mixture optimization. Figure 1.2 shows the comparison of shrinkage of different materials over-drying period. As cement is also the most costly ingredient in concrete, by reducing the cement content, more durable concrete pavement can be achieved.



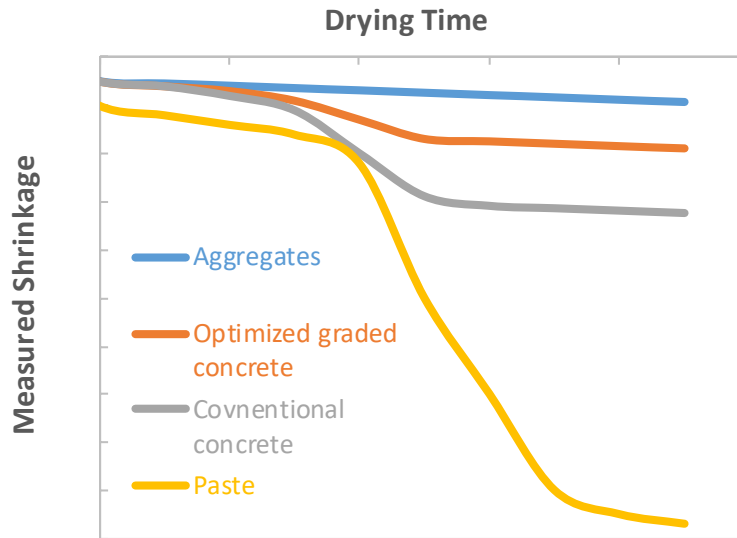


**Figure 1.2. Comparison of shrinkage of aggregate, paste, and concrete.**

The most common approach to reducing cement content is to improve the particle packing of the aggregate skeleton that consists of fractions of particles at different sizes, shapes, and textures. In general, aggregates occupy around 70-80% of the concrete mixture by volume. Optimization of particle packing implies to achieve as dense matrix as possible, i.e., with the lowest possible amount of voids in between particles. De Larrard (1999) stated that the main three factors affecting particle packing are particle size distribution, particle geometry, and compaction method. Kennedy (1940) claimed that to provide appropriate concrete workability simply filling the voids among the aggregate matrix is not enough, and excess paste is required to achieve different levels of workability. Figure 1.3 illustrates the reduced cement content with optimum aggregate gradation. It can be seen that the lower the amount of voids, the less cement paste is needed to fill them, which in turn resulted in a higher amount of excess paste that is available to provide sufficient workability and bonding to ensure concrete strength.

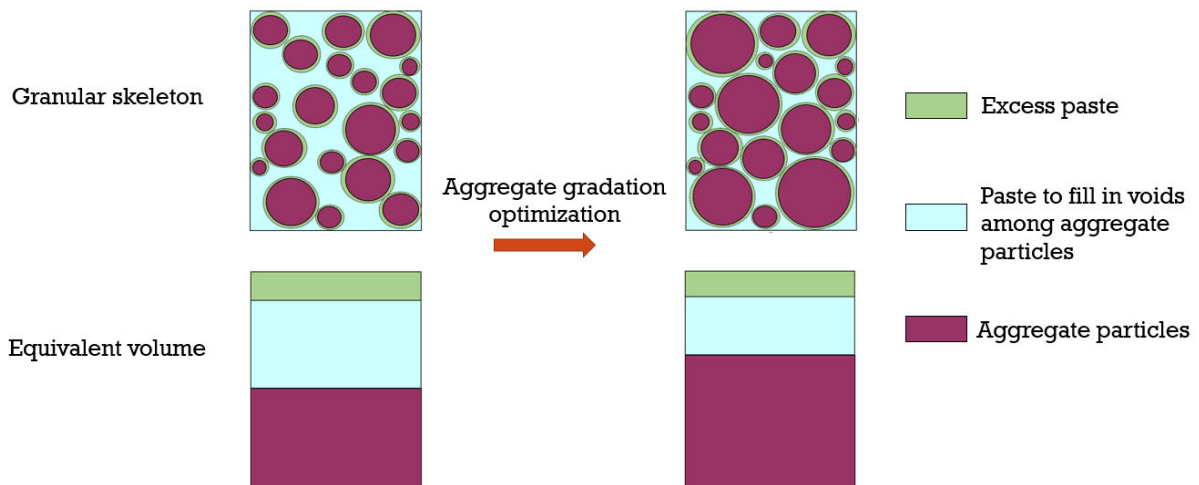


**Figure 1.3. Illustration of cement content reduction through aggregate gradation optimization**

Sometimes contingent upon the application and circumstances, it is not practical to vary aggregate geometry or compaction method to optimize particle packing, leaving the option of optimizing aggregate gradation to be the most feasible one. There are many different aggregate optimization approaches currently being used in the concrete arena. Researches showed that aggregate proportioning techniques such as the 45 Power chart, Shilstone chart and 8-18 chart not necessarily provides the lowest void content (Ley et al., 2012; Obla et al., 2007; Quiroga et al., 2004) and might not be the best tool to obtain aggregate blends for slip-form pavement mixtures (Taylor et al., 2015). A newly developed Tarantula curve is a modified version of the 8-18 chart with adjusted upper and lower limits at different aggregate sizes (Ley et al., 2014) created based on a large amount of empirical data from hundreds of mixes. While the Tarantula curve is likely the most recognized gradation for pavement concrete and has been adopted by many agencies and contractors, like other aggregate optimization methods, the biggest issue of these methods mentioned above is that none of them accounts for the shape and texture of aggregates. Also, although methods including the Tarantula curve can likely distinguish whether a gradation is good or bad, these approaches do not provide information on the optimum blend to obtain a higher packing degree. Due to this limitation, these methods can serve as a supplemental tool in concrete mix design, but not capable of guiding the gradation optimization process. It is believed that the use of necessary particle packing models, such as discrete theoretical models can be useful. Besides obtaining optimum proportions, such models are capable of predicting the particle packing degree.

Moreover, because modeling inputs required factors such as individual packing of aggregates, these models indirectly account for aggregate shape and texture. Previous studies have shown that the Modified Toufar Model has a good correlation between experimental and estimated packing degree. It is believed that using the Modified Toufar Model to obtain an optimum packing, accompanied by experimental tests of the actual void content of aggregate can provide simple and more effective guidance for aggregate optimization and concrete mix design.

Nebraska is known for its unique type of aggregates for concrete, where the major proportion of aggregate is a combination of sand and gravel that is mostly fine aggregate yet with a small portion of particles within the coarse aggregate size range; further, a relatively small amount (approximately 30%) of limestone is generally used as coarse aggregate. The relatively small amount of limestone implies a less expensive total cost of aggregate and a lower amount of angular aggregates in the design, which generally results in a relatively high pavement concrete workability compared to other states. More importantly, the combined aggregate gradation could be compromised, which leads to a higher cement content required for the concrete mixture. The current specification requires a minimum of 564 lb/yd<sup>3</sup> (335 kg/m<sup>3</sup>) cement content for pavement concrete.

Figure 1.4 represents aggregate sources in the state of Nebraska and Iowa. As shown in the figure, there is a lack of limestone sources in West Nebraska, making granite and dolomite the more widely used coarse aggregate in that region. Granite and dolomite might significantly differ from limestone in terms of gradation, shape, and texture. While sand and gravel are used through the state of Nebraska, it is also important to note that sand and gravel aggregate becomes coarser in West Nebraska. Therefore, it is critical to use an effective aggregate gradation optimization tool that can be applied to different types and sizes of aggregates.

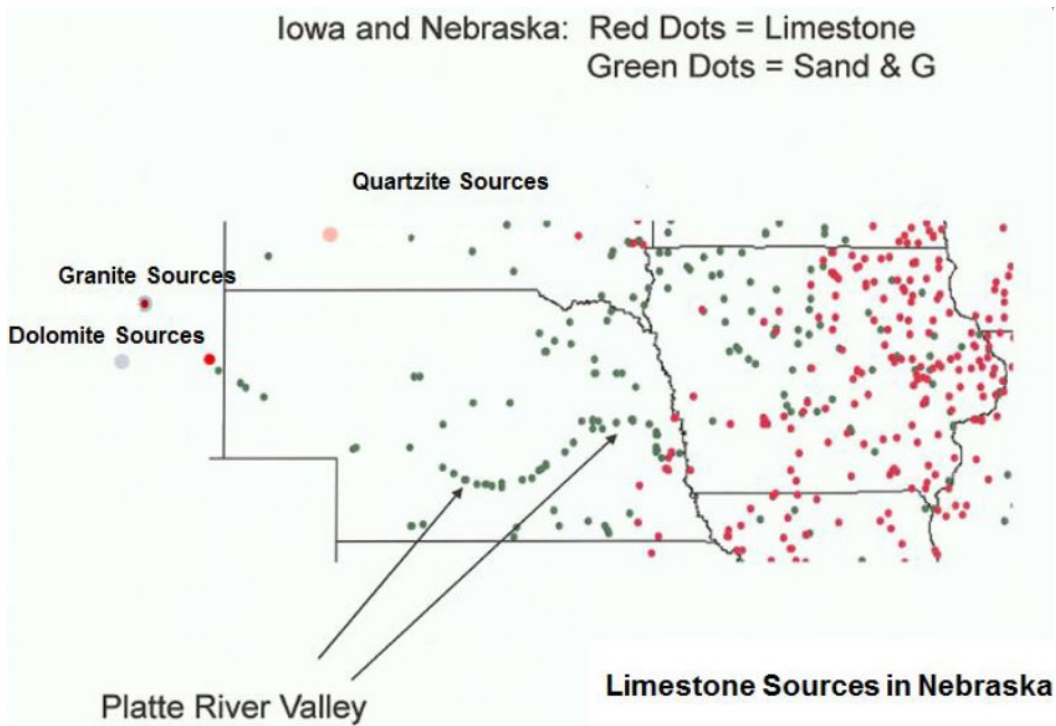


**Figure 1.4. Aggregate sources in Nebraska and Iowa**

To ensure successful concrete optimization, it is important to adopt specific tests to examine slip-formed pavement concrete workability. Box test and VKelly tests were developed by Cook et al. (2014) and Taylor et al. (2012) respectively with the purpose of evaluating fresh pavement concrete behavior under vibration. It is believed that both tests have to be tested for applicability in Nebraska, where low coarse aggregate concrete mixtures are being used. Moreover, the possibility of improving test rankings should be discussed and tried.

## **1.2 Research Objectives**

Besides developing an effective mix design method based on both theoretical and experimental packing and fresh concrete performance, the main objective of this work is to identify optimized concrete designs for pavement applications in Nebraska. Therefore, historical data and information of Nebraska aggregate availability and gradation have to be collected and analyzed. The study provides recommended pavement concrete mixtures to ensure workability and constructability so that the mixes can be easily used in engineering applications, and appropriate mechanical properties and durability characteristics meet the Nebraska Department of Transportation (NDOT) specifications.

## **1.3 Organization of the report**

The report is divided into seven chapters. Chapter 1 is an introduction, where the general background and main objectives are provided. A literature review is presented in Chapter 2, which includes a summary of different theoretical and empirical particle packing models and gradation optimization tools, factors affecting aggregate packing, workability (quality control) tests of pavement concrete, to justify optimized aggregate gradation. Chapters 3 and 4 include the main experimental program and results covering both East and West Nebraska aggregates. Cost-effectiveness and feasibility study are discussed in Chapter 5. Chapter 6 summarizes all conclusions and provides recommendations for future studies.

## CHAPTER 2. BACKGROUND

### 2.1 Introduction

There are many different approaches to optimize particle packing including empirical methods, theoretical models, and experimental tests. In order to select the most effective method for this particular study in terms of optimization and prediction of the particle packing degree, a comprehensive literature review was conducted. Various theoretical models, empirical optimization tools were evaluated for their advantages, limitation, and simplicity. Besides, factors impacting aggregate gradation and workability of pavement concrete such as the maximum size of aggregate, gradation, aggregate shape and texture, and microfine content were discussed. Quality control tests to justify optimized aggregate gradation were also presented. Moreover, mixture design development for pavement concrete proposed by other researchers is discussed. Finally, NDOT historical data was presented, and it was justified that the majority of the blends used nowadays in the state are not optimum.

### 2.2 Particle packing theories and models

Concrete is composed of a skeleton of granular particles bound together with cementitious paste. The philosophy of particle packing is to combine grains with the lowest possible porosity to minimize the amount of binder. It is believed that the packing degree mainly depends on three parameters: particle size distribution, particle shape, and method of processing the packing (De Larrard, 1999). There are various theories and models developed to predict particle packing of different granular matrices as accurate as possible.

#### 2.2.1 Furnas model

Furnas (1928) is the first who started to run basic research on particle packing theory in his study of the flow of gases through beds of broken solids. His discrete theory of binary system was based on the assumptions that particles are spherical in shape; small and large particles are significantly different in size (particle diameter  $d_1 \ll$  particle diameter  $d_2$ ); and small particles fill out the voids among large particles without disturbing their packing. There are two scenarios possible based on volumes of fine and coarse particles: “fine-grain domain” and “coarse domain” meaning the volume fraction of small particles is dominant and the volume fraction of large particles is dominant, respectively. The model can be described as:

$$\Phi^* = \varphi_2 + (1 - \varphi_2) * \varphi_1 \quad (2.1)$$

Where,  $\Phi^*$  is the maximum packing density of the binary system,  $\varphi_1$  and  $\varphi_2$  are individual packing densities for small and large particles respectively. If  $d_1 \approx d_2$ , the so-called “wall effect” and “loosening effect” occur (Figure 2.1). Wall effect is a phenomenon when an isolated coarse particle in the fine particle matrix disturbs the packing and increases voids around. Loosening effect is when an isolated fine particle in the coarse particle matrix appears to be too large to fit the space between coarse particles, thus disturbing the packing. If the difference in particle diameters is not significant, the  $d_1/d_2$  ratio has to be taken into consideration, which this model does not account for. Therefore, the main limitation of this model is that it does not consider “wall effect” and “loosening effect”.

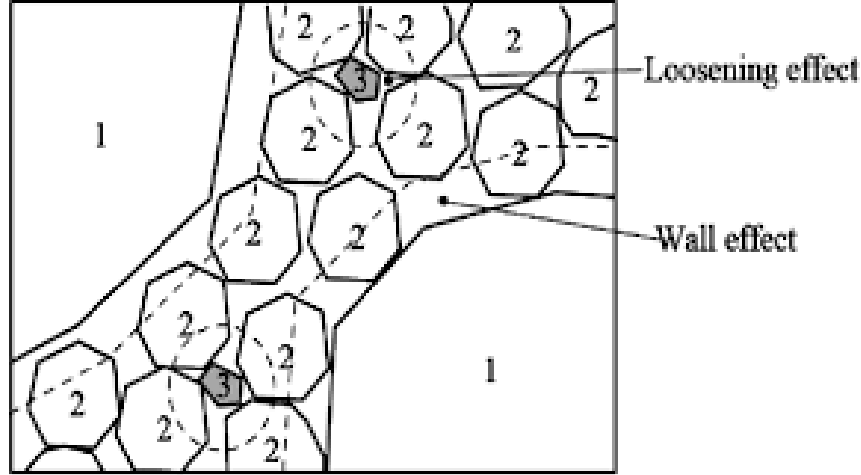


Figure 2.1. Wall effect and loosening effect (De Larrard 1999)

### 2.2.2 Aim's and Goff's model

According to Rudy (2009), in 1967, Aim and Goff suggested a simple geometrical model to predict the packing density of binary systems. The main improvement was that this model takes into consideration the “wall effect” in the first layer of spherical particles in contact with a smooth and plain wall. Similarly to the previous model, two scenarios are considered in this method: the amount of fine particles is much less than the number of coarse particles, or the amount of fine particles is much more than the number of coarse particles. The first scenario implies that fine particles serve to fill the voids among coarse particles, whereas the second scenario implies that fine particles serve as a media for coarse aggregates to be embedded. The fraction of fine particles,  $V_1^*$  resulting in maximum packing density can be calculated using the following equation:

$$V_1^* = \frac{[(\varphi_1/\varphi_2) - (1 + 0.9 * d_1/d_2) * \varphi_1]}{[(\varphi_1/\varphi_2) - (1 + 0.9 * d_1/d_2) * \varphi_1 + 1]} \quad (2.2)$$

Where,  $d_1$  and  $d_2$  are the diameters of fine and coarse particles, and  $\varphi_1$  and  $\varphi_2$  are individual experimental packing densities respectively,  $(1 + 0.9 * d_1/d_2)$  is the factor due to wall effect, where  $d_1$  and  $d_2$  are the diameters of fine and coarse particles respectively. The packing degree can be calculated based on two cases depending on whether the volume fraction of fine particles ( $V_1$ ) is higher or lower than  $V_1^*$ :

$$\text{For } V_1 < V_1^*, \Phi = \varphi_2 / (1 - V_1) \quad (2.3a)$$

$$\text{For } V_1 \geq V_1^*, \Phi = 1 / [(V_1/\varphi_1 + (1 - V_1) * (1 + 0.9 * d_1/d_2))] \quad (2.3b)$$

In the experimental study of Goltermann et al. (1997), this model did not correlate appropriately with the test results. It was concluded that Aim's and Goff's model cannot be used for realistic aggregates.

### 2.2.3 Modified Toufar's model

Toufar model is the method to design multicomponent mixtures of particles by maximizing the packing degree, which was created in the 1970s and then modified in the 1990s (Goltermann et al., 1997). The main concept implies that fine particles are not able to fill interstices between coarse particles, and as a result, the whole matrix consists of two systems: one mostly composed of densely packed coarse particles and the other consisting of areas of packed fine particles with discretely distributed coarse particles. The main unrealistic assumptions made in this theoretical model are that 1) all particles are spherical in shape, 2) monosized, and 3) coarse and fine particles differ in size ( $d_1 \ll d_2$ ). The first two assumptions can be corrected by introducing a characteristic diameter of the aggregates and individual packing degree of the aggregates. Characteristic diameter can be obtained by the position parameter of Rosin-Raimmler-Sperling-Bennet distribution curve, which stands for the diameter, where 36.8% of particles are retained. Goltermann et al. (1997) stated that characteristic diameter and individual packing degree minimize the deviations from the first two assumptions. The third assumption can cause problems in case of overlapping fractions of fine and coarse particles with fairly different characteristic diameters. However, it was found from an experimental study that overlapping effect has an insignificant effect on packing degree close to maximum packing or when the fraction of fine particles is high (Goltermann et al., 1997). Once characteristic diameter and individual packing degrees are obtained, they can be used to obtain combined packing degree,  $\Phi$  as follows:

$$\Phi = \frac{1}{\left[\frac{V_1}{\varphi_1} + \frac{V_2}{\varphi_2} - V_2 * \left(\frac{1}{\varphi_2} - 1\right) * k_d * k_s\right]} \quad (2.4)$$

Where  $V_1$  and  $V_2$  are the volume fractions of fine and coarse particles respectively,  $\varphi_1$  and  $\varphi_2$  are packing degrees of fine and coarse particles respectively,  $k_d$  is the diameter ratio factor

$k_d = \frac{(d_2 - d_1)}{(d_2 + d_1)}$ , where  $d_1$  and  $d_2$  are characteristic diameters of fine and coarse particles respectively,  $k_s$  is a statistical factor. This factor was introduced after a later comparison by Goltermann et al. (1997) showed that introducing a small number of fine particles to a sample of coarse particles does not increase the packing degree, as expected. It is caused by the assumption that each fine particle placed is limited only to four coarse particles to surround it. Introducing a statistical factor can overcome this unrealistic behavior (Goltermann et al., 1997).

$$\text{For } x < x_0, k_s = \left(\frac{x}{x_0}\right) * k_0 \quad (2.5a)$$

$$\text{For } x \geq x_0, k_s = 1 - \frac{(1+4*x)}{(1+x)^4} \quad (2.5b)$$

$$\text{Where, } x_0 = 0.4753, k_0 = 0.3881, x = \frac{(V_1/V_2) * (\varphi_1/\varphi_2)}{(1-\varphi_2)}$$

According to the works of Goltermann et al. (1997), Rudy (2009), Jones et al. (2001), and Moini (2015), the Modified Toufar Method has a good correlation of theoretical and experimental packing results for binary blends of aggregates. Besides, Goltermann et al. (1997) collected more than 800 experimental results from their own studies and other authors and compared them with the predicted packing degree (Figure 2.2). It can be seen that the Modified Toufar Model predicts packing degree very well.

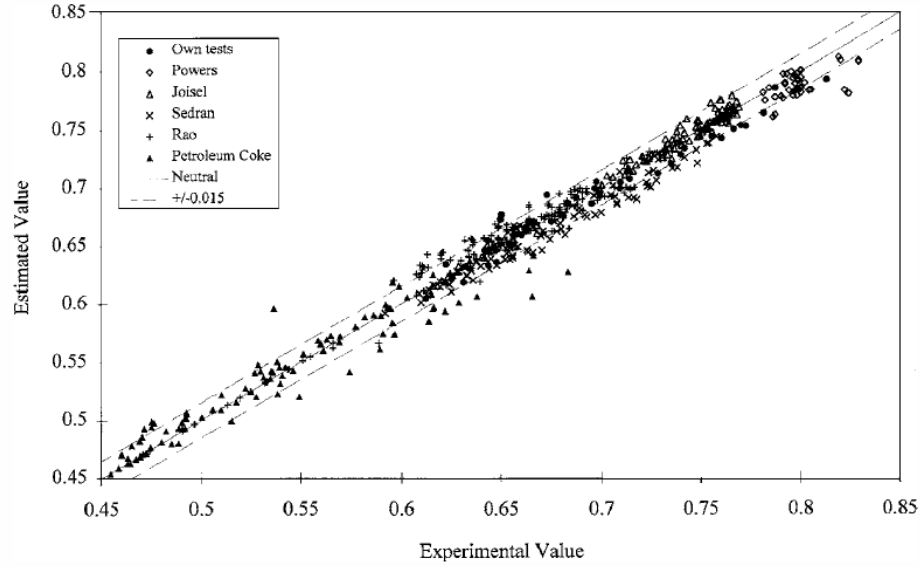


**Figure 2.2. Correlation between predicted and experimental packing degrees (Goltermann, 1997)**

### 2.2.4 The Linear Packing Density Model (LPDM)

Stovall (1986) suggested a model for the packing density of multisized grains in, where the packing density is a function of the fractional solid volume of each grain size in the mixture. The input required to use this model includes the diameter of each grain component ( $d_i$ ), the individual packing density ( $\varphi_i$ ), and individual fractional solid volume ( $\eta_i$ ). The assumption made is that grain sizes are continually distributed. The packing density of multisized grains can be calculated as the infimum, which is the lowest number in a set of numbers:

$$\Phi = \inf_{d \leq t \leq D} \left[ \frac{\varphi(t)}{1 - [1 - \varphi(t)] * \int_d^t dx * \eta(x) * g(x,t) - \int_t^D dx * \eta(x) * f(x,t)} \right] \quad (2.6)$$

Where,  $\varphi(t)$  is the packing density of the grains group with diameter  $t$  ( $d \leq t \leq D$ ), “f” and “g” are the functions of local packing disturbance due to the introduction of smaller or larger particles respectively and can be calculated as:

$$f = \left(1 - \frac{d_i}{d_j}\right)^{3.1} + 3.1 * \left(\frac{d_i}{d_j}\right) * \left(1 - \frac{d_i}{d_j}\right)^{2.9} \quad (2.7)$$

$$g = \left(1 - \frac{d_i}{d_j}\right)^{1.6} \quad (2.8)$$

According to Mangulkar et al. (2013), LPDM is a good tool in predicting optimum proportions. However, based on the experimental study of different models by Jones et al. (2001), LPDM underestimated the void ratio of the binary blend of fine and coarse particles.

### 2.2.5 The Compressible Packing Model (CPM)

This model presented by De Larrard (1999) bases on the fact that the process of compaction impacts the packing density. This mathematical model is developed to predict the performance of

concrete properties in the fresh and hardened stage, packing density of aggregates and cementitious materials (Quiroga 2004). The method allows using any number of fractions of aggregate/cementitious materials. The input required includes the mean diameter and packing density of each fraction. It was also stated that packing density is affected by the compaction method. There are several methods of compacting aggregates, such as loose placement, rodding, vibrating with or without external pressure, and wet packing. Table 2.1 presents packing processes with corresponding compaction indices. The higher the compaction index, the higher the packing degree (Figure 2.3). It can be seen that with the increase of compaction index packing degree grows exponentially. Besides, no matter what compaction method is applied, an ideal packing degree (1.0) cannot be reached. For coarse and fine aggregates De Larrard suggested using vibration plus 1.45 psi (10 kPa) pressure, whereas for microfine water demand test is suggested.

**Table 2.1. Compaction Index with different packing processes**

(According to de Larrard 1999)

<b>Packing process</b>	<b>K</b>
Loose	4.1
Sticking with a rod	4.5
Vibrated	4.75
Vibrated + pressure	9
Wet packing	6.5

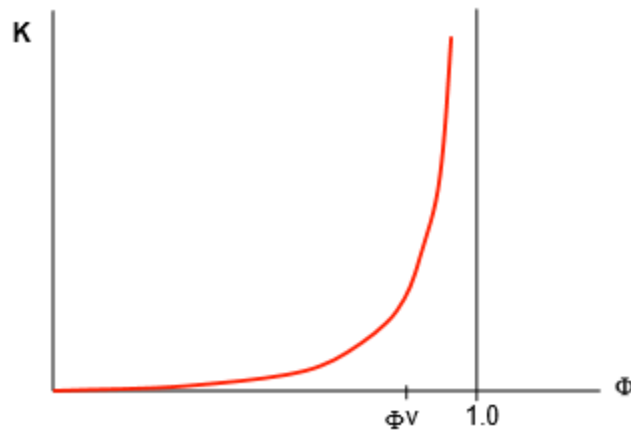


**Figure 2.3. Compaction index versus packing degree (De Larrard, 1999)**

Jones et al. (2001) analyzed the CPM for its suitability in proportioning mixtures. In the scenario of binary blends with fine and coarse fractions, the CPM overestimated the void ratio. In terms of prediction of fresh concrete performance, the CPM model was calibrated using data of mixtures with slump more than 4 in, which implies that for stiff mixes (slump lower than 4 in.) there is a high probability that CPM predictions will be inaccurate.



### 2.2.6 Modified Andreasen and Andersen Model

This model is based on a continuous approach rather than a discrete approach that all models mentioned above. The model that was modified by Funk and Dinger (Mangulkar, 2013) can be represented by the following equation:

$$P_t = \frac{d^q - d_{min}^q}{d_{max}^q - d_{min}^q} \quad (2.9)$$

Where  $P_t$  is the fraction of total solids being smaller than  $d$ ,  $d_{max}$  indicates the maximum sieve size (100% passing),  $d_{min}$  is the minimum size of the particle, and  $q$  is the distribution modulus. Since fine particles are not able to pack similarly as coarse particles (same in shape), Andreasen, and Andersen limited distribution modulus to a range 0.33-0.50 (Wang et al. 2014). The main limitation of this model is that it bases only on particle size distribution, and does not account for aggregate shape and texture.

## 2.3 Empirical gradation optimization methods

While some particle packing methods are based on theory and scientific explanations, other methods are based on the strategy of proportioning particles by trial and error. These empirical methods provide a criterion of “ideal” packing and suggest to proportion particles attempting to meet the given criteria.

### 2.3.1 0.45 Power Chart

0.45 Power Chart was developed by the concrete industry in 1907, which is a graph of percent passing versus sieve size raised to power 0.45. According to this method, the optimum grading is defined by a straight line from the origin to the nominal maximum size of aggregate (Figure 2.4). However, according to the study results of Taylor et al. (2015), aggregate combinations obtained from the 0.45 Power Chart did not always provide the lowest void content. Ley et al. (2012) also found in their research that the 0.45 Power Chart is not the best way to obtain the aggregate combination for a slip formed concrete pavement mixture. However, according to Cook et al. (2016), this method can be useful in predicting water reducer (WR) dosage that was required to pass box test: the closer a combined aggregate curve to the optimum one, the less amount of WR is required. Ramakrishnan (2004) stated that the mixes obtained using the 0.45 Power Chart resulted in higher strength and better workability compared to such methods as Shilstone Chart, and 8-18 Curve.

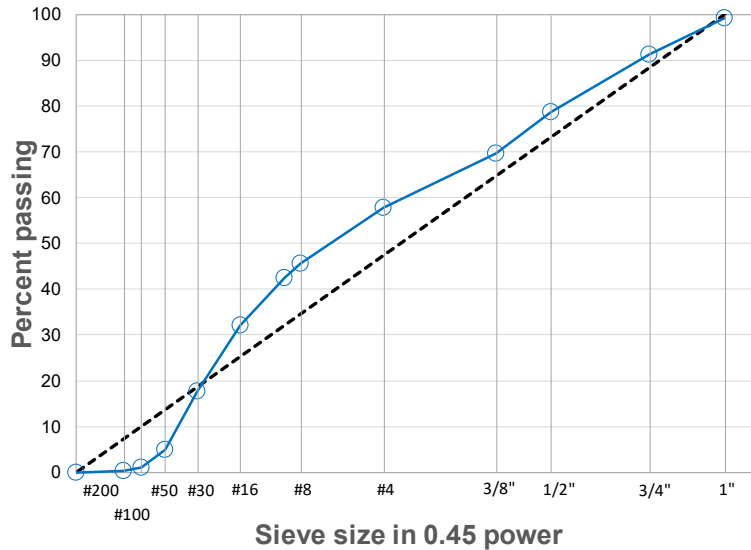


**Figure 2.4. 0.45 Power Chart of the current NDOT combined aggregate gradation**

### 2.3.2 8-18 curve

The 8-18 Curve is a tool based on an individual percent retained (IPR) to provide uniform blend by limiting the amount of each sieve size particles. It focuses on graphically evaluating excess and deficiency of particles of particular sieve size. Traditionally “8-18” boundaries (Figure 2.5) are suggested for each sieve size from 1/2 in. to #30. According to Cook et al. (2016), it is a useful tool in predicting required WR dosage to achieve appropriate workability. However, Quiroga et al. (2004) stated that “8-18” boundaries do not guarantee good workability, and sometimes low packing cannot be achieved due to lack or excess of either small or large particles, which is why this method should not be used when dealing with aggregates with a high amount of microfines.

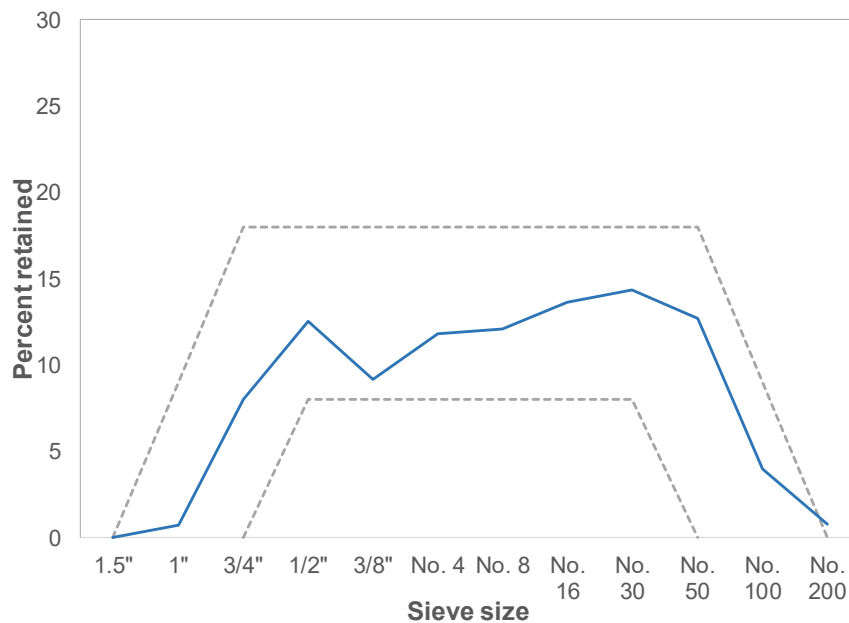


**Figure 2.5. The current NDOT combined aggregate gradation on the IPR chart with ‘8-18’ limits**

### 2.3.3 Tarantula Curve

Tarantula Curve is an empirical method to proportion aggregate content developed by Ley (2012) after comparing the workability of the mixtures with different gradations using the Box test. Consequently, boundary limits on an individual percent retained chart were modified (Figure 2.6). There are also recommendations for the amount of coarse sand to provide appropriate cohesion (total volume retained on #8 to #30 sieves must be at least 15%), and for the amount of fine sand to provide adequate workability (total volume retained on #30 to #200 must be within 24% and 34%). Historical data from the Minnesota Department of Transportation shows that with time aggregate combinations were developed by trial and error to fall into Tarantula limits without knowing of Tarantula curve (Ley, 2013). According to Taylor (2015), similar results were reported in Iowa, North Dakota, and South Africa. Moreover, in Texas slip formed pavement sections with the mixture obtained with this method showed a good response to vibration and resulted in low cementitious materials content (4.75 sacks). This method cannot be used for roller-compacted concrete, self-consolidating concrete, and pervious concrete since the scope of the work focused on slip formed pavement concrete and traditional flowable concrete applications. However, the main issue of this approach is that although it can define if a blend is good or bad (within Tarantula limits or not), it is not able to compare good blends, i.e. if several blends are within the provided limits, it is hard to tell which one is exactly the optimum one.

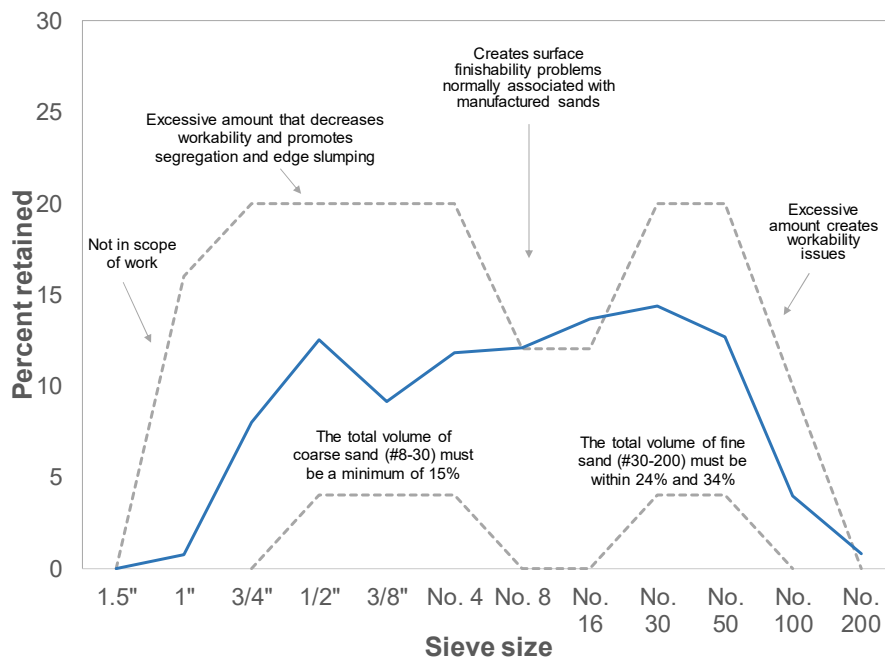


Figure 2.6. The current NDOT combined aggregate gradation Tarantula Curve

### 2.3.4 Coarseness Factor Chart

Coarseness Factor Chart, also called as Shilstone Chart, is a graphical method to analyze combined aggregate particle distribution. The chart is made up of a coarseness factor (CF) as a horizontal axis and a workability factor (WF) as a vertical axis. CF and WF can be calculated using equations (2.10) and (2.11). The chart is divided into five different zones (Figure 2.7). Zone I stands for the gap-graded mixtures. Due to the deficiency of intermediate aggregates, there is a high risk of segregation during consolidation. Zone II indicates a well-graded mixture with maximum aggregate size from 1.5 in. to 3/4 in. Zone III is a continuation of Zone II but with the

maximum aggregate size equal or smaller than ½ in. Zone IV represents mixtures with an excess of fine particles, which can lead to segregation and high permeability. Mixtures falling to Zone V have an excess of coarse particles.

$$WF = W + \left( 2.5 * \frac{C-564}{94} \right) \quad (2.10)$$

Where, W is the cumulative percent passing No.8 sieve, and C is the cementitious materials content (lb/yd<sup>3</sup>).

$$CF = \left( \frac{Q}{R} \right) * 100 \quad (2.11)$$

Where, Q is the cumulative percent retained on the 3/8 sieve, and R is the cumulative percent retained on the No.8 sieve.

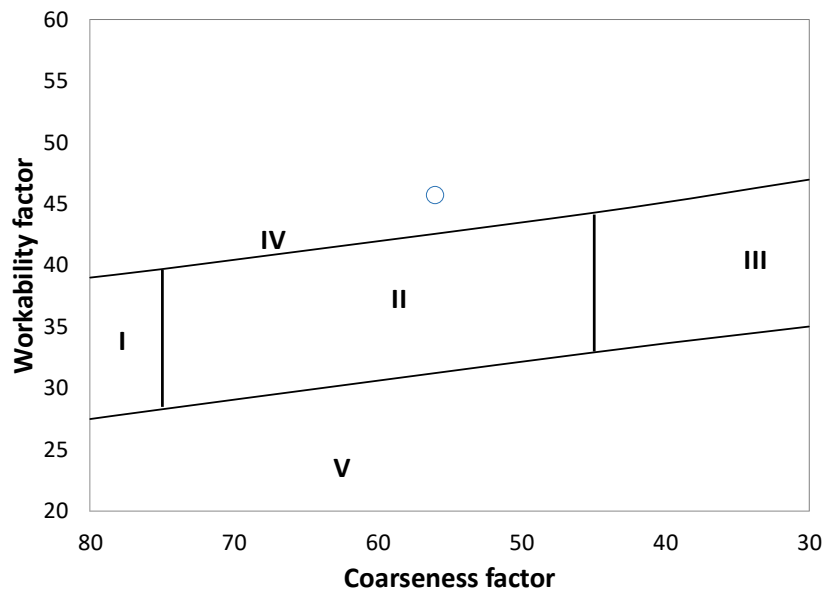


**Figure 2.7. The current NDOT combined aggregate gradation on the Coarseness Factor Chart**

According to Ley et al. (2012), the location on a Coarseness Factor Chart does not necessarily have a significant relationship to the response of a concrete mixture to vibration. However, it was found that mixes falling into Zone II were able to hold an edge. Cook et al. (2016) concluded that the Coarseness factor is not a useful tool to predict the water reducer dosage required for adequate workability of pavement concrete. A single location on the chart did not result in similar WR demand; and oppositely, some mixtures were located at different regions but resulted in almost the same WR dosage to pass the box test. According to Obla (2007), optimizing aggregate gradation using Shilstone Chart does not result in lower void content within the aggregate matrix.

## **2.4 Factors impacting aggregate packing and workability of pavement concrete**

### **2.4.1 Maximum size of aggregate**

A larger maximum size of aggregate is reported to positively impact concrete workability due to less specific surface area of aggregate (Quiroga et al., 2004). In his investigation of optimized graded concrete, Cook et al. (2013) examined the influence of the maximum size of

aggregate by analyzing mixtures with three different maximum sizes with the same sand content and no particles of one sieve size exceeding 20%. Larger aggregate size resulted in lower WR dosage to pass box test, but the difference is too insignificant to state that increasing maximum size can lead to better workability. It was also mentioned that using larger aggregate size could be beneficial in producing aggregate gradation with no excessive content of material on a single sieve size because there will be more sizes to distribute aggregate. Ley (2012) attempted to correlate results from the slump test and box test. It was found that due to the stronger aggregate interlocking, mixes with coarse aggregate with a maximum size of 1.5 in. required higher slump to pass the box test compared to  $\frac{3}{4}$  in. coarse aggregate.

#### **2.4.2 Gradation**

It is useful to analyze the combined aggregate grading, as they present in a concrete mixture. Sometimes, there is a deficiency of mid-sized aggregate (around 3/8 in), which leads to concrete with high shrinkage properties, poor workability, and high water demand (Kosmatka et al. 2008). Kosmatka et al. (2008) referred to Abrams (1918) and Shilstone (1990) who mentioned benefits of combined aggregate analysis: by keeping cement content constant, the optimum aggregate combination can be found that will lead to the most effective water to cement ratio and higher strength. Besides, mixtures with optimum gradation respond best to a high-frequency vibrator.

#### **2.4.3 Aggregate shape and texture**

The aggregate shape is a very important characteristic that has an impact on paste demand, workability, and strength. According to Kosmatka et al. (2008), aggregate shape and texture have more impact on fresh concrete rather than hardened concrete. The shape is mainly associated with sphericity, flatness, angularity, and roundness (Quiroga et al. 2004). The aggregate texture is mainly related to the roughness of a particle. Rached et al. (2009) found that mixtures with the poor shape of aggregates required more cement paste. Cook et al. (2016) concluded that angularity and the number of flat particles play a big role in workability of pavement concrete. Based on Quiroga (2004), a high amount of flat coarse aggregates can lead to finishability issues. Aggregate shape and texture significantly influence particle packing. Kwan (2002) in his research compared the correlation between different aggregate shape characteristics (flakiness ratio, elongation ratio, sphericity, shape factor, convexity ratio, and fullness ratio) and particle packing. Results indicated that the two factors most affecting the particle packing are shape and convexity factors. They had a correlation coefficient of 0.859 and 0.828 respectively when considered as an alone factor; when they are considered together, the correlation coefficient was 0.893. Obla (2011) and Quiroga et al. (2004) stated that concrete workability is affected by the shape and texture of fine aggregate more than the coarse aggregate.

#### **2.4.4 Micro fines content**

Aggregate particles finer than 75 microns (#200 sieve), usually referred to as silt or clay, can present in sand and gravel deposits (Lamond et al., 2006). It can also present as dust from crushing and mechanical processing. Typically, the higher the amount of microfines leads to increased water demand and reduced air content (Obla, 2011).

### **2.5 Mixture design development**

There are several mixture design procedures reported for pavement concrete developed by research groups from the University of Texas-Austin and the National Concrete Pavement Technology Center. Siddiqui et al. (2014) proposed a mix design method for pavement concrete,

where the optimum aggregate blend is selected based on the 0.45 power chart. Once the optimum blend is obtained, a combined aggregate void content test is used to determine how much of paste is to be added. This design procedure suggests designing concrete, so the paste volume equals the void content of combined aggregate blend, and start adjusting it after trial batches. However, it is well known that excess paste is required to provide adequate workability. Therefore, the design procedure seems to have unnecessary steps of trial mixes without an excess paste. Also, as was mentioned before, the 0.45 power chart does not always provide the optimum blend because it does not take into consideration aggregate shape and texture. The mix design procedure proposed by Tylor et al. (2015) is based on a similar technique as described in Siddiqui et al. (2014). In addition to the 0.45 power chart, the Tarantula curve is used to optimize aggregate gradation. Once the void content of the combined aggregate is obtained experimentally, the volume of paste over the volume of voids ratio ( $V_{\text{paste}}/V_{\text{voids}}$ ) was the main driving criteria. The recommended initial  $V_{\text{paste}}/V_{\text{voids}}$  is 1.25-1.75. Besides the slump test, VKelly test was used to evaluate the behavior of fresh concrete under vibration.

## 2.6 Quality control tests

ASTM C29 (Standard Test Method for Bulk Density (Unit Weight) and Voids in Aggregate) is a test used to determine the bulk density and void content of aggregate in compacted or loose conditions. Standard compaction methods included in the standard test are rodding, jiggging, and shoveling. However, the test is limited to one aggregate only. According to Kosmatka (2008), it is important to analyze the combined aggregate gradation, as the way they present in a concrete mixture. Therefore, the test was modified to determine the void content of the combined aggregate matrix. The combined void content test is a tailored adoption of the test procedure as described in ASTM C29 that was developed to measure the particle packing density and void content with the incorporation of multiple aggregates at different proportions (Obla, 2007). Moreover, it is believed that introducing vibration plus pressure compaction method is appropriate. This method results in a higher compaction factor, and it is more representative for pavement application as pavement concrete is generally vibrated during placing

It is important to justify the optimum blends based on fresh concrete performance. Both works discussed in the previous subchapter lacked a more appropriate analysis of fresh concrete properties to justify pavement concrete performance. For slip-forming paving, it is necessary for the concrete to be consolidated under vibration, but also to be able to hold an edge after vibration is stopped and formwork is removed. The slump test is not sufficiently sensitive to evaluate low workability mixtures for slip-forming applications. Therefore, it is necessary to conduct additional tests to better understand the fresh properties of pavement mixtures. Box test was developed to examine the response of fresh concrete under vibration, which can be assessed by the number of surface voids observed on the sides and appearance of edge slump (Cook et al., 2014).

As the Box test is largely subjective in the surface evaluation, another test, i.e., VKelly test, which is a quantitative test, can be used. VKelly Test is the modified test from the standard test method for ball penetration in freshly mixed hydraulic cement concrete (ASTM C360) and was developed by Taylor et al. (2012). The main purpose of the test is to observe the dynamic behavior of pavement concrete under vibrations, by evaluating the penetration depth of a vibrating ball against time.

## 2.7 NDOT historical data

Figures 2.8-2.11 illustrate some documented blends used in pavement mixes in Nebraska that were obtained from Heyen et al. (2013) and Nebraska Department of Transportation (NDOT) internal reports. Figure 2.8 shows that most of Nebraska blends fall within the specified limits of 47BR concrete provided by Heyen et al. However, from Figures 2.9 and 2.10, it can be noticed that the blends used in Nebraska have a significant excess in No. 8 and No. 16 sieve sizes, and a lack of 3/4 in. and 3/8 in. size particles. Figure 2.11 also demonstrates that the majority of the blends with standard cement content used are out of recommended zones. While it is fair to state that gradations used in Nebraska pavement concrete are far from the optimum packing, it is difficult to determine which gradation will work better due to the unique type and gradation of aggregate being used.

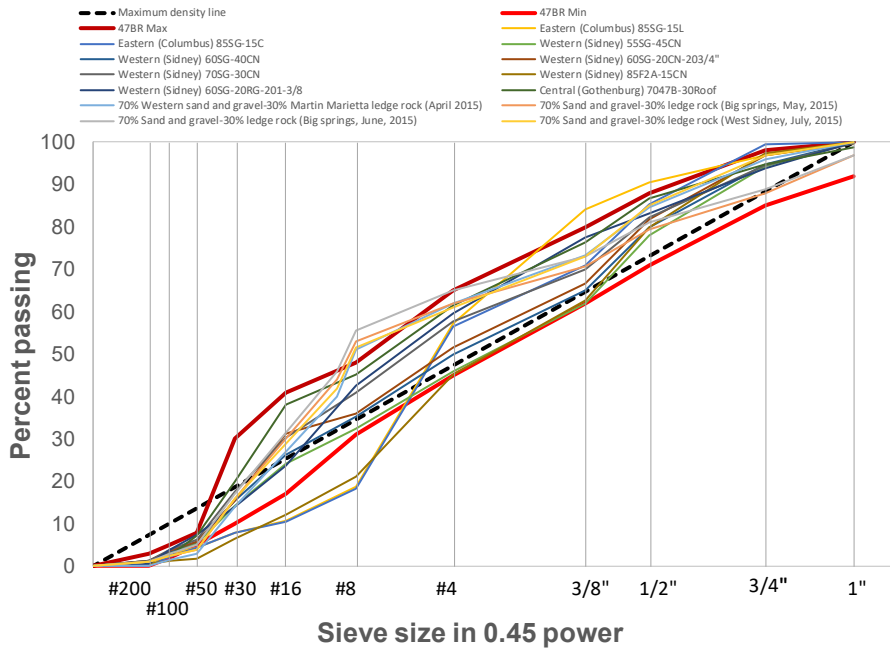
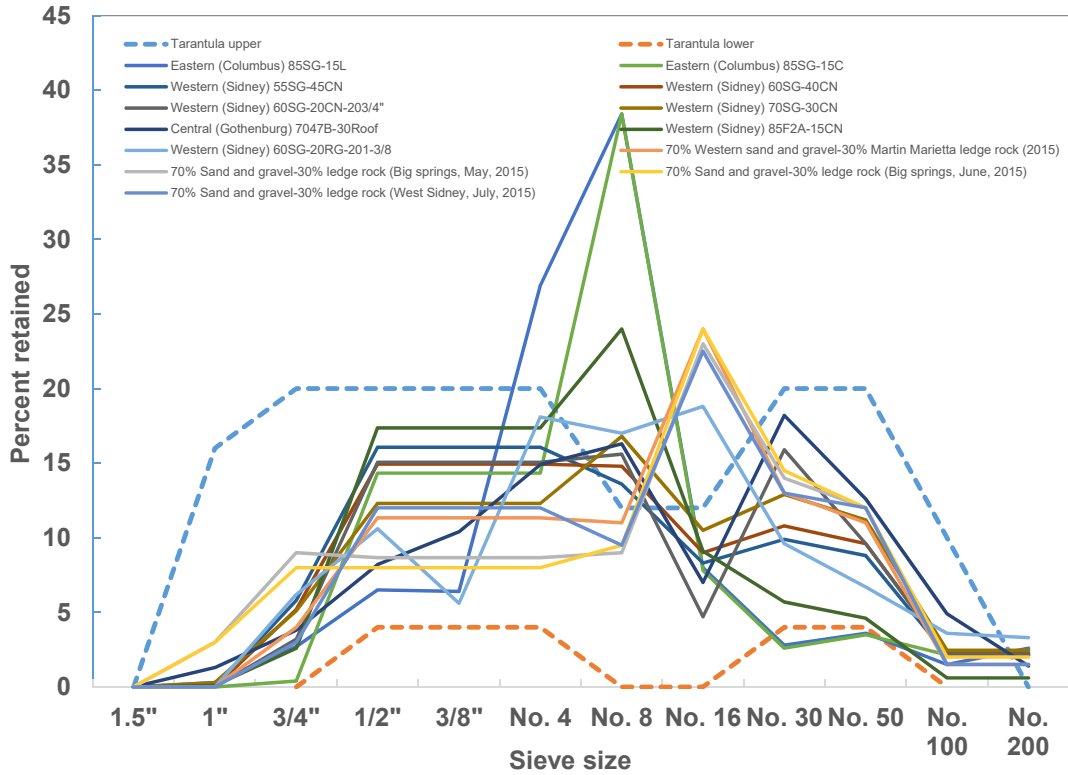
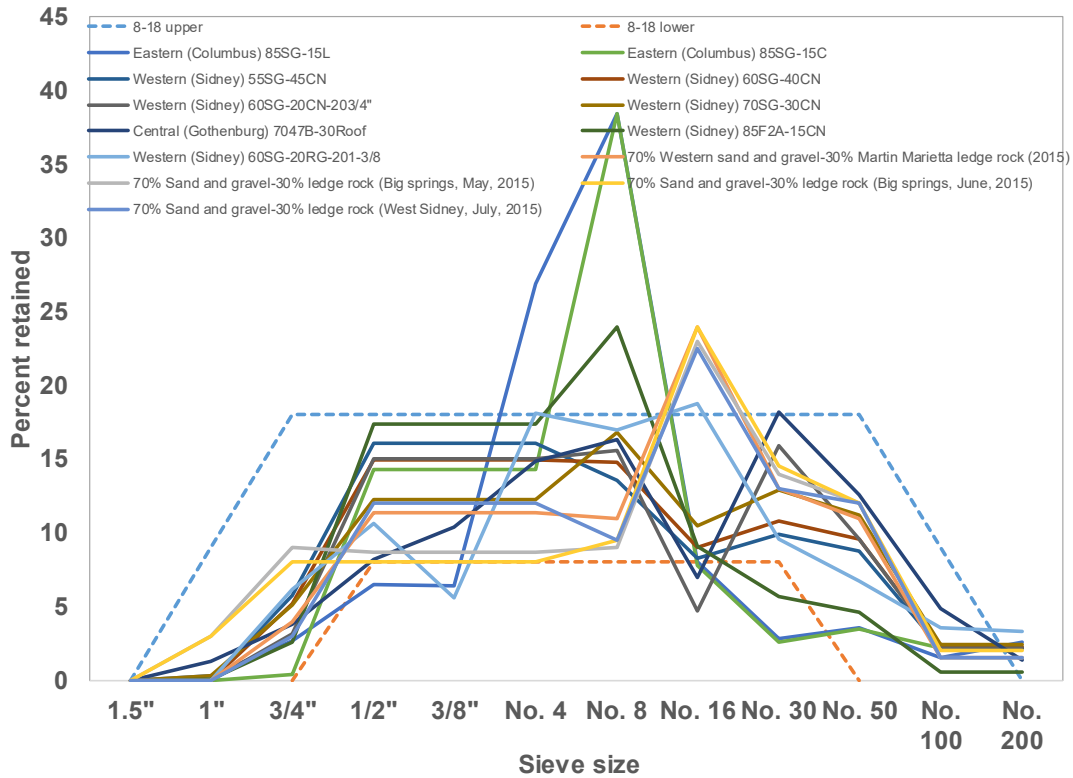


Figure 2.8 Nebraska gradation on 0.45 Power Chart



**Figure 2.9. Nebraska gradations on Tarantula Curve**



**Figure 2.10. Nebraska gradations on 8-18 Curve**



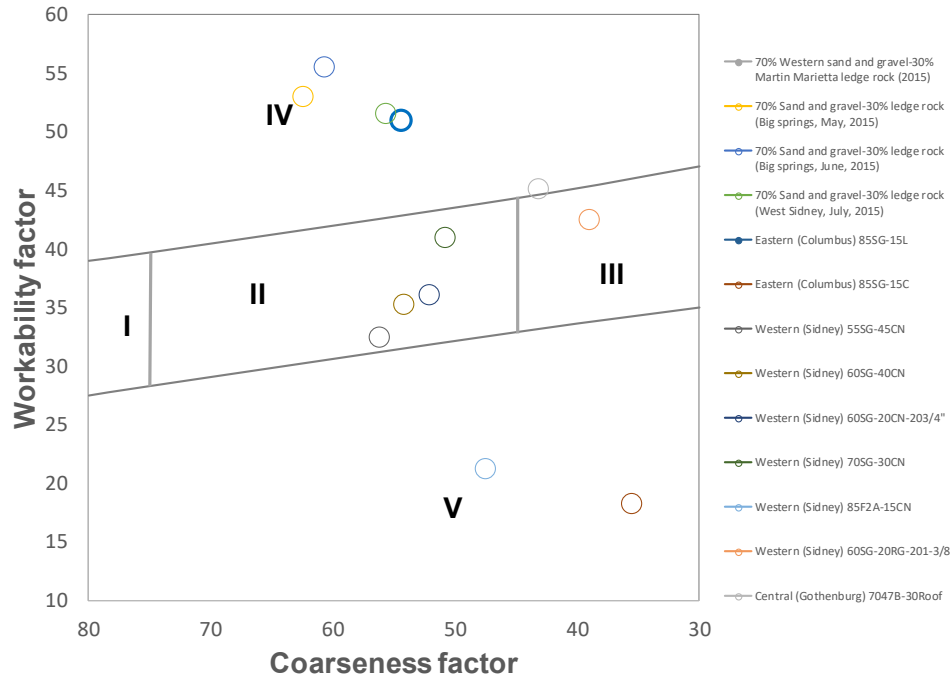


**Figure 2.11. Nebraska gradations on Shilstone Chart**

## 2.8 Summary

Based on the literature review conducted, it was determined to proceed with a discrete theoretical model. The first advantage of this model is that the approach includes the consideration of aggregate shape and texture, although they are accounted for indirectly. Another advantage of discrete theoretical models is that they can quantitatively predict the packing degree, whereas the empirical models are only capable of comparing aggregate blends. Among presented models, the Modified Toufar Model was selected for binary blends due to its accurate correlation with experimental results based on historical data provided by Goltermann et al. (1997), and relative simplicity compared to such complex models as the LPDM or the CPM due to less amount of input parameters. For ternary blends, Modified Andersen & Andreassen Model was selected.

Various factors impacting aggregate packing and pavement concrete workability were discussed. It was found that the aggregate gradation, shape, and texture are the driving criteria in aggregate packing. It is believed that the shape and texture of fine aggregate play a more important role compared to coarse aggregate. Besides these two parameters, the maximum size of aggregate and microfine content are critical in fresh concrete performance.

Different mixture design procedures developed by other researchers were reviewed. It was found that even though the philosophy is reasonable, there is a lack of fresh pavement concrete performance analysis. In addition, methods used to optimize aggregate gradation in these studies do not account for aggregate shape and texture.

In terms of quality control tests, it was decided to proceed with the combined void content test with an additional compacting method, which is vibration plus pressure. The performance of fresh pavement concrete can be justified with the help of special tests such as Box Test, which will be used in this study.

Finally, gradations of different aggregate blends that are being used in Nebraska were obtained from the previous research project reports and NDOT internal reports. Since only gradation information was available, it was only practical to analyze blends based on empirical methods. Shilstone chart, 8-18 curve, and Tarantula curve have shown that the currently used aggregate blends are far from optimum.

## CHAPTER 3. MATERIALS AND TEST METHODS

### 3.1 Introduction

It was critical to select representative materials for Nebraska for efficient research. This chapter presents the materials, i.e. cementitious materials, aggregates, and chemical admixtures selected for this study including necessary properties and justification. The main materials used in this study were IP cement with 25% blended class F fly ash as the main cementitious material; limestone, granite, and two types of sand and gravel as representative aggregates; air-entraining agent and mid-range water reducer as chemical admixtures.

Test methods with corresponding standards to evaluate concrete behavior in fresh state, hardened state, and in the long-term are also presented. Besides standard tests including slump and setting time, fresh concrete behavior was characterized by special pavement workability tests such as Box and VKelly tests, which are also presented in this chapter. To examine hardened concrete properties, compressive strength, flexural strength, and modulus of elasticity tests were used. Moreover, procedures of such test as freeze/thaw resistance, surface and bulk resistivity, free shrinkage, and restrained shrinkage, which were used to observe long-term durability behavior, are presented.

### 3.2 Materials

#### 3.2.1 Cement and cementitious materials

NDOT Standard Specifications for Highway Construction (2017) requires the use of IP interground/blended cement for pavement application. IP cement was designed to mitigate Alkali-Silica Reaction (ASR), provide sulfate resistance and reduced chloride permeability. For this study, type IP Portland-pozzolan cement with 25% blended class F fly ash content that meets ASTM C595 (Standard Specification for Blended Hydraulic Cements) was used as the cementitious material. The chemical composition and physical properties of cement used in the study are reported in Table 3.1.

**Table 3.1. Chemical composition and physical properties of IP cement**

Chemical Properties	Pozzolan content, %	25
	MgO, %	2.45
	SO <sub>3</sub> , %	3.10
	Loss in Ignition, %	1.00
Physical Properties	Blaine Fineness, cm <sup>2</sup> /g	4400
	Specific Gravity	2.95

#### 3.2.2 Aggregates

In order to evaluate the effectiveness of the aggregate gradation optimization, aggregate from different locations were collected and used in the present study. From East NE combined sand and gravel (SG) and 1 in. nominal maximum size aggregate of limestone (LS) were used, which are the most commonly used aggregates for pavement concrete in East NE. Besides, ½ in. limestone was used as an intermediate aggregate (IA). In order to select aggregates from West and Central NE, gradations from different aggregate sources were collected and analyzed. Figure 3.1 represents the gradations of representative West and Central NE aggregates. It was noticed that

aggregates from Central NE identified in this study are very similar to the aggregates from East NE. Therefore, it was decided to only incorporate East NE and West NE aggregates in this study. In West NE usage of sand and gravel, limestone, and granite is predominant. In general, sand and gravel in West NE is coarser, however, limestone and granite aggregates are finer than East NE limestone.

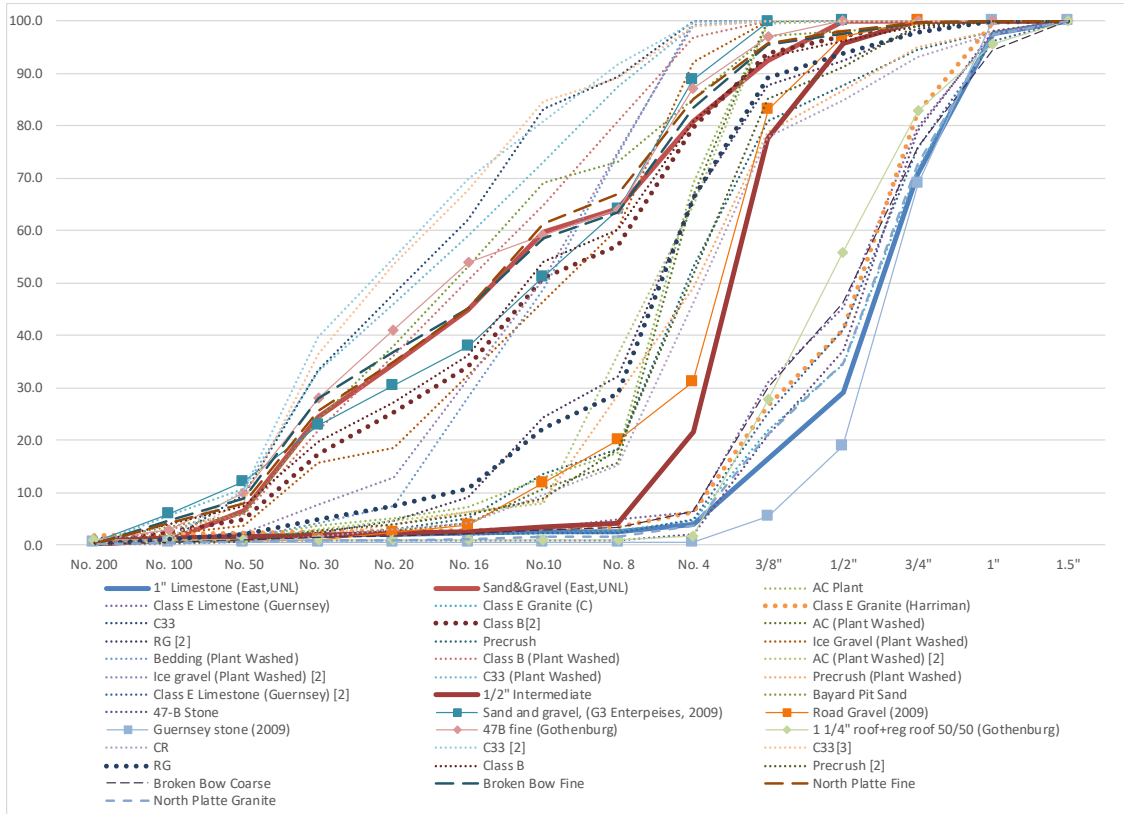


**Figure 3.1. Nebraska aggregates gradations**

Since the purpose was to evaluate the impact of aggregate gradation on concrete performance and justify the approach, it was decided to intentionally pick representative aggregate from West NE that significantly differ from East NE aggregates; combined sand and gravel (SG\_W) with the highest fineness modulus, and 1 in. nominal maximum size granite (GR) with the lowest fineness modulus were selected from West NE. Selected aggregates can be seen in Figure 3.2.



**a) 1" Limestone**

**b) Sand and gravel (East NE)**

**c) Intermediate aggregate**



**d) 1" Granite**

**e) Sand and gravel (West NE)**

**Figure 3.2. Selected aggregates**

Figure 3.3 presents the particle size distribution of aggregates based on sieving analysis performed according to ASTM C136 (Standard Test Method for Sieve Analysis of Fine and Coarse Aggregates).

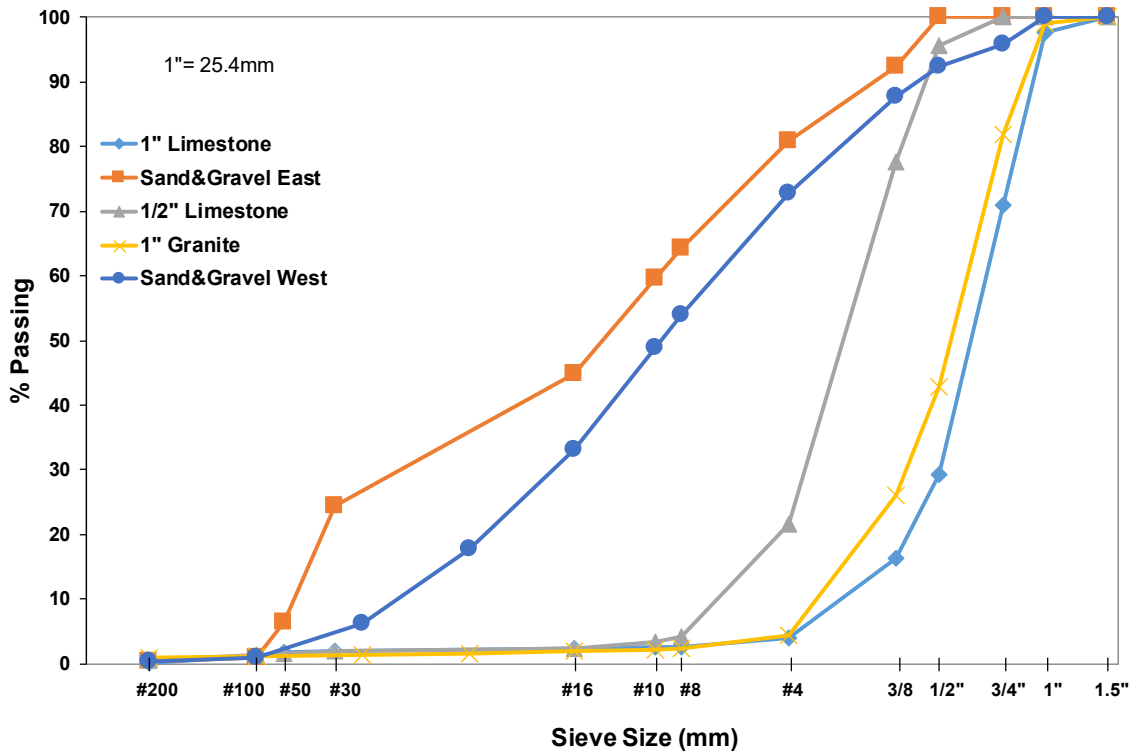


**Figure 3.3. Gradation curve of aggregates used in this curve**

Specific gravity at saturated surface dried (SSD) condition, and absorption of coarse and fine aggregates were obtained in accordance with ASTM C127 (Standard Test Method for Relative Density (Specific Gravity) and Absorption of Coarse Aggregate) and ASTM C128 (Standard Test Method for Relative Density (Specific Gravity) and Absorption of Fine Aggregate) respectively. The obtained values along with the fineness modulus (FM) are presented in Table 3.2.

**Table 3.2. Aggregates properties**

Properties	SG	LS	IA	SG W	GR
Specific gravity	2.586	2.671	2.605	2.567	2.652
Absorption (%)	0.96	0.91	1.35	1.35	0.70
Fineness modulus	3.86	6.99	5.90	4.32	6.79

### 3.2.3 Chemical admixtures

A MasterAir AE200 for East NE mixes/ AE290 for West NE and performance evaluation mixes admixtures that meets ASTM C260 (Standard Specification for Air-Entraining Admixtures for Concrete) and Eucon X-15 that meets ASTM C494 (Standard Specification for Chemical Admixtures for Concrete) were used as an air-entraining agent (AEA) and mid-range water reducer (WR) respectively.

### 3.3 Combined aggregate void content test

To obtain the amount of excess paste in each specific mix, a combined void content test was conducted. The test is a tailored adoption of the test procedure as described in ASTM C29 that was developed to measure the particle packing density and void content with the incorporation of multiple aggregates at different proportions (Obla, 2007). Figure 3.4 is an example of the mixed aggregates (3.4a) and representative aggregate combinations demonstrating different packing degrees (3.4b). To ensure proper mixing, aggregates were mixed in a 1.7 ft<sup>3</sup> (0.0481 m<sup>3</sup>) capacity drum mixer for one minute followed by hand mixing for another minute. In addition to the three standard compaction methods, i.e., shoveling, rodding, and jiggling procedures, a vibration plus pressure method as suggested by De Larrard (1999) were used for the void content measurement. The fourth method results in a higher compaction factor, and it is more representative for pavement application as pavement concrete is generally vibrated during placing. In this method, a steel container of a volume of 0.25 ft<sup>3</sup> (0.0071 m<sup>3</sup>) filled with aggregates was placed on a vibration table with a 1.45 psi (10 kPa) applied external pressure on top and was vibrated at a medium amplitude for one minute (see Figure 3.5). The specific gravity of the blended fiber-aggregate mixture was calculated as:

$$G_{sb,combined} = \frac{1}{\frac{P_{LS}}{G_{sb,LS}} + \frac{P_{SG}}{G_{sb,SG}}} \quad (3.1)$$

Where  $G_{sb}$  and  $P$  represent the specific gravity and fraction of each component.

Bulk density of the combined mixture can be calculated as:

$$Bulk\ Density = \frac{Mass}{Volume} \quad (3.2)$$

Where Mass is the total mass of material in the measure, and Volume is the volume of the measure.

The void content (%Void) of the mixture was calculated as:

$$\%Void = \frac{G_{sb,combined} \times UW_{water} - Bulk\ Density}{G_{sb,combined} \times UW_{water}} \quad (3.3)$$

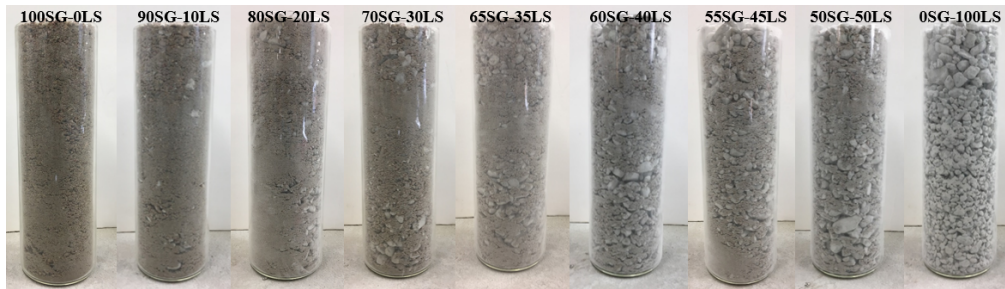
Where  $UW_{water}$  is the unit weight of water.

Void contents of each aggregate combination were measured three times, and the average value was reported.





a) Test setup



b) Visual examination of aggregate packing with different combinations

Figure 3.4. Combined void content test

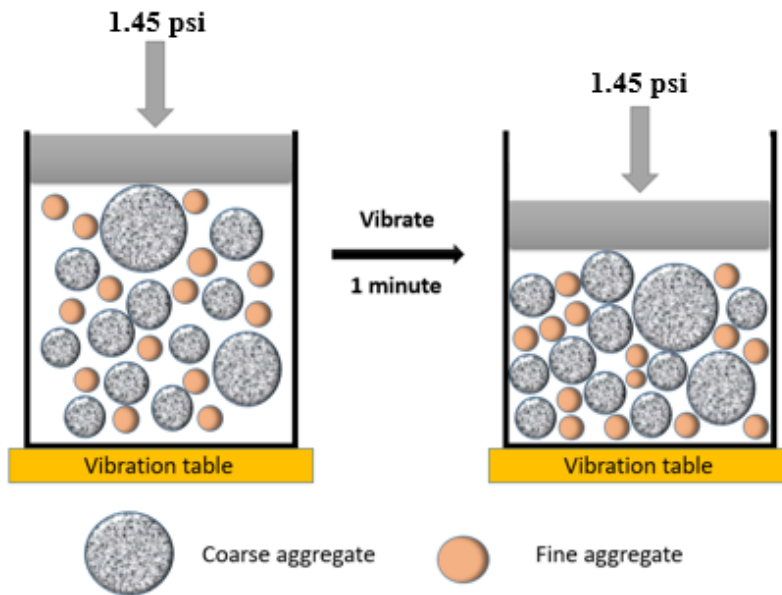


Figure 3.5. Vibration plus pressure method sketch

### 3.4 Concrete mixing

A drum mixer with 3 ft<sup>3</sup> (0.0849 m<sup>3</sup>) capacity was used to mix concrete following the procedure described in ASTM C192 (Standard Practice for Making and Curing Test Specimens in the Laboratory). First, the coarse aggregate was mixed with approximately half of the mixing water containing AEA for 30 seconds. Then, sand and gravel, cement, and the remaining water were



added and mixed for 3 minutes followed by 3 minutes resting and additional 2 minutes mixing. If it was necessary to adjust workability, WR was added and concrete was mixed for additional 3 minutes. In the performance evaluation phase, when WR dosage was already known for a particular mixture, it was added with the second half of the water. Prior to mixing, aggregates were brought to saturated condition and the water amount was adjusted accordingly prior to batching of each mix, which was 1.3 ft<sup>3</sup> (0.0368 m<sup>3</sup>) in size.

### **3.5 Fresh concrete tests**

#### **3.5.1 Slump test**

A concrete slump was measured according to ASTM C143 (Standard Test Method for Slump of Hydraulic-Cement Concrete) to measure the consistency of concrete (Figure 3.6). The test was performed immediately after the concrete mixing was completed.



**Figure 3.6. Slump test setup**

#### **3.5.2 Air content test**

Air content of the mixtures was measured according to ASTM C231 (Standard Test Method for Air Content of Freshly Mixed Concrete by the Pressure Method) using type B meter (Figure 3.7).



**Figure 3.7. Air pressure meter**

### **3.5.3 Setting time test**

Concrete time of setting was tested in accordance with ASTM C403 (Standard Test Method for Time of Setting of Concrete Mixtures by Penetration Resistance). Once mixing is completed, coarse aggregates were sieved out from the concrete, and mortar was tested for setting time (Figure 3.8).



**Figure 3.8. Setting time test setup**

### 3.5.4 Box test

For Box test, fresh concrete was loosely placed into a temporarily fixed wooden box with open top and bottom and a dimension of 1ft× 1ft× 1ft (0.3m× 0.3m× 0.3m) (Figure 3.9). A portable electrical vibrator was then used to consolidate the concrete for 6 seconds. A vibrator was inserted vertically at the center of the specimen to full depth for 3 seconds, and the raised for 3 seconds. The wooden box was then removed sideways and the surface was visually examined for surface voids and straight edge is used to exam edge slumping. While a visual examination of the surface void content is commonly used, in order to have a more objective measurement, a commercial image process software name ImageJ was used to obtain the exact value of surface voids using photos of the four sides taken after the removal of sides. As shown in Figure 3.10a, the original method determined the visual ranking largely based on eyeballing the number of surface voids. Even with the recent attempt to improve the accuracy with a procedure to place a piece of transparency paper with dots on the concrete surface to count the voids, the measurement is still relatively subjective. The new methods using the image software to calculate the percentage of voids in all the four sides, which largely eliminate the human factor. Figure 3.10 illustrates the difference in surface void evaluations based on the original method and the one used image software in the current study. The example as illustrated in Figure 3.10b demonstrated that the image software can clearly identify surface voids. Note that the new method resulted in a lower amount of voids identified compared to the original method. According to the comparison of voids based on the original visual measurement and the image software from box tests with over thirty difference mixes, a revised ranking system based on the software calculated surface voids was determined. The new ranking range using the image analysis method was designed as follows: 0-3% classified as ranking 1, 3-5% as 2, 5-15% as 3, and over 15% as 4.



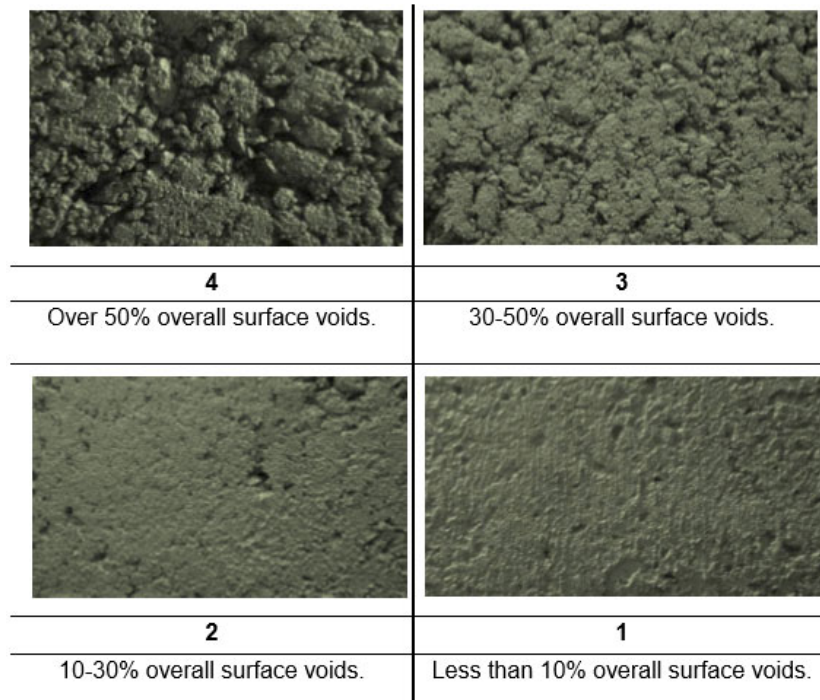
a) Box Test setup

b) Vibrating concrete during Box Test

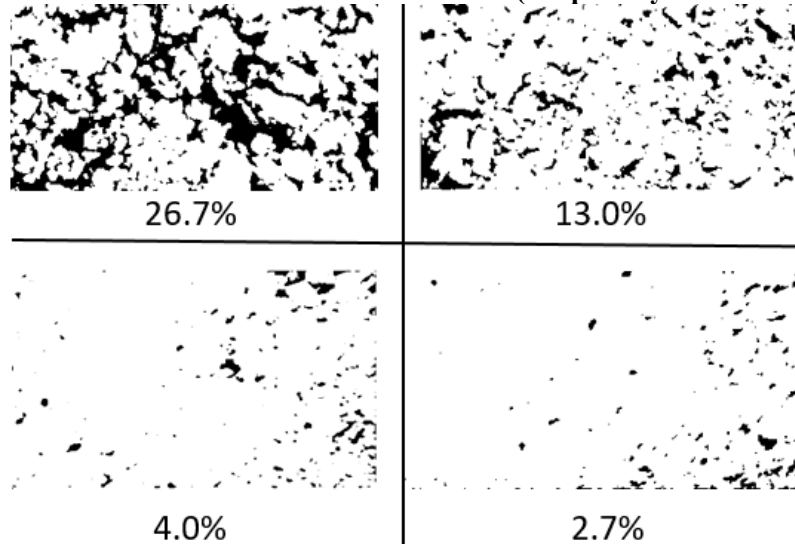


c) Example of poor performance d) Example of good performance

Figure 3.9. Box Test setup



(a) Surface voids based on visual examination (adopted by Cook et al. 2016)



(b) Surface voids based on the digital image process

Figure 3.10. Comparison of surface voids of box test rankings from different methods

In terms of the edge holding ability, standard procedure differentiates only passing and failing according to edge slump by classifying a mix as “fail” if the deflection is more than 1/4”. However, even if the mixture passes, the holding edge quality might differ. Therefore, it was decided to modify the rating based on the smoothness of edges. The idea was borrowed from the old measurement of Floor Flatness ( $F_F$ ) number, where the greatest defect along specified length was measured. The edge quality ranking was modified as follows and bases on the greatest defect



along edges: 1-good ( $<1/16$  in), 2-average ( $1/16$ - $1/8$  in), 3-poor ( $1/8$ - $1/4$  in), 4-failed ( $>1/4$  in) (Figure 3.11). If it failed because of a notable lack of paste, ranking 4a was assigned; and if a failure is due to abundance of excess of paste, ranking 4b was assigned. Finally, a dual index was used to describe Box test performance with “E” standing for edge quality, and “S” for surface quality. For example, “E2-S1” stands for a mixture with an average edge quality and ranking 1 in terms of surface voids.



**a) 1-good edge quality**



**b) 2-average edge quality**



**c) 3-poor edge quality**



**d) 4a-failed edge quality**



**e) 4b-failed edge quality (abundance of excess paste)**

**Figure 3.11. Examples of Box test results with different edge holding abilities**

### 3.6 Specimen casting and curing

Upon the completion of mixing, specimens were prepared according to ASTM C192 (Standard Practice for Making and Curing Test Specimens in the Laboratory). All specimens were stored in a  $73.5 \pm 3.5$  °F ( $23.0 \pm 2.0$ °C) room prior to demold at 24 hours and then stored in a curing room with 100% R.H. and  $73.5 \pm 3.5$  °F ( $23.0 \pm 2.0$ °C) until testing.

### 3.7 Hardened concrete tests

#### 3.7.1 Compressive strength test

Three 4" by 8" cylinders per each mixture were tested for compressive strength based on ASTM C39 (Standard Test Method for Compressive Strength of Cylindrical Concrete Specimens) at 7 and 28 days ages. All specimens were mechanically end-ground before each test. Forney compressive machine with a capacity of 400 kips (1,779 kN) was used (see Figure 3.12).



Figure 3.12. Compressive strength test setup

#### 3.7.2 Flexural strength test

One 6" by 6" by 20" beam per mixture was tested for modulus of rupture at the age of 28 days according to ASTM C78 (Standard Test Method for Flexural Strength of Concrete (Using Simple Beam with Third-Point Loading)). Forney beam tester machine with a capacity of 30 kips (133 kN) was used (see Figure 3.13).



**Figure 3.13. Flexural strength test setup**

### **3.7.3 Static modulus of elasticity test**

Modulus of elasticity test was performed at 28 days age according to ASTM C469 (Standard Test Method for Static Modulus of Elasticity and Poisson's Ratio of Concrete in Compression). A frame with two dial gauges to monitor both axial and radial deformations was used (see Figure 3.14). Each test was recorded and later used to build a graph, from which according properties were calculated.



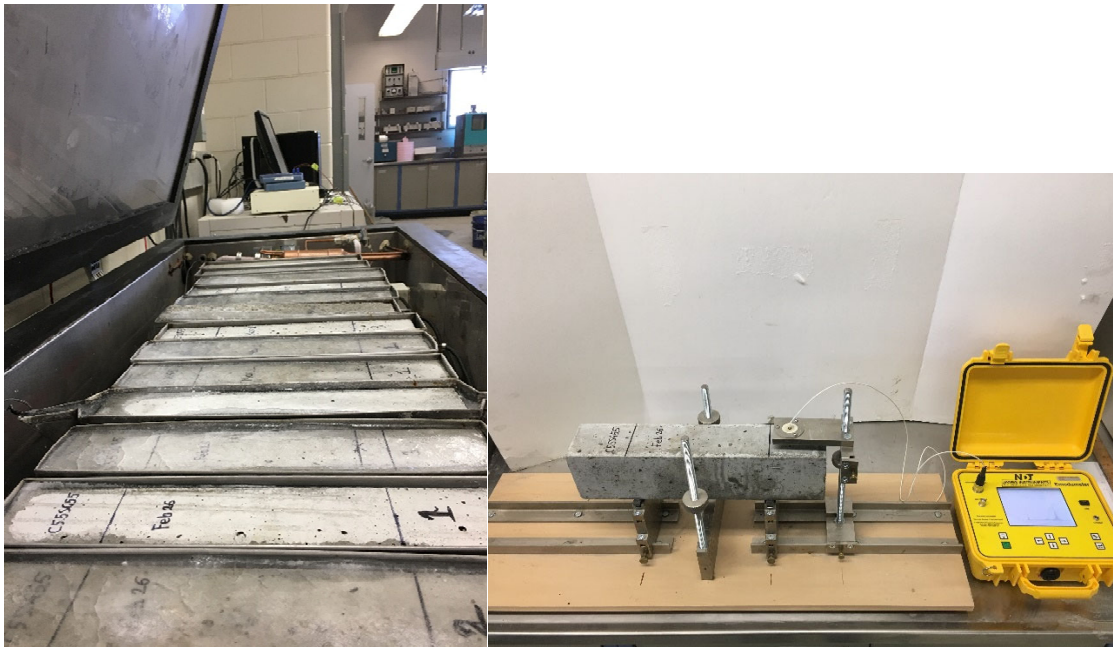
**Figure 3.14. Static Modulus of Elasticity test setup**



### 3.8 Durability tests

#### 3.8.1 Freeze/thaw resistance

The freeze/thaw test was conducted according to ASTM C666 (Standard Test Method for Resistance of Concrete to Rapid Freezing and Thawing) Procedure A. Humboldt freeze-thaw cabinet, which has multiple channels with one being a control, was used (see Figure 3.15a). Three 3”× 4”× 16” prisms per mixture were tested and the average values were reported. Specimens were exposed to freezing/thawing cycles after 14 days of standard curing. NDT E-meter MK II was used to obtain the fundamental transverse frequency of the specimens approximately every 30 cycles. Mass loss was also measured at about 30 cycles frequency. The equipment setup can be seen in Figure 3.15b.



a) Freeze/thaw chamber

b) NDT E-meter

Figure 3.15. Setup used for freeze/thaw resistance test.

#### 3.8.2 Surface and bulk resistivity

One cylinder specimen was randomly selected from each mixture to be tested for the surface (Figure 3.16a) and bulk resistivity (Figure 3.16b) using a Proceq Resipod testing device at 28-day based on AASHTO TP95 (Standard Method of Test for Surface Resistivity Indication of Concrete’s Ability to Resist Chloride Ion Penetration). The Resipod works based on the Wenner probe principles and measures the electrical resistivity of concrete. The specimen needs to be in a fully saturated condition. Electric current is applied through the outer probes, while the inner probes measure the voltage.



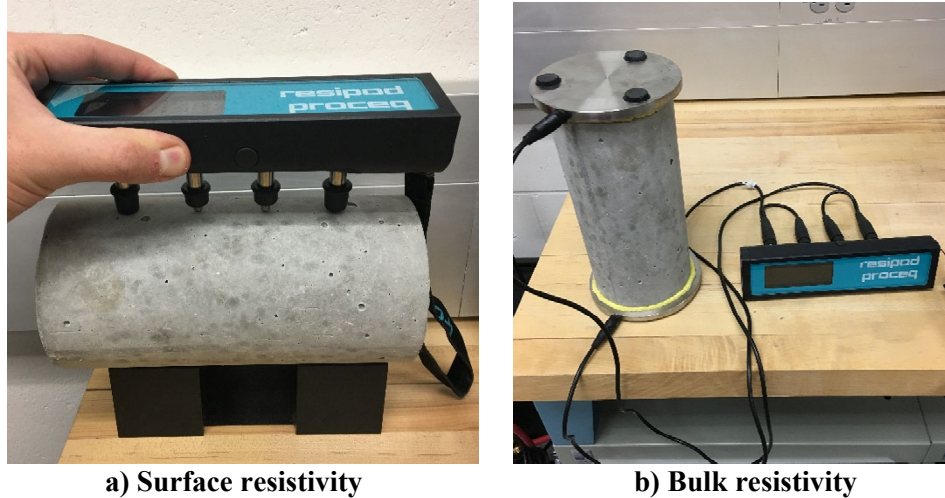


Figure 3.16. Resistivity test setup.

### 3.8.3 Free shrinkage

Three shrinkage bars 3" by 3" by 11.25" per mixture were casted for free shrinkage test according to ASTM C157 (Standard Test Method for Length Change of Hardened Hydraulic-Cement Mortar and Concrete). Specimens were cured until 28 days of age and then stored in an environmental chamber with  $73.5 \pm 3.5^\circ\text{F}$  ( $23.0 \pm 2.0^\circ\text{C}$ ) and  $50 \pm 4.0\%$  R.H. The initial reading was taken right after the specimens were moved from curing room to environmental chamber using the length comparator (see Figure 3.17). The average value from three specimens was recorded. The next readings were taken at 1, 3, 7, 14, 28 days after the initial reading.



Figure 3.17. Length comparator used for shrinkage measurement

### 3.8.4 Restrained shrinkage

One concrete ring per mixture was casted for restrained shrinkage test in accordance with ASTM C1581 (Standard Test Method for Determining Age at Cracking and Induced Tensile Stress Characteristics of Mortar and Concrete under Restrained Shrinkage). One of the test specimens is

shown in Figure 3.18a as an example. The specimens were stored in an environmental chamber with  $73.5 \pm 3.5$  °F ( $23.0 \pm 2.0$  °C) temperature and  $50 \pm 4.0$ % R.H. for 28 days or until the stress release is noticed due to concrete cracking. As shown in Figure 3.18b, the strain gauges were attached to the inner side of the steel ring using special adhesive and then were covered with wax coating. The readings were taken every one hour and monitored for sudden strain reduction. The sudden reduction of strain greater than 30 microstrains can be considered as cracking. The age at which cracking occurred was reported to the nearest 0.25 day.



**a) Test specimen**

**b) Strain gauge attached to the steel ring**

**Figure 3.18. Restrained shrinkage test setup**

## CHAPTER 4. EXPERIMENTAL DESIGN AND RESULTS

### 4.1 Introduction

The objective of this chapter is to present the details of the testing plan development and results obtained from the experimental study. The scope of the work includes aggregate analysis and three phases on the concrete study, which are aggregate blend investigation, performance of concrete with reduced cement content and durability evaluation.

The first step was to analyze different aggregate matrices for East NE, and West NE blends by using experimental and theoretical particle packing methods. Experimental packing degrees were obtained using the combined void content test and then compared to packing degrees obtained from the Modified Toufar Model.

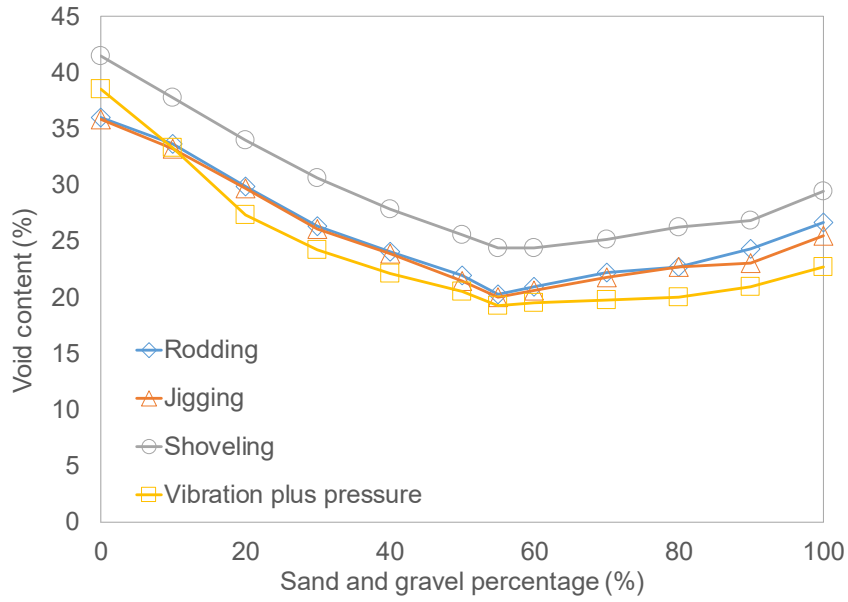
Once various aggregate systems were evaluated, promising blends were selected for further investigation. The testing matrix was developed and consisted of three phases. Phase 1 included evaluating performances of concrete mixtures with promising aggregate blends at standard cement content. Blends that showed better performance were selected to proceed further to Phase 2, where cement content was reduced at 0.5 sack step. Once the first two phases were completed, selected promising mixtures were tested for performance evaluation, which mainly included durability tests.

Finally, once all the results were collected and evaluated, corresponding conclusions were drawn, and some recommended changes to NDOT specifications of pavement concrete were proposed.

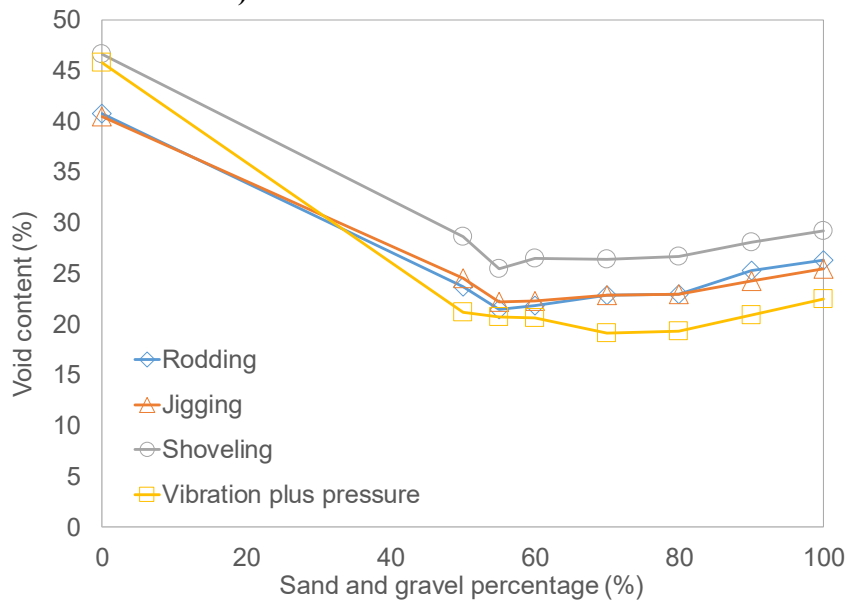
### 4.2 Aggregate system evaluation and selection

#### 4.2.1 Experimental packing results

In order to develop a testing matrix, the aggregate system was first analyzed in terms of experimental particle packing. As shown in Figure 4.1, as expected, except for the LS only case, the condition of vibration plus pressure resulted in a higher degree of compaction, followed by jiggling, rodding, and shoveling respectively. According to Figure 4.1a, the blend with the maximum packing is 55SG-45LS (identification represents a 55% SG and 45% LS blend) followed by promising blends as 60SG-40LS and 50SG-50LS. In terms of West NE aggregate system, based on the experience from East NE aggregates system analysis, along with the results of blends  $SG\_W/A > 0.50$ , it was determined that the optimum blend would not be a blend with  $SG\_W/A < 0.50$ . To minimize the experimental effort, experimental tests for blends  $SG\_W/A < 0.50$  were not performed. From Figure 4.1b, it can be noticed that the vibration plus pressure method resulted in 70SG\_W-30GR (identification represents a 70% SG\_W and 30% GR blend) being the optimum blend, while other three methods showed that the blend with the lowest amount of voids is 55SG\_W-45GR.



**a) East NE blends void contents**



**b) East NE blends void contents**

**Figure 4.1. Results of the combined aggregate void content test for binary blends**

As shown in Figure 4.2, for the ternary blends, as it was expected after the tests for binary blends, vibration plus pressure provided better compaction followed by jigging, rodding and shoveling respectively. Blend 55SG-40LS-5IA resulted in the lowest amount of voids. The possible reason is that this blend is very close to the best binary blend 55SG-45LS, if intermediate aggregate is to be considered as coarse aggregate.

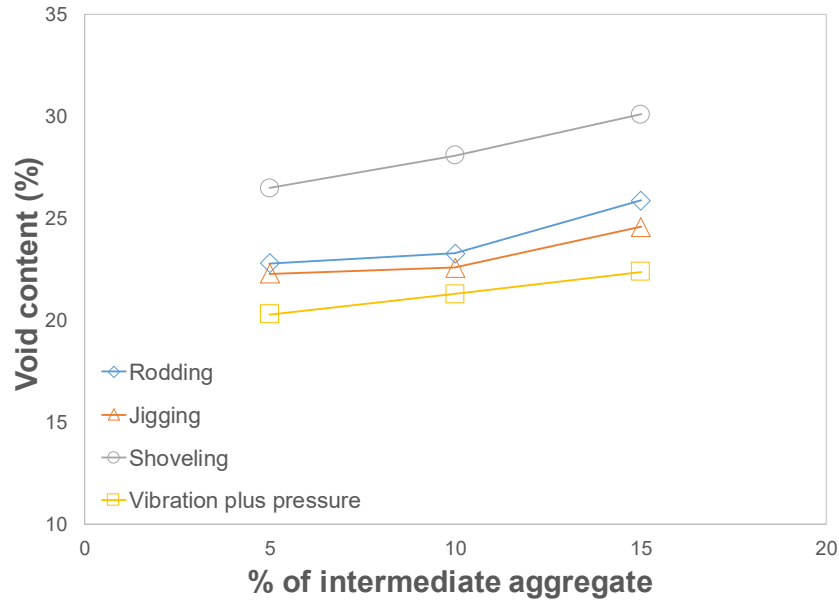


**Figure 4.2. Results of the combined aggregate void content test for ternary blends**

#### 4.2.2 Theoretical packing results

Results from the theoretical packing degree were compared with the experimental results from the four different compaction methods. According to the individual void contents of SG, LS, SG\_W, and GR, together with the volume fractions of aggregates in different combinations, the theoretical packing degree can be calculated based on the modified Toufar Model as described earlier in Equation (2.4). As shown in Figures 4.3 and 4.4, there is a good correlation between the experimental and theoretical packing degrees in the blends. From East NE aggregate system analysis, it was noticed that as the proportion of limestone exceeds 50%, i.e.,  $SG/A < 0.50$ , the correlation is not as clear, except for vibration plus pressure method. Moreover, the maximum theoretical and experimental packing degree matched only when vibration plus pressure is used, which is 55SG-45LS. Regarding West NE aggregates system analysis, results showed that the optimum blend is whether 55SG\_W-45GR based on vibration plus pressure method or 70SG\_W-30GR based on the other three methods. Besides the good match with the theoretical packing, as mentioned earlier, it is believed that the vibration plus pressure method is the most representative method for the pavement concrete application procedure. Thus, the void contents from this procedure was used in further study.

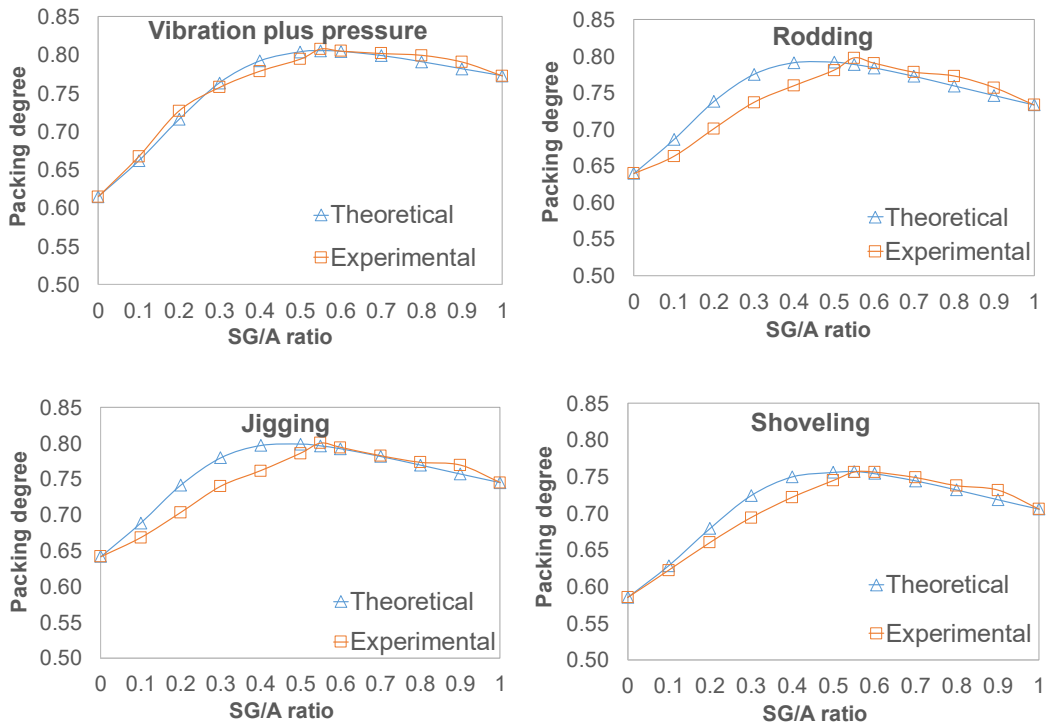


Figure 4.3. Comparison between experimental and theoretical packing degrees of East NE blends

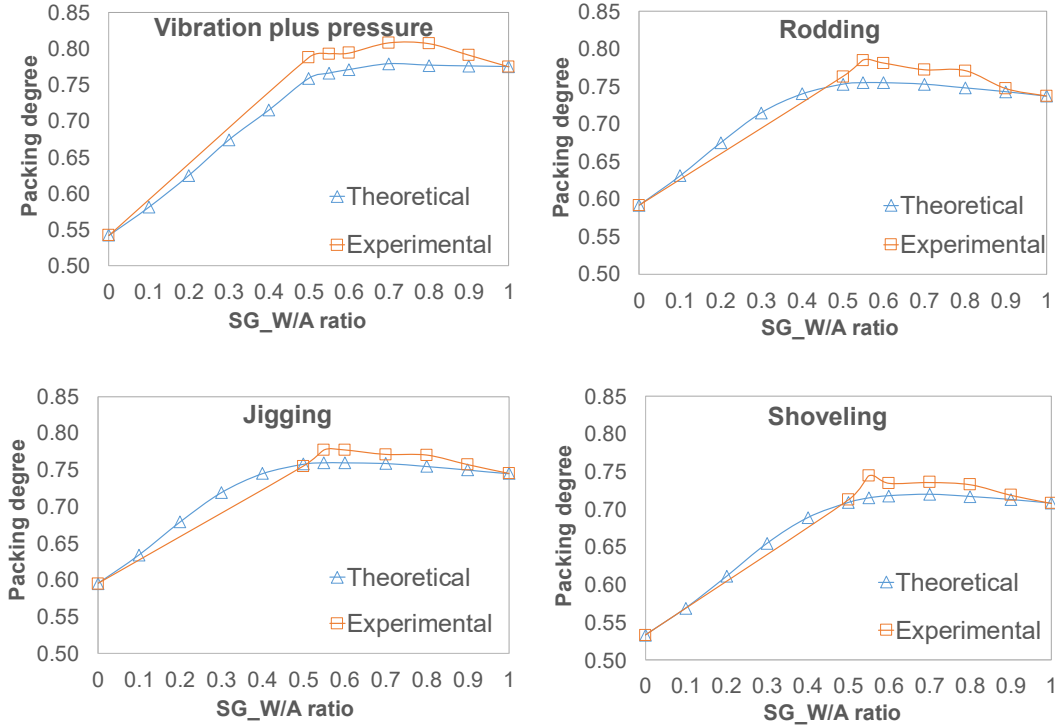
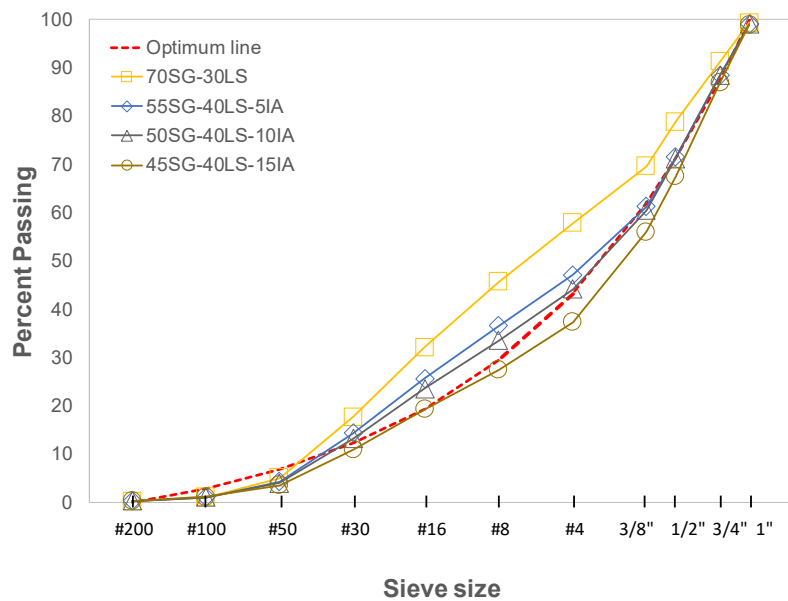


Figure 4.4. Comparison between experimental and theoretical packing degrees of West NE blends

Since Modified Toufar Model has a good correlation with experimental results mostly for binary blends, it was not used for ternary blends. Besides, it was not practical to conduct combined void content test for that many ternary blends. Therefore, it was decided to find few promising blends using the Modified A&A model and Solver function within Excel, and follow by conducting experimental part for those few blends. Distribution modulus ( $q$ ) was selected as 0.45, which is a common value for pavement applications. Maximum and minimum diameters were used as 1 in (25 mm) and 75 microns respectively. Based on the results, it was found that the optimum packing is provided when LS proportion is 40%, and proportion of IA is 5%, 10%, or 15%. Figure 4.5 illustrates these blends along with the reference blend, which is 70SG-30LS. It can be clearly seen that the reference blend is farther from the optimum packing line compared to the three promising ternary blends.



**Figure 4.5. Theoretical Optimum curve with the reference blend and promising ternary blends,  $q=0.45$ ,  $d_{max}=1$  in,  $d_{min}=75$  microns**

### 4.3 Testing matrix development

After the particle packing analysis was completed, 70SG-30LS (reference), 60SG-40LS, 55SG-45LS, 50SG-50LS, 55SG-40LS-IA5, 50SG-40LS-IA10, and 45SG-40LS-IA15 blends from East NE, and 70SG\_W-30GR, 55SG\_W-45GR blends from West NE were selected for concrete mixtures. These blends were also examined to determine if they satisfied the Tarantula curve criteria (see Figure 4.6). It can be seen that the reference blend is out of Tarantula limits with an excess of No. 8 and No. 16 particles. It worth noticing that one of the promising blends with West NE aggregates (70SG\_W-30GR) based on combined aggregate void content test and Modified Toufar Model is out of Tarantula limits too with an abundance of #8 and #16 size particles.



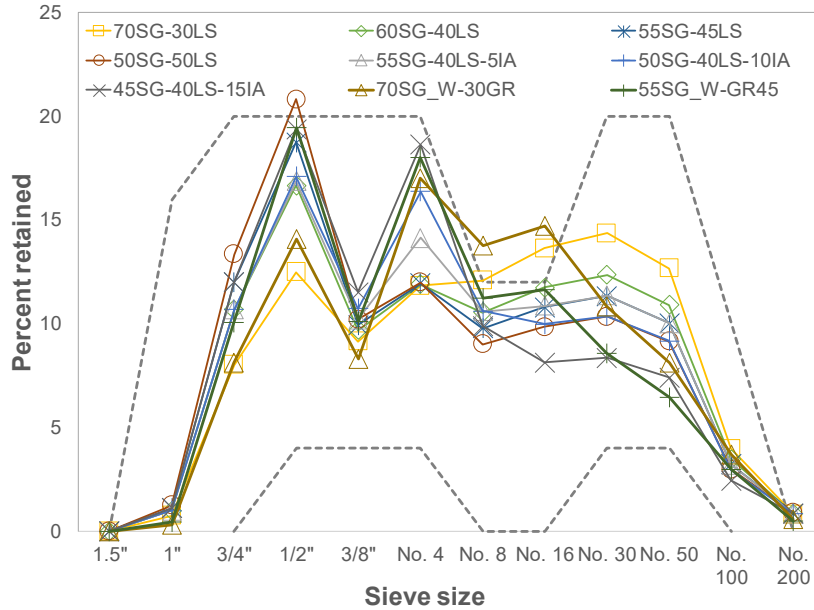


**Figure 4.6. Reference blend and blends chosen for further study plotted on Tarantula curve.**

In order to evaluate the impacts of aggregate gradation and cement content on pavement concrete performance, the testing matrix was divided into three Phases. Phase 1 was focused on obtaining the best blend performance while keeping the cement content at a standard 6.0 sacks (564 lb/yd<sup>3</sup>). The best blend was selected mainly based on the highest amount of excess paste shown in the box test performance and meeting the minimum mechanical property criteria. In Phase 1 mixes, the following blends were evaluated: 70SG-30LS (reference mix), 60SG-40LS, 55SG-45LS, 50SG-50LS, 45SG-40LS-IA5, 50SG-40LS-IA10, 55SG-40LS-IA5 from East NE, and 70SG\_W-30GR, 55SG\_W-45GR from West NE. Once Phase 1 was completed, the most promising mixtures would be obtained. In Phase 2, promising blends along with the reference one were subjected to a stepwise reduction of cement content. Cement factor was reduced by 0.5 sack (47 lb/yd<sup>3</sup>) steps, i.e. from 6.0 sacks (564 lb/yd<sup>3</sup>), to 5.5 sacks (517 lb/yd<sup>3</sup>), 5.0 sacks (470 lb/yd<sup>3</sup>) and 4.5 sacks (423 lb/yd<sup>3</sup>) respectively. After Phase 2, promising mixtures with reduced cement content were selected and along with the reference mixture were evaluated for performance, which includes setting time, air content, modulus of elasticity, resistance to freeze/thaw cycles, drying shrinkage, and restrained shrinkage tests.

#### **4.4 Phase 1 - Aggregate Blends Study**

##### **4.4.1 Mix proportions**

Table 4.1 shows the mix proportions for mixtures included in Phase 1. The mix identification is based on three parameters, i.e., cement content in sacks (C) and the fractions of SG and LS. For example, C6SG70LS30 stands for a mixture with a cement content of 6.0 sacks, SG fraction of 70, and LS fraction of 30 (Figure 4.7). For the mixes with ternary aggregate blends, additional parameter is added (IA). Water-to-cement ratio (w/c) was fixed at 0.43 for East NE mixes. For West NE mixes it was decided to use, a lower w/c at 0.41 was used. The calculated total paste volume (P<sub>t</sub>%), excess paste volume (P<sub>e</sub>%), and excess paste-to-aggregate volume ratio (P<sub>e</sub>%/V<sub>B\_agg</sub>%) are also shown in Table 4.1. The procedure of calculating excess paste-to-aggregate ratio can be found in the Appendix A.



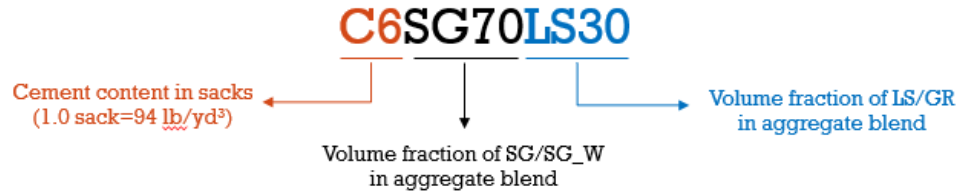


**Figure 4.7. Mix identification**

**Table 4.1. Mix proportions for mixes of Phase 1**

	Mix ID	w/c	CF	LS/GR	SG/SG_W	IA	Water	AEA	WR	P <sub>t</sub> %	P <sub>e</sub> %	P <sub>e</sub> %/V <sub>B<sub>agg</sub></sub> %
East	C6SG70LS30	0.43	564	912	2060	0	243	0.125	0.0	31.88	14.91	0.17388
	C6SG60LS40	0.43	564	1216	1766	0	243	0.125	0.0	31.89	15.24	0.17840
	C6SG55LS45	0.43	564	1368	1619	0	243	0.125	0.0	31.88	15.52	0.18231
	C6SG50LS50	0.43	564	1520	1472	0	243	0.125	0.0	31.88	14.11	0.16300
	C6SG45LS40IA15	0.44	564	1216	1324	445	248	0.125	0.0	32.15	12.35	0.13986
	C6SG50LS40IA10	0.43	564	1216	1472	297	243	0.125	0.0	31.88	13.26	0.15165
	C6SG55LS40IA5	0.43	564	1216	1619	148	243	0.125	0.0	31.88	14.54	0.16992
West	C6SG_W70GR30	0.41	564	897	2027	0	231	3.00	0.0	32.33	16.28	0.19425
	C6SG_W55GR45	0.41	564	1345	1592	0	231	4.00	2.5	32.49	14.83	0.17388

Note: all ingredients are in lb/yd<sup>3</sup>, except for the chemical admixtures (WR and ARA), which are in fl oz/cwt (1 lb/yd<sup>3</sup>= 0.5935 kg/m<sup>3</sup>, 1 fl oz/cwt= 0.6519 mL/kg)

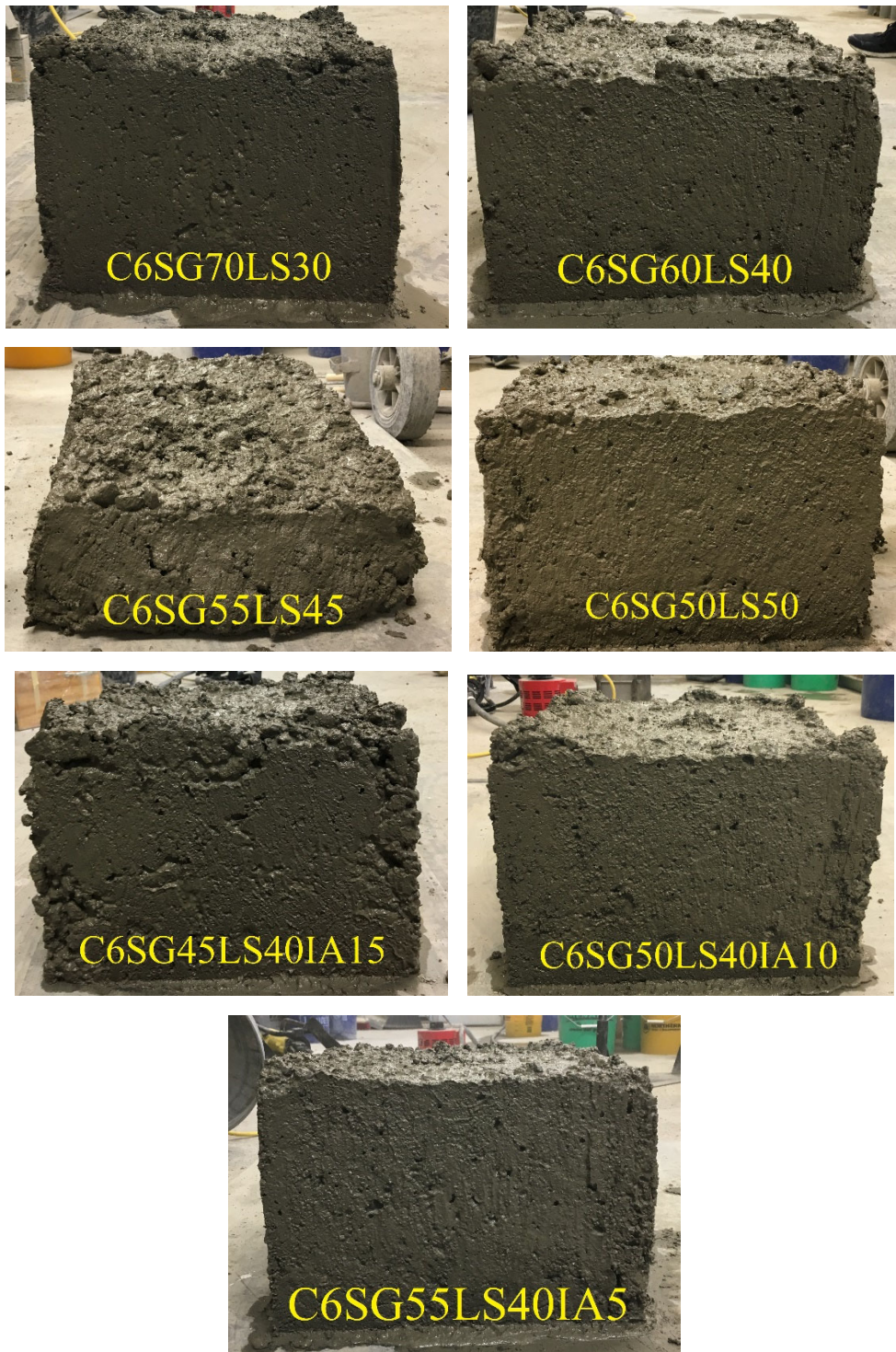
#### 4.4.2 Fresh concrete properties

Fresh concrete properties, in particular the Box test, were used as the main criteria to select the most promising blend. Table 4.2 summarizes fresh concrete properties of Phase 1 East NE mixes. In addition, box test images for all mixes are shown in Figure 4.8. Results revealed that all mixes except C6SG45LS40IA15 have low surface voids content, which indicated sufficient paste content to cover the aggregates. Noted that although results shown below presented a lower box ranking for the C6SG55LS45 mix, the blend was still considered as a more promising blend. Even though the mix was considered failed per box test, it was apparently largely due to the high amount of excess paste. This result also indicated that more paste can be reduced in this mix.

**Table 4.2. Fresh concrete properties of Phase 1 East NE mixes**

Mix ID	C6SG70LS30	C6SG60LS40	C6SG55LS45	C6SG50LS50	C6SG45LS40IA15	C6SG50LS40IA10	C6SG55LS40IA5
# of adjustments	0	0	0	0	0	0	0
Slump (in)	1.5	2.5	5	3.5	3.0	4.0	4.0
Box test ranking	1	1	failed	2	3	2	1
Surface voids (%)	3.8	3.6	NA	3.7	6.0	2.8	1.9
Revised box test ranking	E1-S2	E1-S2	E4b-S4	E3-S2	E3-S3	E2-S1	E2-S1

Note: 1 in= 25.4 mm



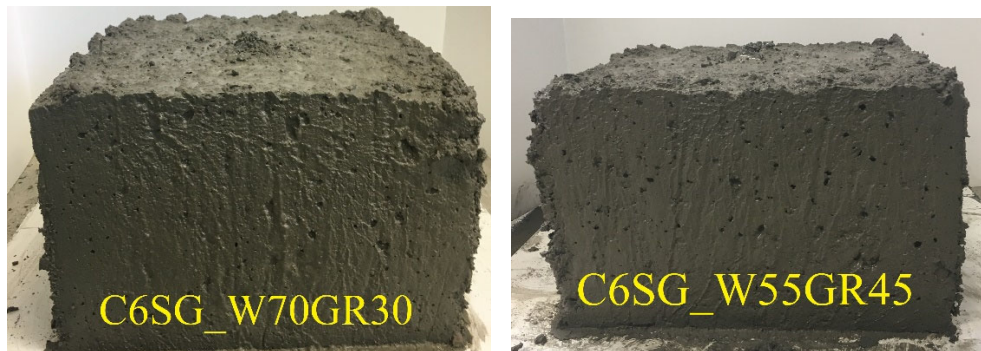
**Figure 4.8. Box test images from Phase 1 East NE mixes**

Table 4.3 presents the fresh concrete properties of Phase 1 West NE mixes. Box test images are shown in Figure 4.9. According to the results, it can be seen that two mixtures have almost identical results, although C6SG\_W55GR45 mixture required a small dose of WR. It was decided to move on to the next Phase with both mixtures.

**Table 4.3. Fresh concrete properties of Phase 1 West NE mixes**

Mix ID	C6SG W70GR30	C6SG W55GR45
# of adjustments	0	1
Slump (in)	4.0	4.0
Box test ranking	1	1
Surface voids (%)	2.7	2.5
Revised box test ranking	E2-S1	E3-S1

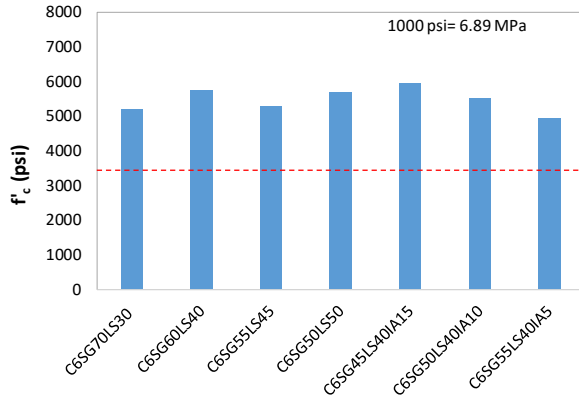
Note: 1 in= 25.4 mm



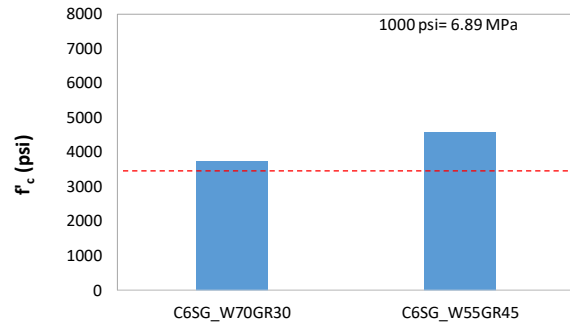
**Figure 4.9. Box test images from Phase 1 West NE mixes**

#### **4.4.3 Hardened concrete properties**

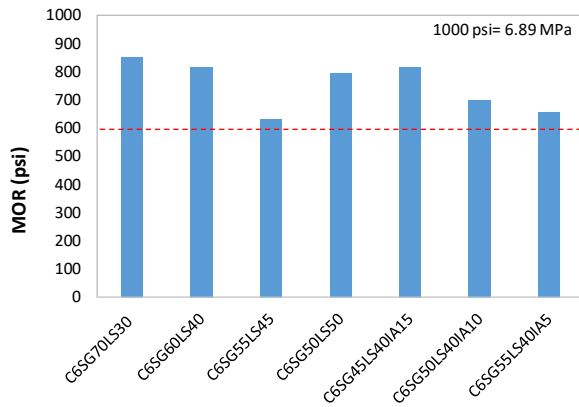
Figure 4.10 demonstrates the mechanical properties of Phase 1 mixes. All mixes met the NDOT criteria, which are 3,500 psi of compressive strength and 600 psi of modulus of rupture at 28 days.



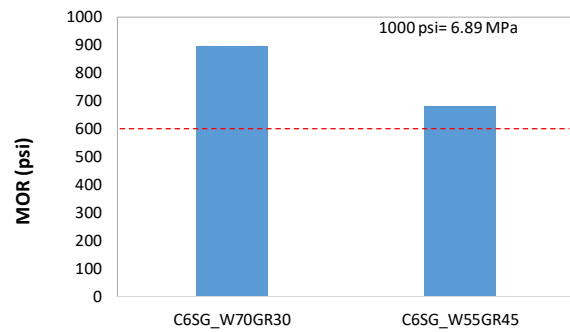
**a) Compressive strength of East NE mixes**



**b) Compressive strength West NE mixes**



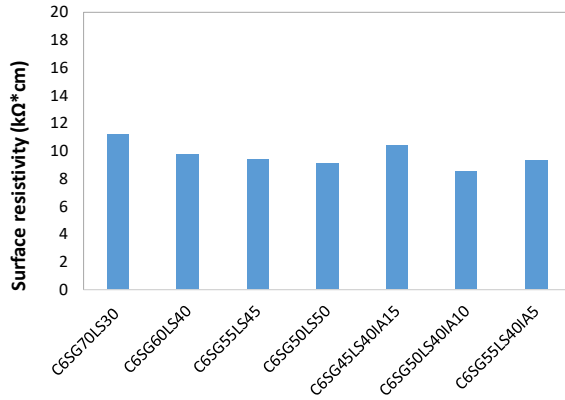
**c) Modulus of rupture of East NE mixes**



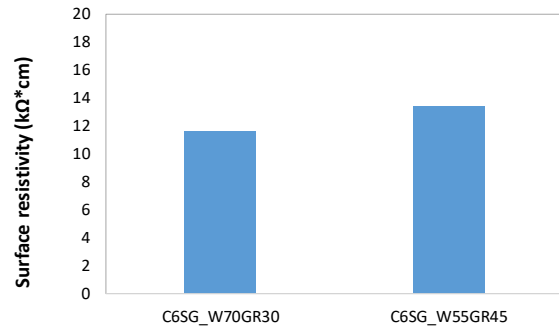
**d) Modulus of rupture of West NE mixes**

**Figure 4.10. Mechanical properties of Phase 1 mixes**

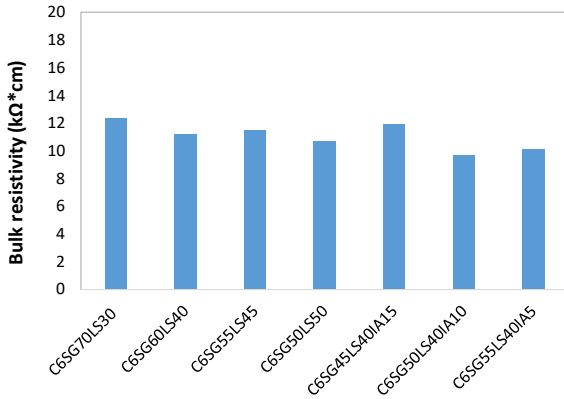
Permeability properties are presented in Figure 4.11. It seems that the change in aggregate gradation does not significantly impact neither surface resistivity nor bulk resistivity.



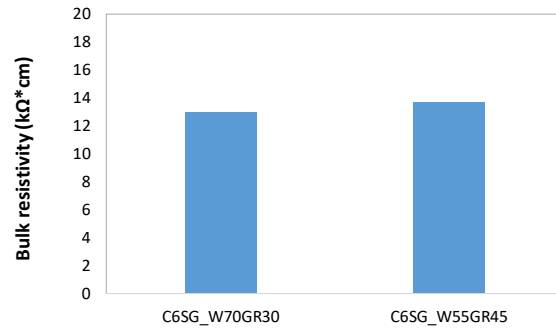
a) Surface resistivity of East NE mixes



b) Surface resistivity of West NE mixes



c) Bulk resistivity of East NE mixes



d) Bulk resistivity of West NE mixes

Figure 4.11. Surface resistivity results of Phase 1 mixes

## 4.5 Phase 2 - Cement Content Study

### 4.5.1 Mix proportions

In terms of East NE mixes, based on results obtained in Phase 1, blends selected for further investigation along with the reference blend are 55SG-45LS and 55SG-40LS-IA5. Regarding the West NE mixes, as it was not that clear which blend is the optimum, it was decided to proceed with both blends. Mixtures with a stepwise reduction of 0.5 sack of cement from 6.0 sacks to 4.5 sacks were developed. Mix proportions for both East NE and West NE mixes are presented in Table 4.4. For East NE mixes, w/c was increased to 0.45 in this phase to accommodate the anticipated reduction of workability due to the reduction of cement content. For West NE mixes, it was decided to keep w/c the same as in Phase 1.



**Table 4.4. Mix proportions for mixes of Phase 2**

	Mix ID	w/c	CF	LS/GR	SG/SG _W	IA	Water	AEA	WR	P <sub>t</sub> %	P <sub>e</sub> %	P <sub>e</sub> %/V <sub>B</sub> _agg%/o
East	C6SG70LS30	0.43	564	912	2060	0	243	0.125	0.0	31.88	14.91	0.17388
	C6SG55LS45	0.43	564	1368	1619	0	243	0.125	0.0	31.88	15.52	0.18231
	C5.5SG70LS30	0.45	517	942	2128	0	233	0.125	4.0	30.21	12.83	0.14609
	C5.5SG55LS45	0.45	517	1413	1672	0	233	0.125	0.0	30.21	13.46	0.15438
	C5.5SG55LS40IA5	0.45	517	1256	1673	153	233	0.500	0.0	30.21	12.29	0.13906
	C5SG70LS30	0.45	470	972	2196	0	212	0.125	20.0	28.02	10.09	0.11129
	C5SG55LS45	0.45	470	1458	1725	0	212	0.125	4.0	28.02	10.74	0.11937
	C5SG55LS40IA5	0.45	470	1296	1725	158	212	0.700	4.0	28.01	9.54	0.10461
	C4.5SG55LS45	0.45	423	1504	1779	0	190	0.125	24.0	25.75	7.93	0.08542
	C4.5SG55LS40IA5	0.45	423	1336	1778	163	190	1.000	20.0	25.81	6.76	0.07191
West	C6SG_W70GR30	0.41	564	897	2027	0	231	3.00	0.0	32.33	16.28	0.19425
	C6SG_W55GR45	0.41	564	1345	1592	0	231	4.00	2.5	32.49	14.83	0.17388
	C5.5SG_W70GR30	0.41	517	925	2089	0	212	4.000	5.0	31.37	14.82	0.17162
	C5.5SG_W55GR45	0.41	517	1388	1642	0	212	4.000	8.0	31.36	13.14	0.14935
	C5SG_W70GR30	0.41	470	952	2154	0	193	1.500	8.0	28.75	11.70	0.13142
	C5SG_W55GR45	0.41	470	1430	1691	0	193	1.500	8.0	28.90	10.14	0.11182
	C4.5SG_W70GR30	0.41	423	981	2217	0	173	0.500	12.0	26.79	9.23	0.10074

Note: all ingredients are in lb/yd<sup>3</sup>, except for the chemical admixtures (WR and ARA), which are in fl oz/cwt (1 lb/yd<sup>3</sup>= 0.5935 kg/m<sup>3</sup>, 1 fl oz/cwt= 0.6519 mL/kg)

#### 4.5.2 Fresh concrete properties

Table 4.5 presents fresh concrete test results for East NE mixes and box test images are shown in Figure 4.12. It can be noted that for the reference blend with 0.5 sacks of reduced cement (C5.5SG70LS30), a WR adjustment of 4 fl oz/cwt was needed to pass the box test. In comparison, mix with the optimum blend (C5.5SG55LS45) resulted in a good performance without any WR addition, proving that 55SG-45LS is the optimum gradation. C5.5SG55LS40IA5 mix performed very similarly to the optimum blend mix. When cement content was reduced by 1.0 sack, for reference blend (C5SG70LS30) even four adjustments at a total WR dosage of 20 fl oz/cwt was not sufficient to pass the Box test, and the final box test ranking was E3-S3. For the C5SG55LS45 and C5SG55LS40IA5 mixes, a minimum WR dosage of 4 fl oz/cwt was necessary to obtain an acceptable mixture and result in E2-S2 and E2-S1 rankings respectively. Results of East NE mixes prove that, although by introducing a higher amount of LS that is more angular compared to SG, the improved gradation and decreased surface area of aggregates helped to reduce the needed cement content. Results showed that it is not feasible to obtain acceptable mixture for the optimized blends with 1.5 sacks reduced cement (C4.5SG55LS45 and C4.5SG55LS40IA5), even with the WR. It seems that 5.0 sacks of cement is the minimum cement content with the materials used in this series.

Fresh concrete properties and images from the box test for West NE mixes are demonstrated in Table 4.6 and Figure 4.13 respectively. In general, both blends worked appropriately with 0.5 and 1.0 sacks cement reduction. However, it can be seen that 70SG\_W-30GR blend resulted in slightly better performance, proving that it is the optimum blend for the aggregates in this series. It could be due to the fact that GR is more angular compared to LS, thus negatively affecting particle packing. The observation is consistent with results from the theoretical and experimental particle packing as shown in Figures 4.1 and 4.3. It is important to note that while the Tarantula curve showed 55SG\_W-45GR blend to be the optimum, results from the Modified Toufar Model and experimental test with vibration plus pressure method predicted the packing were deemed more accurate. The reason is that Tarantula curve takes into account gradation only ignoring aggregate shape.

**Table 4.5. Fresh concrete properties of Phase 2 East NE mixes**

Mix ID	C6SG70 LS30	C6SG55 LS45	C5.5SG70 LS30	C5.5SG55 LS45	C5.5SG55 LS40IA5	C5SG70 LS30	C5SG55 LS45	C5SG55 LS40IA5	C4.5SG55 LS45	C4.5SG55 LS40IA5
Number of adjustments	0	0	1	0	0	4	1	1	3	3
Slump (in)	1.5	5	2.5	4.0	3.0	1.0	2.0	2.0	0.0	0.0
Box test ranking	1	failed	1	1	1	3	3	1	failed	failed
Surface voids (%)	3.8	NA	3.1	2.3	2.6	8.9	3.2	2.6	NA	NA
Revised box test ranking	E1-S2	E4b-S4	E1-S2	E2-S1	E1-S1	E3-S3	E2-S2	E2-S1	E4a-S4	E4a-S4

Note: 1 in= 25.4 mm

**Table 4.6. Fresh concrete properties of Phase 2 West NE mixes**

Mix ID	C6SG_W70 GR30	C6SG_W55 GR45	C5.5SG_W70 GR30	C5.5SG_W55 GR45	C5SG_W70 GR30	C5SG_W55 GR45	C4.5SG_W70 GR30
Number of adjustments	0	1	1	2	1	1	2
Slump (in)	4	4	2.25	3.5	3	4.25	0.75
Box test ranking	1	1	1	2	1	2	4
Surface voids (%)	2.7	2.5	2.7	3.7	2.5	3.4	10.5
Revised box test ranking	E2-S1	E3-S1	E2-S1	E2-S2	E2-S1	E2-S2	E4a-S3

Note: 1 in= 25.4 mm





Figure 4.12. Box test images for East NE mixes

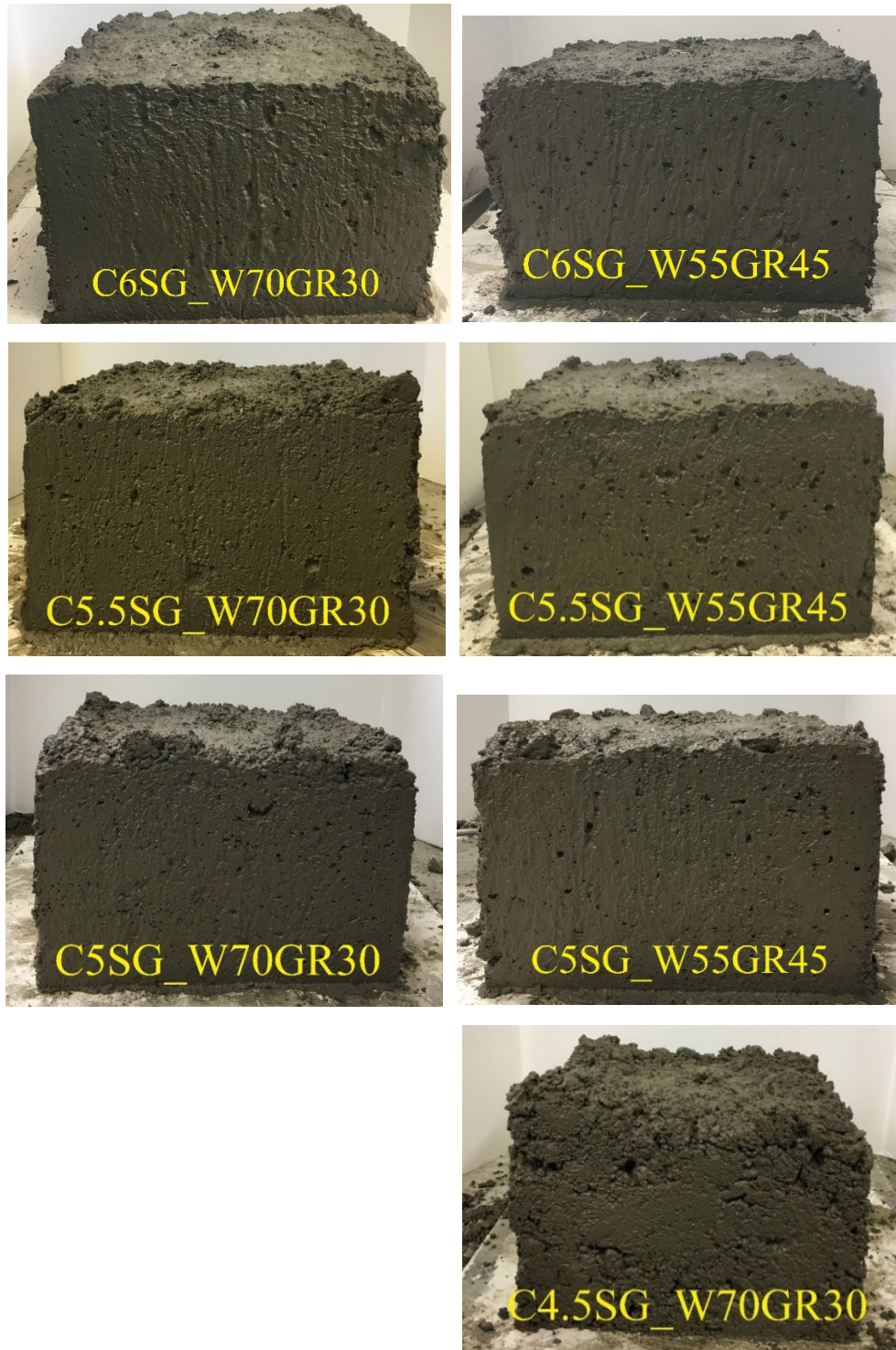


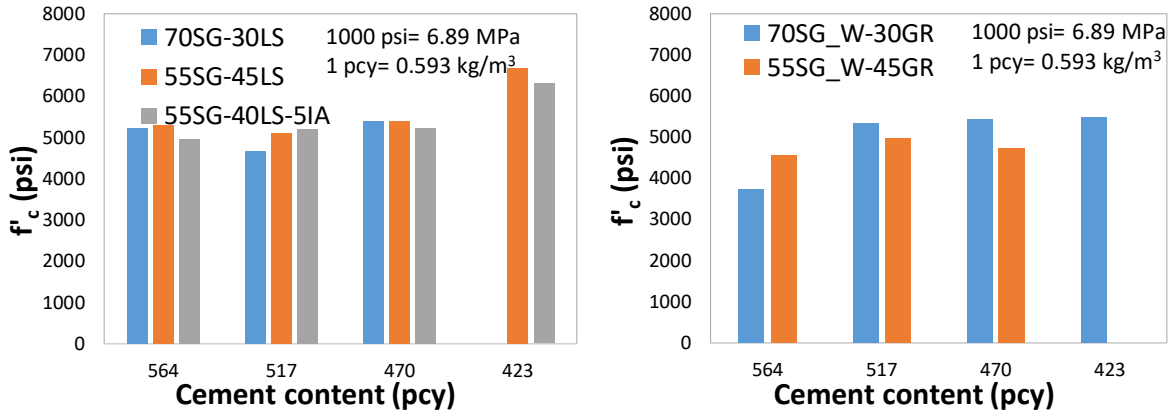
Figure 4.13. Box test images for West NE mixes

#### 4.5.3 Hardened concrete properties

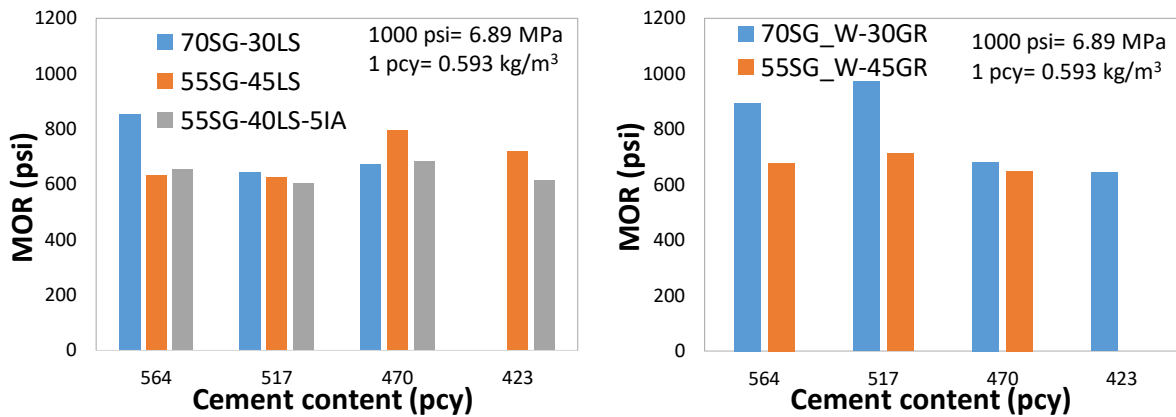
In terms of hardened concrete properties, the effect of cement reduction on properties including compressive strength, modulus of rupture, surface and bulk resistivity was evaluated.



Note that even with the reduction of cement content, there is no significant change in strength (Figure 4.14a). These results are consistent with Yurdakul (2010) and Wassermann et al. (2009). There is also no significant effect of cement content on the modulus of rupture (Figure 4.14b). West NE mixes resulted in slightly higher flexural strength. It might be due to the more angular aggregate used. The developed mixes were all deemed acceptable based on the minimum compressive strength and modulus of rupture at 28 days specified for pavements in Nebraska, which are 3,500 psi and 600 psi respectively. Surface and bulk resistivity are also not compromised by the reduction of cement content (Figure 4.15). However, values seem to be relatively low, which is believed to be due to high pozzolan content in mixes.

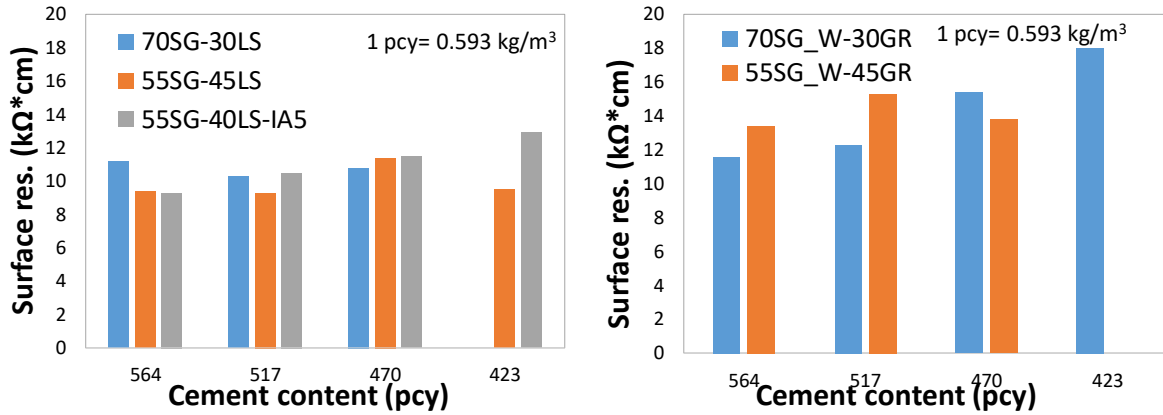


a) Effect of cement content on compressive strength (f'c)

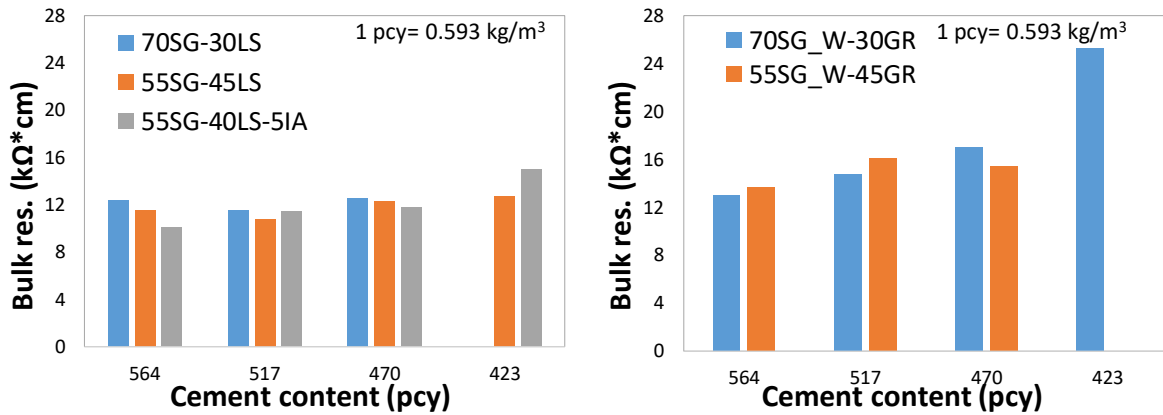


b) Effect of cement content on modulus of rupture (MOR)

Figure 4.14. Effect of cement content on mechanical properties



a) Effect of cement content on surface resistivity



b) Effect of cement content on bulk resistivity

Figure 4.15. Effect of cement content on permeability

#### 4.6 Phase 3 - Performance Evaluation

Once it was found that reducing cement content does not compromise basic fresh concrete, mechanical and permeability properties, it was important to evaluate few promising mixes for additional properties such as setting time, modulus of elasticity, free shrinkage, restrained shrinkage, and freeze-thaw resistance.

##### 4.6.1 Mix proportions

For performance evaluation, in addition to the reference mixture (C6SG70LS30), three mixes (C5.5SG55LS45, C5SG55LS45, and C5.5SG55LS40IA5) were selected for East NE. For West NE C6SG\_W70GR30, C5.5SG\_W70GR30, and C5SG\_W70GR30 were evaluated. Mix proportions of the abovementioned seven mixes are presented in Table 4.7.

**Table 4.7. Mix proportions for performance evaluation mixes**

	Mix ID	w/c	CF	LS/GR	IA	SG/SG_W	Water	AEA	WR
East NE	C6SG70LS30	0.41	564	904	0	2042	231	2.00	0.0
	C5.5SG55LS45	0.41	517	1398	0	1654	212	2.50	0.0
	C5SG55LS45	0.41	470	1438	0	1702	193	2.00	6.0
	C5.5SG55LS40IA5	0.41	517	1242	151	1654	212	3.50	4.0
West NE	C6SG_W70GR30	0.41	564	897	0	2027	231	3.00	0
	C6SG_W70GR30	0.41	517	925	0	2089	212	2.50	2.0
	C6SG_W70GR30	0.41	470	952	0	2154	193	1.50	8.0

Note: all ingredients are in lb/yd<sup>3</sup>, except for the chemical admixtures (WR and AEA), which are in fl oz/cwt (1 lb/yd<sup>3</sup>= 0.5935 kg/m<sup>3</sup>, 1 fl oz/cwt= 0.6519 mL/kg)

#### 4.6.2 Fresh concrete properties

Fresh concrete properties of East NE and West NE performance evaluation mixes are tabulated in Tables 4.8 and 4.9 respectively. NDOT Standard Specifications for Highway Construction (2017) requires 6.5-9.0% of the air in pavement mixes. It can be seen that air content obtained in all seven mixes is within an acceptable range. In terms of setting time of East NE mixes, it can be noticed that both initial and final sets of C5.5SG55LS45 happened slightly earlier compared to the reference mix, which can be explained by a lower amount of cement paste volume. Mix C5SG55LS45 showed a dramatic increase in initial and final set time mix with even lower cement content, which is believed to cause by to the presence of WR, which can delay hydration and extend initial and final sets. A similar trend was noticed with West NE mixes, where setting time delays with the higher WR dosage.

**Table 4.8. Fresh concrete properties of East NE performance evaluation mixes**

Mix ID	C6SG70LS30	C5.5SG55LS45	C5SG55LS45	C5.5SG55LS40IA5
Slump (in)	3.00	3.50	4.50	4.75
Air content (%)	7.0	7.2	8.0	7.6
Unit weight (lb/ft <sup>3</sup> )	139.24	140.28	134.08	138.88
Initial set (min)	275	255	395	360
Final set (min)	395	380	520	495

Note: 1 in= 25.4 mm

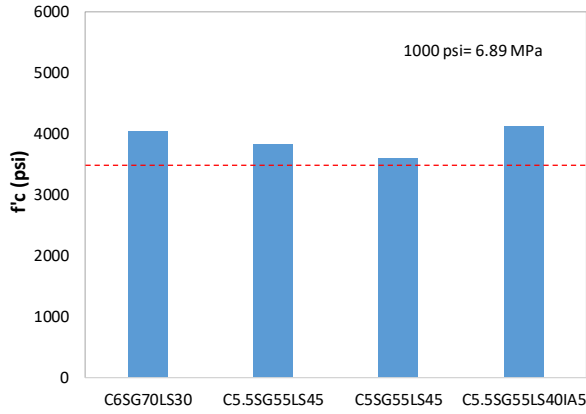
**Table 4.8. Fresh concrete properties of West NE performance evaluation mixes**

Mix ID	C6SG_W70GR30	C5.5SG_W70GR30	C5SG_W70GR30
Slump (in)	5.00	5.25	4.25
Air content (%)	7.6	8.5	8.0
Unit weight (lb/ft <sup>3</sup> )	137.84	135.08	139.40
Initial set (min)	315	360	370
Final set (min)	450	480	505

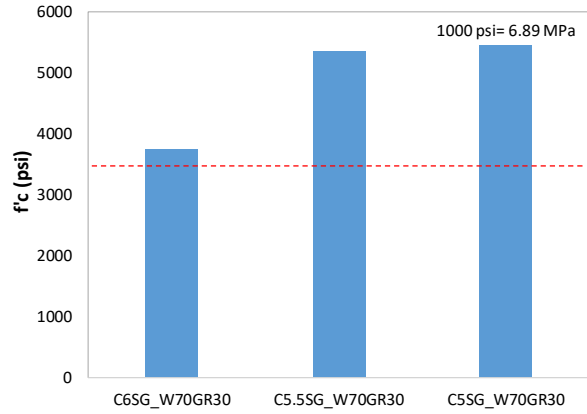
Note: 1 in= 25.4 mm

#### **4.6.3 Hardened concrete properties**

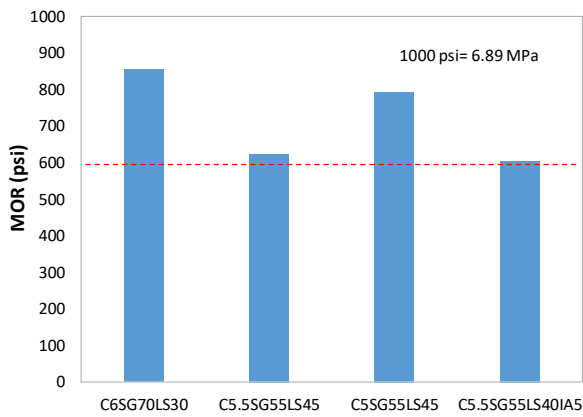
Results of mechanical properties including compressive strength, modulus of rupture (from the Phase 2 results), and modulus of elasticity can be found in Figure 4.16. All the mixtures passed the minimum NDOT criteria of 3,500 psi of compressive strength and 600 psi of modulus of rupture at 28 days. There was no considerable negative effect of cement reduction on mechanical properties of concrete observed.



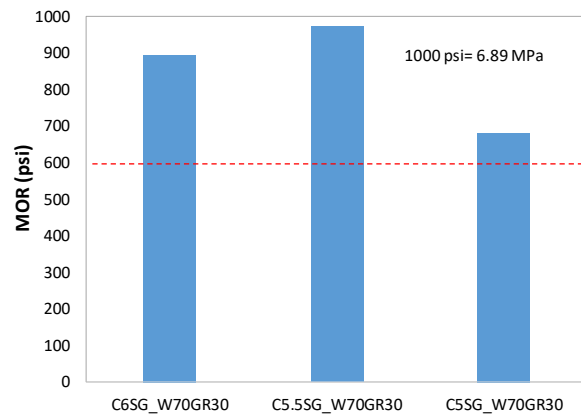
a) Compressive strength of the East NE mixes



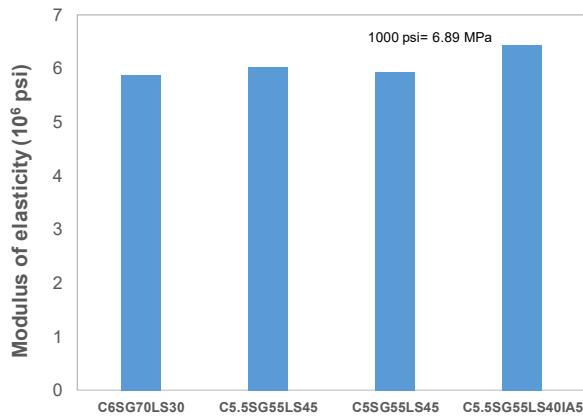
b) Compressive strength of the West NE mixes



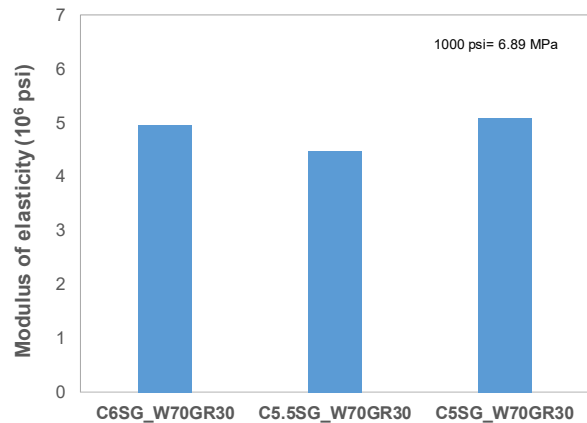
c) Modulus of rupture of the East NE mixes



d) Modulus of rupture of the West NE mixes



e) Modulus of elasticity of the East NE mixes



f) Modulus of elasticity of the West NE mixes

Figure 4.16. Mechanical properties of the promising mixes

Figure 4.17 illustrates the permeability results of Phase 3 mixes. The reduction of cement content resulted in a slight increase in permeability. The potential reason for it is the denser aggregate matrix in the optimized concrete mixes.

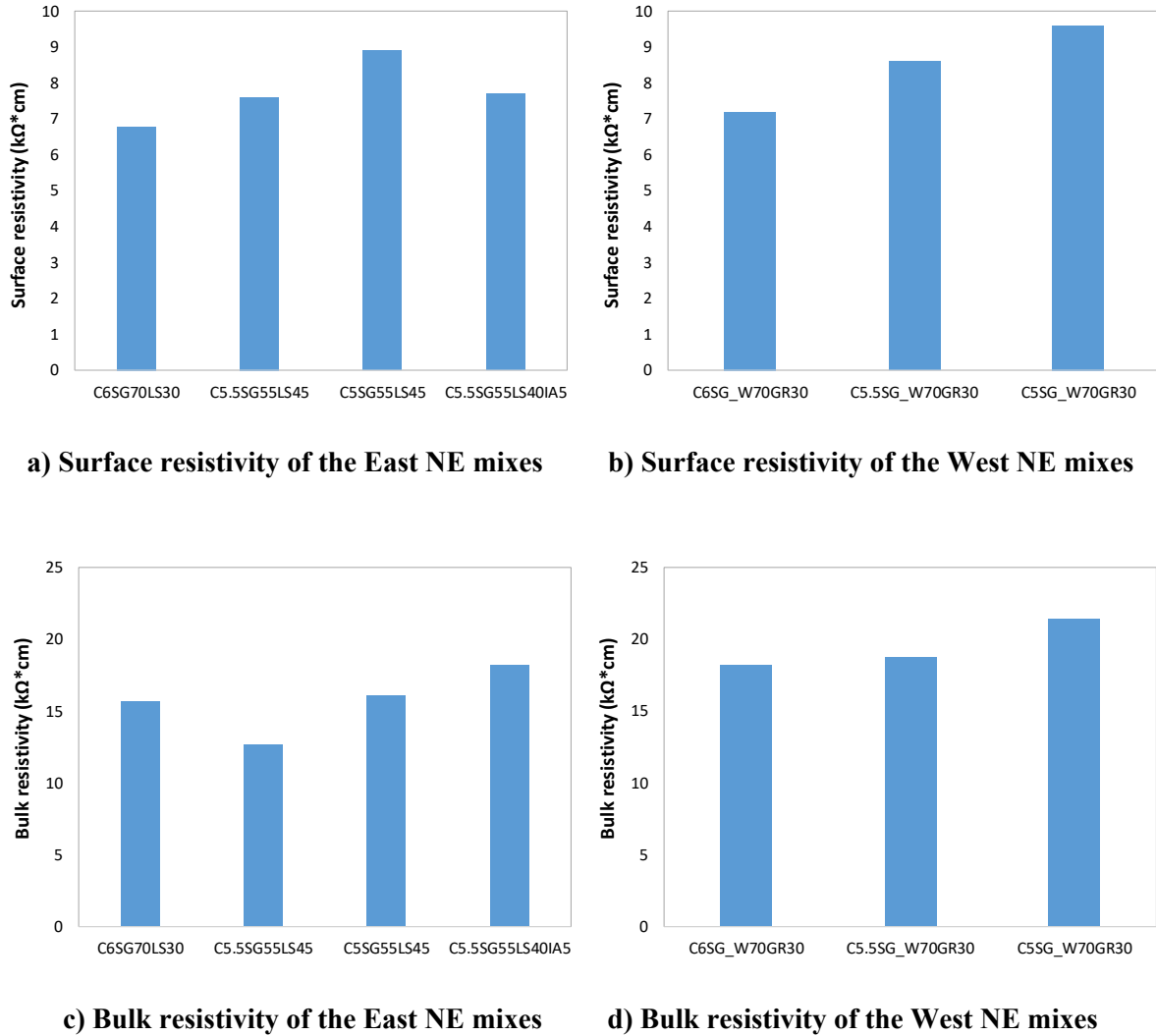


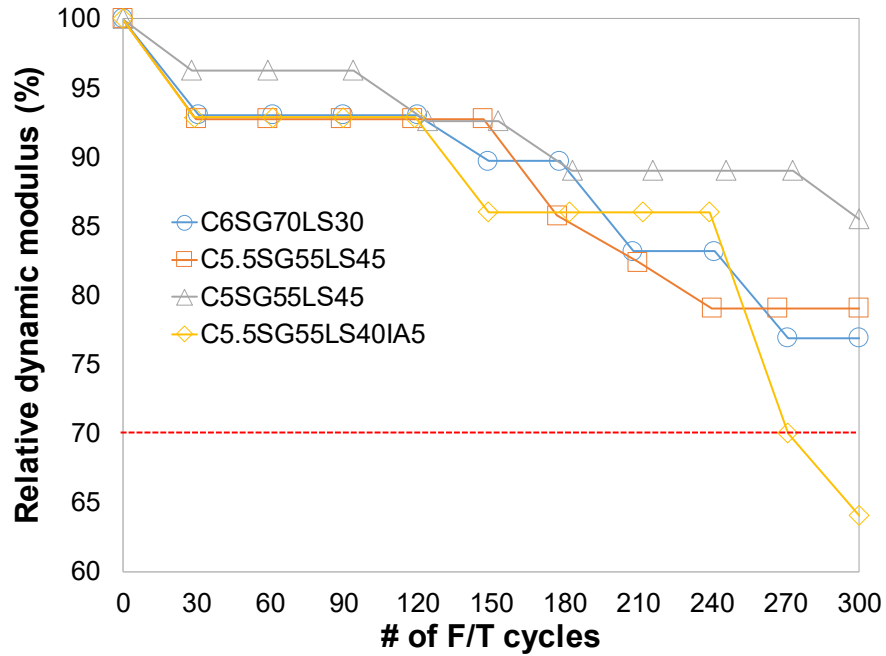
Figure 4.17. Permeability properties of the promising mixes

#### 4.6.4 Durability properties

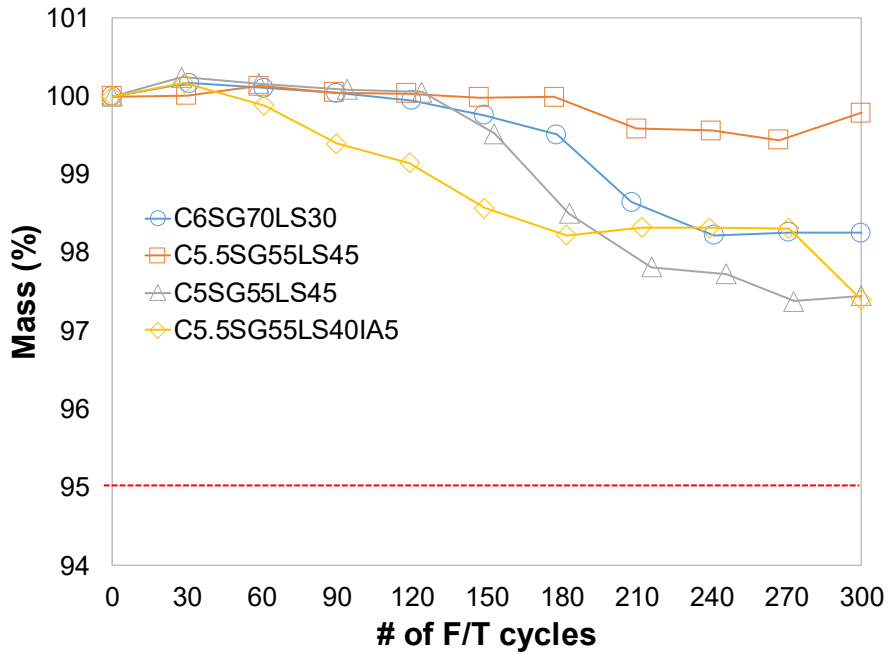
Figure 4.15 demonstrates the relative dynamic modulus and mass change of East NE mixes. From Figure 4.15a, it can be seen that mixtures with optimum gradation are demonstrating very similar performance despite the difference in cement content and air content. It can be stated that 0.5 sacks difference in cement content and 0.8% difference in air content does not significantly influence freeze-thaw resistance. C5.5SG55LS45 and C6SG70LS30 have almost identical air content, and yet the optimum blend mixture is performing better. It is believed that mixtures with a higher amount of coarse aggregates have higher freeze/thaw resistance. NDOT specifies the requirement of minimum relative dynamic modulus of 70% at 300 cycles. It can be seen that one mixture C5.5SG50LS45IA5 failed to pass this criteria. Figure 4.15b illustrates mass change over



freeze-thaw cycles. NDOT specification requires no more than 5% of mass change at 300 cycles. It can be noticed that all four mixtures met the requirement with C5.5SG55LS45 mix showing the best performance. Figure 4.16 shows the representative specimens of each mix after 300 freeze-thaw cycles.

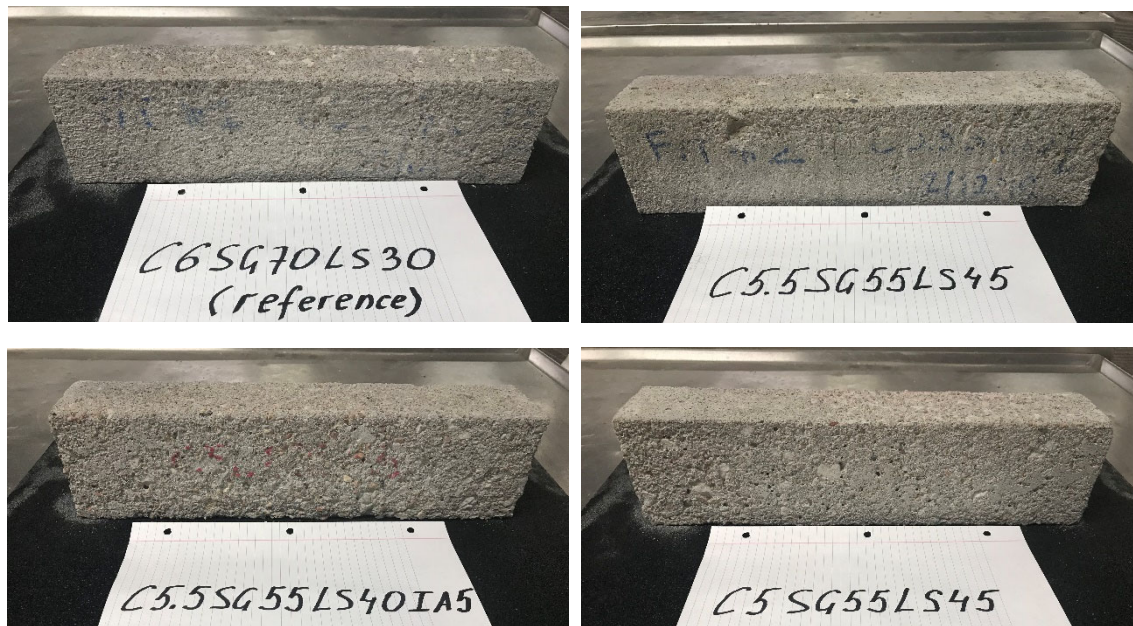


a) Relative dynamic modulus change



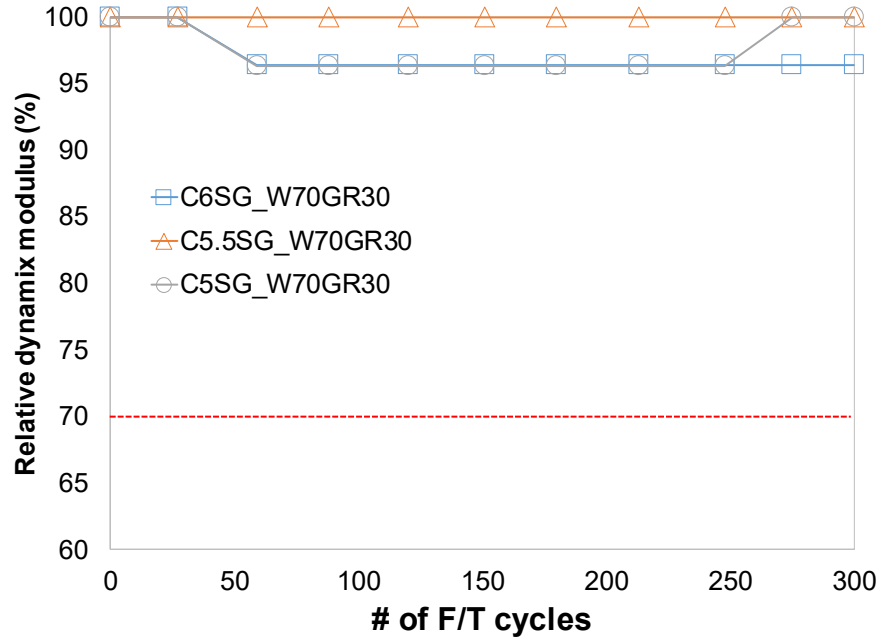
b) Mass change

Figure 4.18. Freeze/thaw resistance results of East NE mixes

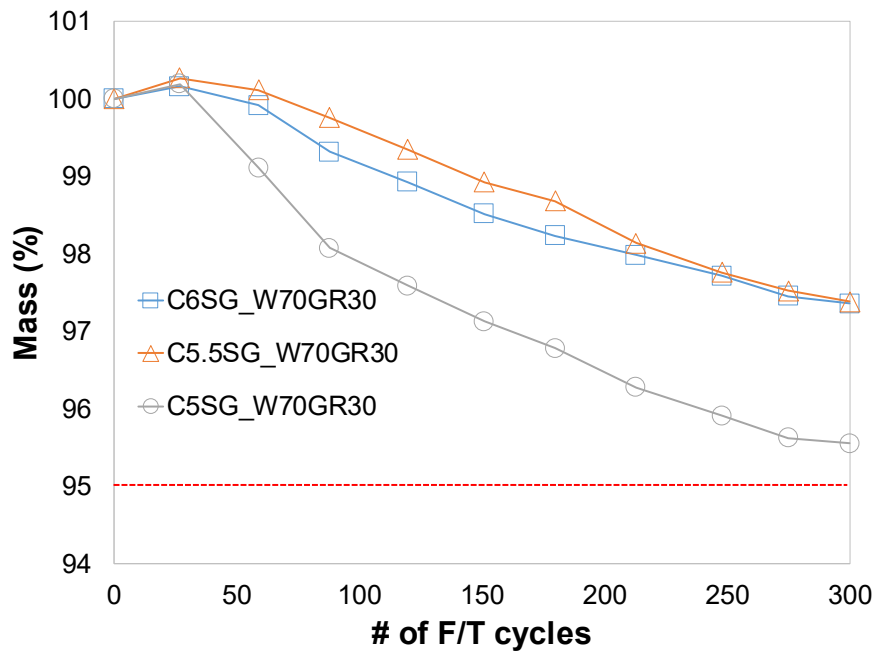


**Figure 4.19. Representative specimens of East NE mixes after 300 cycles of freezing-thawing**

Figure 4.17 demonstrates the relative dynamic modulus and mass change of West NE mixes. All three mixes met both mass loss and dynamic modulus loss requirements per NDOT. The variation of both parameters is too low to draw any conclusions. This insignificant variation may fall within the variation of the test. Figure 4.18 shows representative specimens of West NE mixes after 300 freeze-thaw cycles.

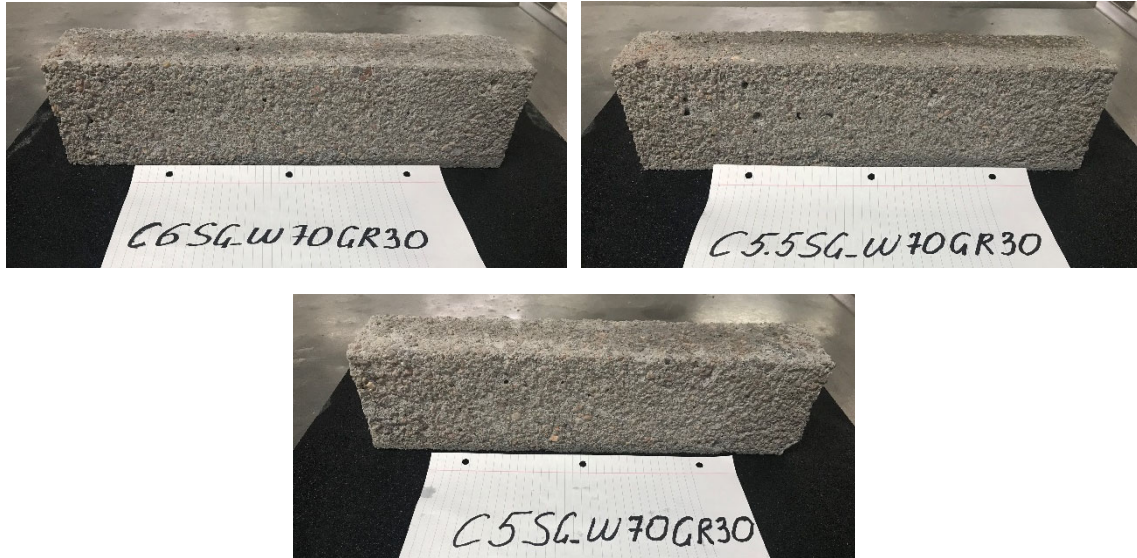


a) Relative dynamic modulus change



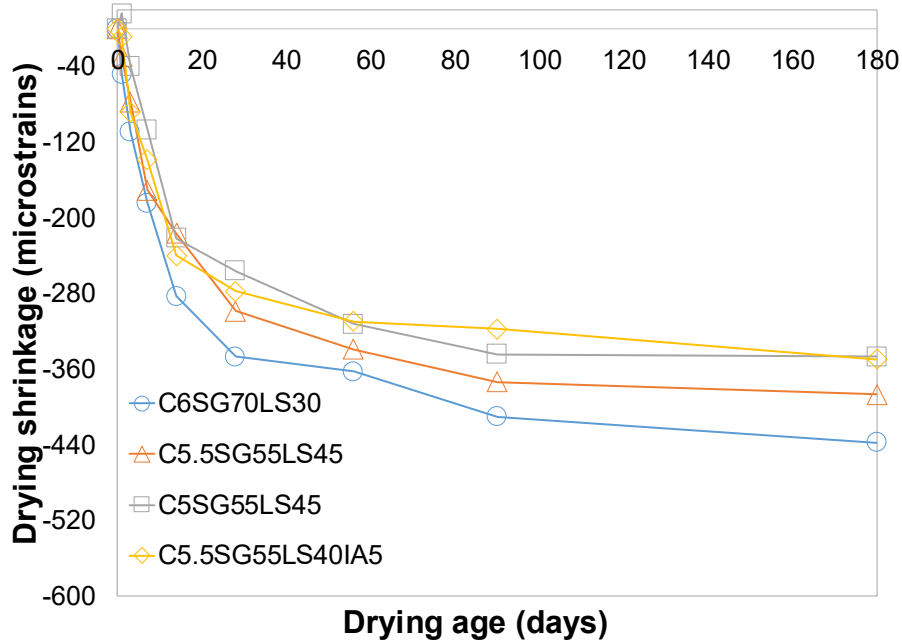
b) Mass change

Figure 4.20. Freeze/thaw resistance results of West NE mixes

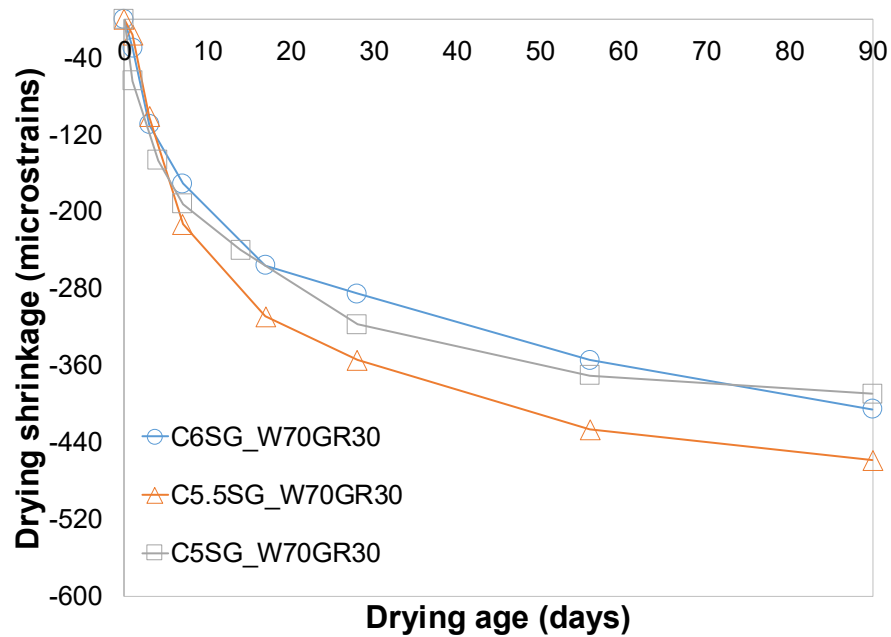


**Figure 4.21. Representative specimens of West NE mixes after 300 cycles of freezing-thawing**

Figure 4.19 demonstrates the results of the free shrinkage test. As expected, the reference mixture (C6SG70LS30) resulted in a higher shrinkage rate due to higher cement paste volume. The difference at 180 days is about 50, 90, and 90 microstrains compared to C5.5SG55LS45, C5SG55LS45, and C5.5SG55LS40IA5 respectively. However, free shrinkage results of West NE were not expected, where 0.5 sacks reduced mix is experiencing higher shrinkage. It could be due to the lower modulus of elasticity of this mix. Further monitoring is necessary to observe if the trend will continue.



a) Free shrinkage results of East NE mixes



b) Free shrinkage results of West NE mixes

Figure 4.22. Free shrinkage results

Figure 4.20 shows the results of the restrained shrinkage test of East NE mixes. As expected, with the reduction of cement content the age at cracking under restrained shrinkage increases. For C6SG70LS30, C5.5SG55LS45, C5SG55LS45, and C5.5SG55LS40IA5 the age at

cracking was 11.5, 13.0, 15.0, and 12.5 days respectively. It worth noting that this test seems to be more representative compared to free shrinkage since pavement concrete is restrained in reality. Due to unforeseen issues with the equipment, restrained shrinkage test was not performed for West NE mixes.

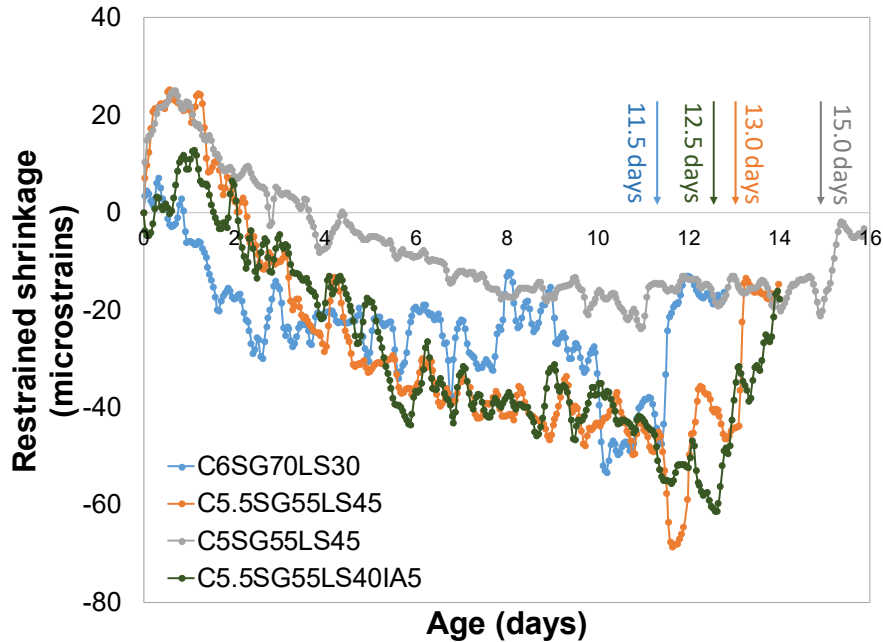


Figure 4.23. Restrained shrinkage results of East NE mixes

#### 4.7 Proposed changes in NDOT specifications

Table 4.9 represents the main requirements for slip formed pavement concrete specified by NDOT (NDOT Standard Specifications for Highway Construction, 2017). From the results obtained in this study, it can be concluded that the requirement of the minimum amount of total cementitious materials can be reduced from 564 lb/yd<sup>3</sup> to 470 lb/yd<sup>3</sup> with the optimum gradation.

Table 4.9. Specification for 47B pavement concrete mix

Specs	Base Cement Type	W/C Ratio Max.	Total Cementitious Materials Min. (lb/yd <sup>3</sup> )	Total Aggregate		Coarse Aggregate (%)
				Min. (lb/yd <sup>3</sup> )	Max. (lb/yd <sup>3</sup> )	
NDOT (2017)	IP	0.45	564	2850	3150	-
Proposed	IP	0.45	470	2850	3150	-*

\*- From the combined gradation optimized using Tarantula Curve

#### 4.8 Summary

According to the aggregate systems evaluation through both experimental and theoretical packing analysis, and it was justified that the reference blend, which is currently being used, does not provide the optimum gradation. Besides, it was found that there is a good correlation between experimental and theoretical particle packing degrees when the vibration plus pressure method is used. Although the Modified Toufar Model worked well for aggregates from this study, it might not work for other aggregates.

According to concrete mixtures performed, it was justified that aggregate gradation plays a significant role in fresh concrete performance. It was found that when optimum gradation is used, cement content can be reduced up to 1.0 sacks. Mechanical properties were not compromised by cement content reduction and still met NDOT requirements. Durability tests showed that concrete mixtures with optimum blend have a higher resistance to freeze/thaw cycles. It was also proved that reducing cement content leads to lower shrinkage, which was demonstrated by both free and restrained shrinkage tests. The summary of the promising mixtures is presented in Table 4.10.

In summary, it can be concluded that cement content can be reduced when the optimum blend is used. In addition, better durability properties were achieved. According to the results obtained, the change of the required cement content to NDOT specifications was proposed.

**Table 4.10. Summary table of Phase 3 mixes**

Mix ID	C6SG70 LS30	C5.5SG55 LS45	C5SG55 LS45	C5.5SG55 LS40IA5	C6SG_W70 GR30	C5.5SG_W70 GR30	C5SG_W70 GR30
Slump (in)	3.00	3.50	4.50	4.75	5.00	5.25	4.25
Air content (%)	7.0	7.2	8.0	7.6	7.6	8.5	8.0
Unit weight (pcf)	139.24	140.28	134.08	138.88	137.84	135.08	139.40
Initial set (min)	275	255	395	360	315	360	370
Final set (min)	395	380	520	495	450	480	505
f <sub>c</sub> , 28 (psi)	4043	3832	3608	4122	3745	5351	5448
MOR, 28 (psi)	854	624	795	605	895	973	681
MoE (x10 <sup>6</sup> psi)	5.89	6.03	5.93	6.43	4.96	4.47	5.09
Surface resistivity, 28 days (kΩ*cm)	6.8	7.6	8.9	7.7	7.2	8.6	9.6
Bulk resistivity, 28 days (kΩ*cm)	15.7	12.7	16.1	18.2	18.2	18.8	21.4
F/T, Mass @300 cycles, %	98.26	99.79	97.45	97.40	97.36	97.38	95.55
F/T, RDM @ 300 cycles, %	76.91	79.04	85.50	64.04	96.40	100.00	100.00
Shrinkage @180 days, microstrains	-437.3	-386.7	-.346.7	-349.3	-466.7	-536	-458.7
Restrained shrinkage, crack initiation age, day	11.5	13.0	15.0	12.5	NA	NA	NA



## CHAPTER 5. COST EFFECTIVENESS AND FEASIBILITY STUDY

### 5.1 Cost Effectiveness Analysis

With the identified aggregate sources and developed mixture designs, a cost analysis was performed based on material and transportation costs. A case-based approach was used for cost analyses in different locations. The cost analysis spreadsheet was prepared for easier use. The results were used to justify if the developed concrete mixtures are cost-effective.

#### 5.1.1 Methodology

Based on the inputs from TAC and local producers the unit costs of the raw materials were obtained and tabulated in Table 6.1.

**Table 5.1. Unit costs of materials**

Material	Unit cost	Unit
IP cement	\$135	Ton
Limestone	\$25	Ton
Granite	\$30	Ton
East NE Sand and Gravel	\$18	Ton
West NE Sand and Gravel	\$18	Ton
Intermediate size limestone	\$40	Ton
Water	\$2.5	Ton
Water reducer	\$9	Gallon
Air entraining agent	\$7	Gallon

#### 5.1.2 Results

Table 6.2 summarizes the base costs of promising mixes obtained based on the individual unit costs of ingredients. Depending on the location and availability of materials, the unit costs are subjected to change. Therefore, a cost spreadsheet was prepared, where the mix base cost is calculated based on the input unit cost. It can be seen from Table 6.2 that for East NE mixes the optimized mixtures do not result in a significantly lower cost due to the fact that even though the cement content is reduced, the higher amount of limestone is introduced to optimize gradation. Since limestone is more expensive than sand and gravel, introducing more limestone compensates the saved cost from the cement content reduction. From West NE mixes cost analysis it can be seen more significant cost reduction with lower cement content due to the aggregate blend remaining the same.

**Table 5.2. Base costs of promising mixes**

Concrete mixture	Base cost (\$/yd <sup>3</sup> )
C6SG70LS30	68.65
C5.5SG55LS45	68.23
C5.5SG55LS40IA5	71.04
C5SG55LS45	67.76
C6SG W70GR30	70.98
C5.5SG W70GR30	69.27
C5SG W70GR30	68.66

## 5.2 Feasibility Analysis

While additional aggregate test and fresh concrete (box) test is required to come up with the revised design and justify the mix performance, there is no additional modification in the batching and casting process. Both aggregate and fresh concrete tests do not require any costly equipment, and the software used for image analysis can be downloaded for free. The developed mixes appear to have acceptable fresh and hardened concrete performance. Similar mixes have already been adopted in local ready mix concrete producers, and better shrinkage and freeze-thaw resistance were observed. NDOT is also in the process of implementing that permit the reducing of cement by 0.5 sack provided that the combined aggregate gradation falls into the Tarantula curve. Based on this study, with the addition of WR even 1.0 sack of cement can be reduced. Some field tests are necessary to justify the feasibility.

There are some concerns such as air content control when aggregates with excessive surface dust are used, especially when it is clay coatings. Specific clays mixed with a particular type of AEA can largely neutralize the function of AEA. It is also becoming challenging to control air content when WR is used to adjust concrete workability. It was found that improving concrete workability with WR can also increase air.

## CHAPTER 6. CONCLUSIONS AND RECOMMENDATION FOR FUTURE STUDIES

### 6.1 Conclusions

Based on the results from the theoretical and experimental study of aggregate packing and the performance of pavement concrete prepared with the standard and optimized aggregate gradations and the reduced cement contents, the following conclusions can be drawn:

- The modified Toufar Model is an effective tool for pavement concrete mix design. By incorporating the packing degree of aggregates, the model accounts for the gradation as well as the shape and texture characteristics.
- Results from the theoretical aggregate particle packing analysis based on the Modified Toufar Model matched well with the experimental results when the vibration plus pressure procedure was used.
- The Box test with the modified index provides a reliable and more objective evaluation of the fresh pavement concrete performance. However, the results in this study imply that the VKelly test does not fit well to evaluate the performance of pavement concrete when coarse aggregate content is low.
- When the optimum aggregate gradation is used, cement content can be effectively reduced by up to 1.0 sack (94 lb/yd<sup>3</sup>) without compromising the fresh properties, mechanical properties, and permeability.
- The results of free and restrained shrinkage indicate that shrinkage and cracking potential can be reduced when the concrete mixture is more optimized. Freeze/thaw resistance can also be improved although it is not significant.
- A mix design procedure considering both the theoretical and experimental void contents and the minimum  $P_c\%/V_{B\_agg}\%$  ratio can be used to reach better design concrete mixtures in a more optimal manner.

### 6.2 Recommendations for Future Studies

#### 6.2.1 Potential modification of Tarantula Curve limits for Nebraska pavement

Figure 7.1 illustrates the promising blends of this study, which lead to a good performance of concrete with reduced cement content, plotted on the Tarantula curve. It can be seen that one of the blends is out of the limits in #8 and #16 sieve size regions with other blends being very close to the limit. The potential reason for this is the use of high amounts of sand and gravel in Nebraska. Considering this fact, there is a potential need in modifying Tarantula Curve limits for a better judgment of NDOT gradations.

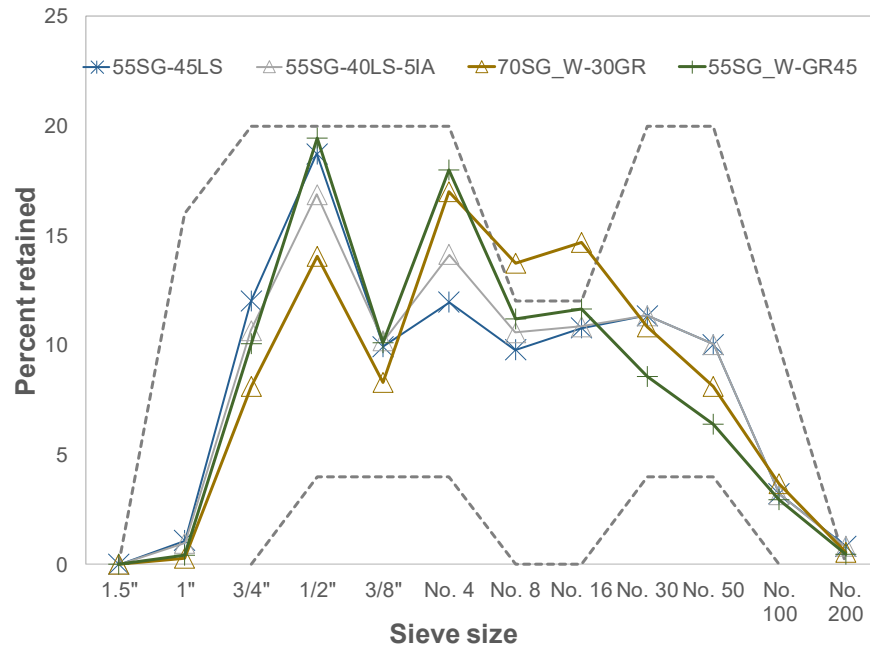


**Figure 6.1. Promising blends plotted on Tarantula Curve**

### 6.2.2 Air content requirement adjustment with the cement reduction

One of the potential things to address in the future is the air content requirement for concrete mixes when the volume of paste is decreased. Since entrained air is introduced into cement paste, and not aggregates, it is more reasonable to maintain the air content within the paste, and not the concrete overall. If the paste volume in concrete is decreased, a lower amount of air is needed for the concrete to maintain the same air in the paste. Figure 7.2 illustrates that to a 6.5-9.0% standard 6.0 sacks concrete mix contains 20.3%-28.1% air in cement. In order to maintain the same air concrete in concrete, when cement content is reduced to 5.5 sacks or 5.0 sacks, a cement paste should have 21.7%-30.3% and 23.2%-32.1% of the air in the cement paste respectively. The higher air content in the cement paste will increase the potential of air void coalescence, which will lead to the larger size of airs and increases spacing factor, and eventually lead to strength, permeability, and F/T resistivity issues. A study is needed to identify if there is any potential issue associated with the air content with the change of cement content, and to determine if an adjustment of NDOT specification on air content is needed.

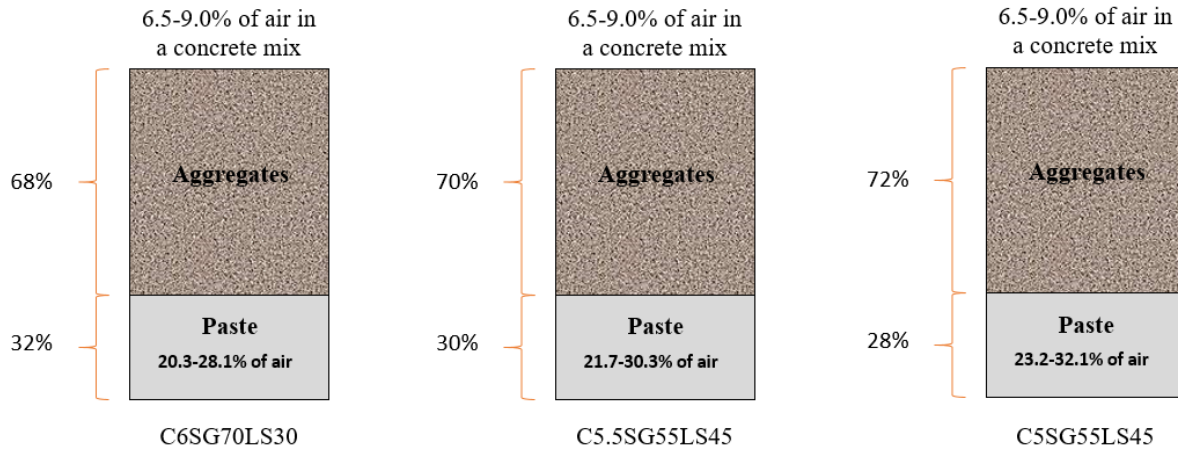


**Figure 6.2. Illustration of increase in paste air content when maintaining concrete air**

### 6.2.3 Mix design adjustment based on specific aggregate characteristics

The main recommendations for future studies include the incorporation of more direct quantitative parameters to develop a more rational mix design procedure of pavement concrete. These additional parameters include direct measurement of aggregate shape and texture, combined aggregate fineness modulus, and microfines type and content.

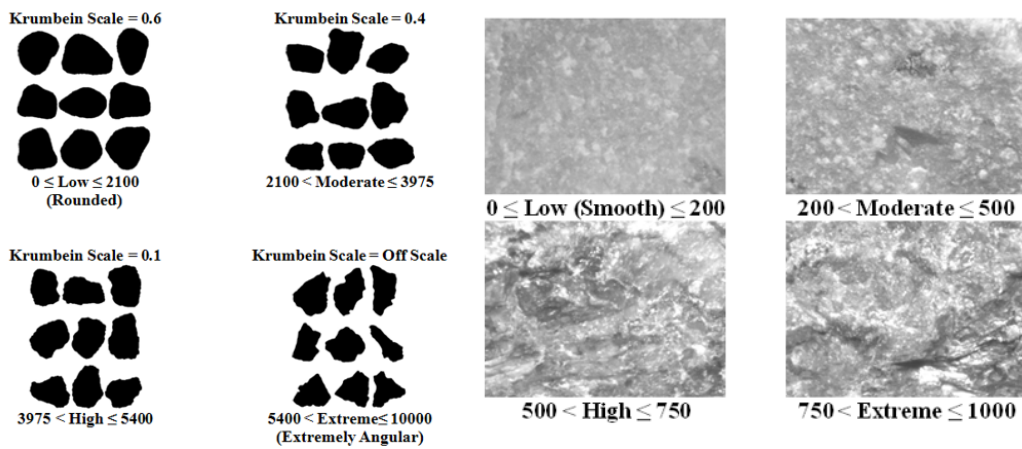
It is believed that different aggregate blends may have comparable volume occupied in a concrete mixture and similar void content, but differ in fineness modulus, i.e., total surface area. This difference will lead to different excess paste demand to coat aggregates. Therefore, consideration of combined fineness modulus could be critical in the mix design.

Aggregate dust is known to cause problems in concrete at different stages. It is also known that the mineralogy of the dust is crucial. For example, clay coatings have a more harmful impact on concrete performance compared to limestone dust. Clay coatings are known to weaken the interfacial transition zone, thus negatively affecting strength and durability. Besides, it was found that specific microfines can neutralize the function of AEA, and reduce entrained air significantly. Therefore, it is important to account for both amount and type of microfines.

Aggregate shape and texture are other factors not included in common mix designs directly. However, it is well known that these properties may have a significant impact on both fresh and hardened concrete properties. Aggregate Image Measurement System (AIMS2) equipment can be used to determine these properties directly. The AIMS2 is an integrated machine that contains image acquisition hardware and a computer for system run and data analysis (Figure 7.3). The equipment can provide information includes angularity, texture, sphericity as well as the distribution of flat and elongated particles. As an example, Figure 7.4 demonstrates angularity and texture rankings from AIMS2 analysis. The software can also provide weighted stockpile properties. These parameters can be very useful during mix design development. However, at this moment a substantial amount of experimental work is needed to obtain sufficient data to correlate these properties with fresh and hardened concrete performance. Therefore, collaboration with other states and agencies is necessary to collect their aggregate and concrete mixes data. Moreover, incorporation of these parameters in mix design can be extended to other types of concrete, not only pavement concrete.



Figure 6.3. AIMS 2 setup



a) Aggregate angularity rankings      b) Aggregate texture rankings  
 Figure 6.4. Direct measurement of aggregate shape and texture

## REFERENCES

AASHTO TP 95-11. Standard Method of Test for Surface Resistivity Indication of Concrete's Ability to Resist Chloride Ion Penetration. *American Association of State and Highway Transportation Officials*, 2011.

ASTM C29. Standard Test Method for Bulk Density (Unit Weight) and Voids in Aggregate. *ASTM International*, 2016.

ASTM C39. Standard Test Method for Compressive Strength of Cylindrical Concrete Specimens. *ASTM International*, 2015.

ASTM C78. Standard Test Method for Flexural Strength of Concrete (Using Simple Beam with Third-Point Loading). *ASTM International*, 2015.

ASTM C127. Standard Test Method for Relative Density (Specific Gravity) and Absorption of Coarse Aggregate. *ASTM International*, 2015.

ASTM C128. Standard Test Method for Relative Density (Specific Gravity) and Absorption of Fine Aggregate. *ASTM International*, 2015.

ASTM C136. Standard Test Method for Sieve Analysis of Fine and Coarse Aggregates. *ASTM International*, 2014.

ASTM C143. Standard Test Method for Slump of Hydraulic Cement Concrete. *ASTM International*, 2016.

ASTM C157. Standard Test Method for Length Change of Hardened Hydraulic-Cement Mortar and Concrete.

ASTM C192. Standard Practice for Making and Curing Concrete Test Specimens in the Laboratory. *ASTM International*, 2016.

ASTM C215. Standard Test Method for Fundamental Transverse, Longitudinal, and Torsional Resonant Frequencies of Concrete Specimens. *ASTM International*, 2014

ASTM C260. Standard Specification for Air-Entraining Admixtures for Concrete. *ASTM International*, 2016.

ASTM C360. Test Method for Ball Penetration in Freshly Mixed Hydraulic Cement Concrete (Withdrawn 1999). *ASTM International*, 1992.

ASTM C403. Standard Test Method for Time of Setting of Concrete Mixtures by Penetration Resistance. *ASTM International*, 2016

ASTM C469. Standard Test Method for Static Modulus of Elasticity and Poisson's Ratio of Concrete. *ASTM International*, 2014

ASTM C494. Standard Specification for Chemical Admixtures for Concrete. *ASTM International*, 2017.

ASTM C595. Standard Specification for Blended Hydraulic Cements. *ASTM International*, 2018.



- ASTM C666. Standard Test Method for Resistance of Concrete to Rapid Freezing and Thawing. *ASTM International*, 2015
- ASTM C1581. Standard Test Method for Determining Age at Cracking and Induced Tensile Stress Characteristics of Mortar and Concrete under Restrained Shrinkage. *ASTM International*, 2018
- Andrew, R.M. *Global Co2 Emissions from Cement Production*. Earth System Science Data, 2018, 10: 195-217.
- Cook, D., Ley, T., and Ghaeezadah, A. A Workability Test for Slip Formed Concrete Pavements. *Construction and Building Materials*, 2014, 68: 376-383.
- Cook, D., Ley, T., Ghaeezadah, A. *Effects of Aggregate Concepts on the Workability of Slip-Formed Concrete*. Journal of Materials in Civil Engineering, 2016, 28-10.
- De Larrard, F. *Concrete Mixture Proportioning: a scientific approach*. Taylor & Francis, New York, 1999.
- Ferrais, C.F., Billberg, P., Ferron, R., Feys, D., Hu, J., Kawashima, S., Koehler, E., Sonebi, M., Tanesi, J., Tregger, N. *Role of Rheology in Achieving Successful Concrete Performance*. Concrete International, 2017, 39-6: 43-51.
- Fly Ash Task Force Report*. AASHTO Subcommittee on Materials, 2016.
- Furnas, C.C. Sun. *Flow of Gases Through Beds of Broken Solids*. Bureau of Mines, United States. 1928.
- Goltermann, P., Johansen, V., Palbol, L. Packing of Aggregates: An Alternative Tool to Determine the Optimal Aggregate Mix. *ACI Materials Journal*, 1997, 94-M51: 435-442.
- Heyen, W., Halsey, L. *Optimized Aggregates Gradations for Portland Cement Concrete Mix Designs Evaluation*. Nebraska Department of Roads, 2013.
- Jones, M.R., Zheng, L., Newlands, D.D. *Comparison of Particle Packing Models for Proportioning Concrete Constituents for Minimum Voids Ratio*. Materials and Structures, 2002, 35: 301-309.
- Kennedy, C.T. The design of concrete mixes. *Journal of the American Concrete Institute*, 1940, 36: 373-400
- Kwan, A.K.H., Mora, C.F. *Effects of Various Shape Parameters on Packing of Aggregate Particles*. Magazine of Concrete Research, 2001, 53-2: 91-100.
- Kosmatka, S., Kerkhoff, B., Panarese, W. *Design and Control of Concrete Mixtures, 14th Edition*. Portland Cement Association, Skokie, IL, 2008.
- Lamond, J.F., Pielert, J.H. *Significance of Tests and Properties of Concrete and Concrete-Making Materials*. ASTM International, 2006, STP169D.
- Ley, T., Cook, D., and Fick, G. *Concrete Pavement Mixture Design and Analysis (MDA): Effect of Aggregate Systems on Concrete Properties*. National Concrete Pavement Technology Center, Ames, IA, 2012.

- Ley, T. and Cook, D. *Aggregate Gradations for Concrete Pavement Mixtures*. CP 9 Road Map. Moving Advancements into Practice (MAP) Brief. FHWA TPF-5-(286), 2014.
- Mangulkar, M.N, Jamkar, S.S. *Review of Particle Packing Theories Used for Concrete Mix Proportioning*. International Journal of Scientific & Engineering Research, 2013, 4-5: 143-148.
- Moini, M. *The Optimization of Concrete Mixtures for Use in Highway Applications*. Master Thesis, The University of Wisconsin-Milwaukee, 2015.
- Obla, K., Kim, H., Lobo, C. *Effect of Continuous (Well-Graded) Combined Aggregate Grading on Concrete Performance Phase A: Aggregate Voids Content (Packing Density)*. National Ready Mix Concrete Association, 2007.
- Obla, K. (2011). *Variation in Concrete Performance due to aggregates*. Concrete infocus: a publication of the national ready mixed concrete association, 2011, 10-5: 9-14.
- Quiroga, P.N. and Fowler, D.W. *The Effects of Aggregates Characteristics on the Performance of Portland Cement Concrete*. Report ICAR 104-1F. International Center for Aggregates Research, University of Texas at Austin, 2004.
- Rached, M., De Moya, M., Fowler, D.W. *Utilizing Aggregates Characteristics to Minimize Cement Content in Portland Cement Concrete*. International Center for Aggregate Research, 2009.
- Ramakrishnan, V. *Optimized Aggregate Gradation for Structural Concrete*. South Dakota Department of Transportation, 2004.
- Rudy, A.K. *Optimization of Mixture Proportions for Concrete Pavements - Influence of Supplementary Cementitious Materials, Paste Content and Aggregate Gradation*. Ph.D. Dissertation, Purdue University, 2009.
- Siddiqui, M.S., Rached, M., and Fowler, D. *Rational Mixture Design for Pavement Concrete*. Transportation Research Record: Journal of the Transportation Research Board, 2014, 2441: 20-27.
- Standard Specifications for Highway Construction. Nebraska Department of Transportation, 2017.
- Stovall, T., de Larrard, F., Buil, M. *Linear Packing Density Model of Grain Mixtures*. Powder Technology, 1986, 48: 1-12.
- Taylor, P., Bektas, F., Yurdakul, E., Ceylan, H. *Optimizing Cementitious Content in Concrete Mixtures for Required Performance*. National Concrete Pavement Technology Center, Ames, IA, 2012.
- Taylor, P., Yurdakul, E., Wang, X., Wang, X. *Concrete Pavement Mixture Design and Analysis (MDA): An Innovative Approach to Proportioning Concrete Mixtures*. National Concrete Pavement Technology Center, Ames, IA, 2015.
- Taylor, P. *Blended Aggregates for Concrete Mixture Optimization: Best Practices for Jointed Concrete Pavements*. FHWA-HIF-019, 2015.
- Taylor, P., Wang, X., Wang, X. *Concrete Pavement Mixture Design and Analysis (MDA): Development and Evaluation of Vibrating Kelly Ball Test (VKelly Test) for the Workability of Concrete*. National Concrete Pavement Technology Center, Ames, IA, 2015.

Wang, X., Wang, K., Taylor, P., Morcous, G. *Assessing Particle Packing Based Self-consolidating Concrete Mix Design Method*. *Construction and Building Materials*, 2014, 70: 439-452.

Wassermann, R., Katz, A., Bentur, A. *Minimum cement content requirements: a must or a myth?*. *Materials and Structures*, 2009, 42: 973–982.

Yurdakul, E. *Optimizing concrete mixtures with minimum cement content for performance and sustainability*. Master thesis, Iowa State University, 2010.

## Appendix A - Excess Paste-to-Aggregates Calculation

To achieve appropriate workability, simply filling voids among aggregate particles with cement paste is not sufficient, and an excess amount of paste is needed to cover aggregates. The amount of excess paste depends on the paste quality and surface area of aggregate particles (Kennedy, 1940). Due to the varied specific gravity of aggregates, two different aggregates with the same mass may differ in the volume occupied in a mix. Therefore, to be able to compare mixes more objectively, it is more reasonable to consider excess paste/aggregates ratio.

Once the bulk density and void content of a particular blend of aggregate is known, the excess paste in a mix can be calculated. The first step was to calculate aggregates bulk volume ( $V_{B\_agg}\%$ ) as presented in a mix by dividing the total mass of aggregates in a specific concrete mix design ( $M_t$ , in  $\text{lb}/\text{yd}^3$ ) with the bulk density of a blend ( $D_b$ , in  $\text{lb}/\text{ft}^3$ ) and 27 ( $\text{ft}^3/\text{yd}^3$ ).

$$V_{B\_agg}\% = \frac{M_t/D_b}{27} \quad (\text{A.1})$$

Then, the void content in a mix ( $VO_{mix}\%$ ) was obtained by multiplying the volume of aggregate in concrete by the void content in the aggregate blend ( $VO_{blend}\%$ ).

$$VO_{mix}\% = V_{B\_agg}\% \times VO_{blend}\% \quad (\text{A.2})$$

As the air content in the cement paste is often unknown, which makes it difficult to calculate the paste volume directly, the total paste volume ( $P_t\%$ ) was calculated by subtracting the coarse and fine aggregate volumes from the total volume of concrete (100%), in which the aggregate volumes were calculated by dividing the mass of aggregate ( $M_1$  or  $M_2$ , in  $\text{lb}/\text{yd}^3$ ), by the specific gravity ( $G_{sb1}$  or  $G_{sb2}$ ) times the specific gravity of water (at  $62.4 \text{ lb}/\text{ft}^3$ ) and then divided by 27 ( $\text{ft}^3/\text{yd}^3$ ).

$$P_t\% = 100\% - \frac{M_1/(G_{sb1} \times 62.4 \text{ pcf})}{27} - \frac{M_2/(G_{sb2} \times 62.4 \text{ pcf})}{27} \quad (\text{A.3})$$

The last step was to obtain the excess paste volume ( $P_e\%$ ) by subtracting  $VO_{mix}\%$  from the total paste volume in the mix ( $P_t\%$ ).

$$P_e\% = P_t\% - VO_{mix}\% \quad (\text{A.4})$$

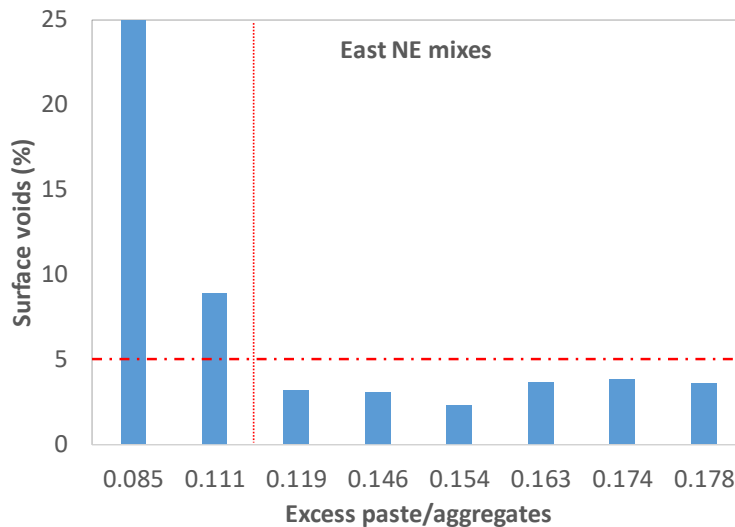
Finally, excess paste-to-aggregates volume ratio ( $P_e\%/V_{B\_agg}\%$ ) can be calculated by dividing  $P_e\%$  by  $V_{B\_agg}\%$ .

## Appendix B - Mix Design Improvement Methodology

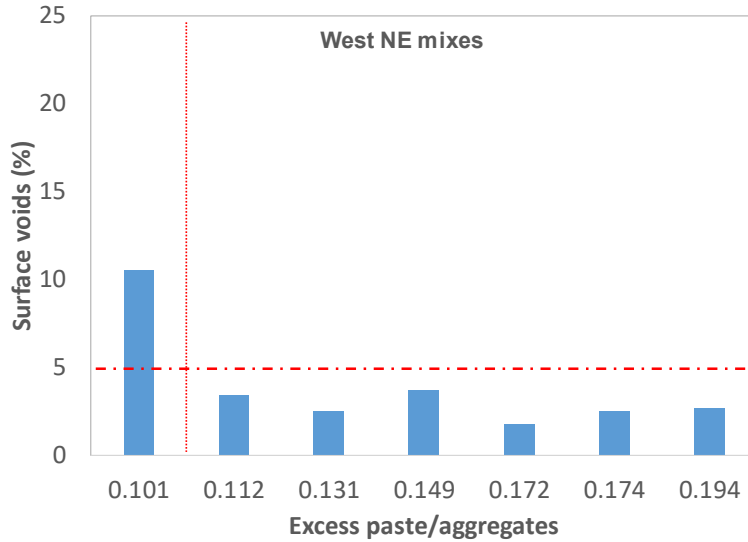
### B.1 Design Philosophy

The design philosophy consists of a systematic selection of the aggregate system and designing concrete with the minimum possible cement content and yet having mechanical and durability properties unaffected or improved. The main contribution of the developed mix design procedure is to use a theoretical particle packing model that accounts for aggregate shape and texture, and then using  $P_e\%/V_{B\_agg}\%$  ratio as the main parameter to drive the mix design. Besides, it is important to evaluate pavement concrete workability with specific tests such as Box Test.

As results indicated in the previous analysis, the relationship between the calculated  $P_e\%/V_{B\_agg}\%$  ratio and the surface void percentage is presented in Figure 5.1. Note that for a convenient visualization, mixtures failed with surface quality ranking 4 were assigned 25% of surface voids, and mixtures failed with edge quality ranking 4b was not included in the figure because it failed due to the too high excess paste volume. Results showed that, based on mixes included in the present study, East NE mixtures with  $P_e\%/V_{B\_agg}\%$  ratio of 0.111 and lower resulted in a dramatic increase and unacceptable surface void amount. For West NE mixes the threshold value was 0.101. The results imply that a minimum excess paste volume is required for pavement concrete to achieve sufficient performance. The reason why East NE and West NE mixtures resulted in slightly different threshold values is that combined fineness modulus of West NE aggregates is higher, resulting in lower total surface area. The lower the total surface area, the less excess paste is required to coat aggregates (Kosmatka et al., 2008). Conservatively, a value of approximately 0.115 for East NE and 0.106 for West NE can be considered as the minimum required  $P_e\%/V_{B\_agg}\%$  ratio based on the materials included in the present study.



a) Effect of  $P_e\%/V_{B\_agg}\%$  ratio on surface voids for East NE mixes



b) Effect of  $P_e\%/V_{B\_agg}\%$  ratio on surface voids for West NE mixes

Figure B.1. Effect of  $P_e\%/V_{B\_agg}\%$  ratio on surface voids

## B.2 Proposed Mix Design Procedure

According to the results obtained and the theoretical and experimental process included in this study, a mix design procedure can be recommended as shown in Figure 5.2. The first step includes obtaining an experimental packing degree of coarse and fine aggregates separately using ASTM C29 and vibration plus pressure method as discussed in the previous chapter. From the aggregate gradation results obtained per ASTM C136, the characteristic diameter of coarse and fine aggregates is obtained, which can be done by looking at cumulative % retained and interpolating where 36.8% of particles are retained. Once individual packing degrees and characteristic diameters are known, the Modified Toufar model should be used to obtain the optimum aggregate proportions and the packing degree of the blend. Then, the combined void content test should be performed for the selected blend, and the void contents from the aggregate skeleton can be obtained. The experimental packing degree obtained should be very close to the theoretical one. Once the aggregate blend is selected, and its void content is known, concrete can be designed with a predetermined minimum  $P_e\%/V_{B\_agg}\%$  ratio (0.106-0.115 contingent upon combined fineness modulus) based on materials used in the present study. Afterward, a trial concrete mix should be prepared in the lab and justified with acceptable pavement concrete performance with the Box test in terms of surface and edge quality. An appropriate WR dosage can be applied if necessary. To account for variables such as aggregate surface texture and shape that are not directly incorporated into the current design approach, in case of mix failing Box test even after WR addition, concrete can be adjusted with an extra 1% of excess paste. Then, the lab trial step is to be repeated and the mix is adjusted until an acceptable mix is obtained.

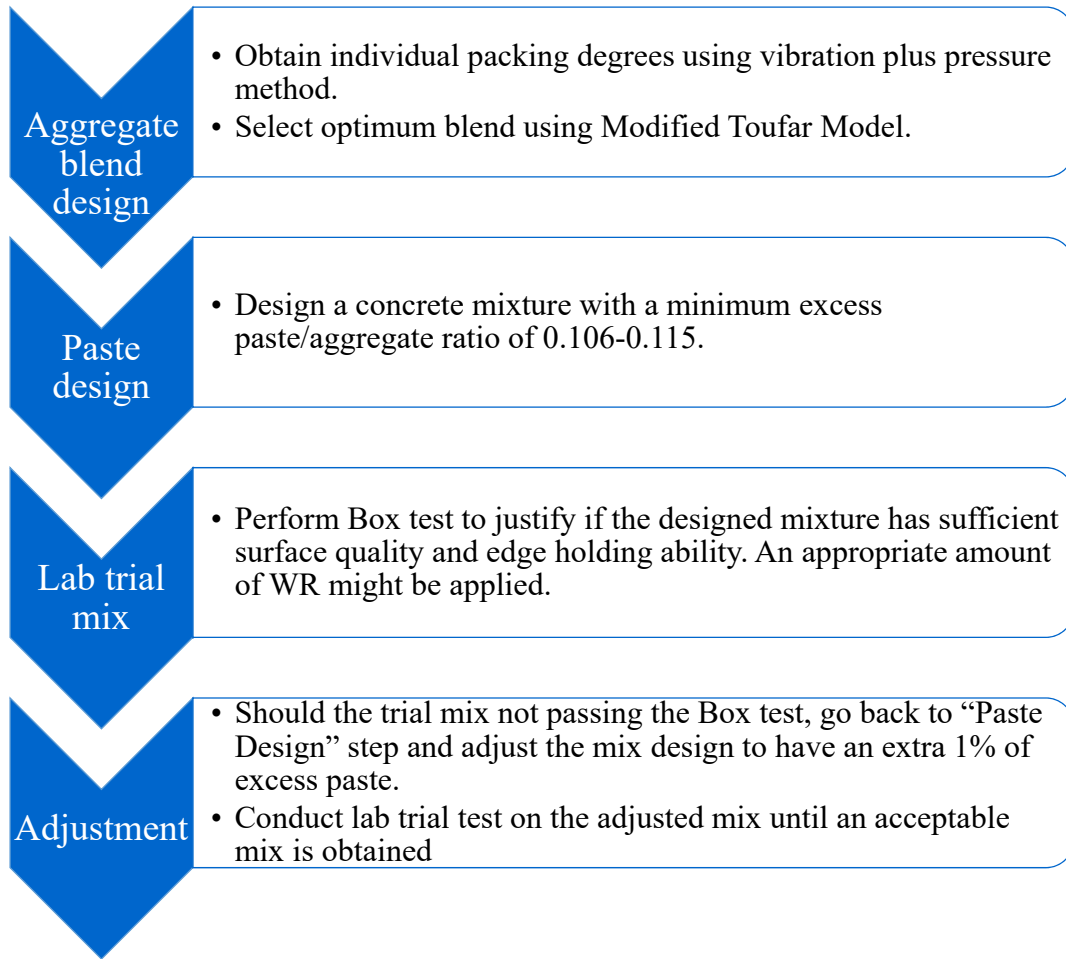


**Figure B.2. The proposed mix design adjustment procedure**

### **B.3 Summary**

Based on Box test results and calculated  $P_e\%/V_{B\_agg}\%$  ratio, the critical parameter of the minimum required  $P_e\%/V_{B\_agg}\%$  ratio was obtained and used for the proposed mix design procedure. The first step includes aggregate blend selection based on both experimental and theoretical particle packing using combined void content test and Modified Toufar Model. The second step required a concrete design with a minimum of  $P_e\%/V_{B\_agg}\%$  ratio of 0.106-0.115. Further steps require lab trial mix and necessary adjustments if needed. Note that the mix design procedure does not account for the combined fineness modulus of the aggregate blend, which can be used as an additional criteria in future studies.